PROPOSAL FOR AN INFN EXPERIMENT
2013 - 2015

ELIMED:
MEDical applications at ELI-Beamlines

July 18, 2013

CONTENTS

1 PROJECT OVERVIEW

Proposal name	ELIMED
Involved INFN Sections	LNS, LNL, INFN-CT, INFN-BO, INFN-MI, INFN-ME, INFN-LE, INFN-RM1, INFN-PI, INFN-TO
National responsibles	G A Pablo Cirrone and M Carpinelli
External participants:	Drug Sciences Department, University of Catania, Catania (I); School of Mathematics and Physics, Queen's University of Belfast, Belfast (UK); ELI Experimental Program Department, Institute of Physics of the ASCR, Prague, (CZ); Russian Academy of Science, Moscow (RU); Vinca Institute of Nuclear Sciences, University of Belgrade, Belgrade (Serbia); INRS-EMT, Montreal in Canada
Temporal schedule	3 years (2013 - 2015)

1.1 SHORT DESCRIPTION

The project aim is the development of innovative instrumentation, technologies and new methodologies for dosimetry and radiobiology in order to realize an hadrontherapy facility based on laser-driven beams. The project will closely follow the activities of the ELIMED project that will realize a hadrontherapy transport beam line using laser-driven beams accelerated at the ELI-Beamlines laser facility in Prague (CZ). One of the project main goals will be the realization of a first prototype of energy selector for laser-driven proton beams and of the necessary diagnostic systems in order to perform the first dosimetric and radiobiological measures at three different laser facilities: the TARANIS laser facility in Belfast (UK), the GIST, Gwangju in Korea and the FLAME laser in Frascati (I).
Part of the developed diagnostic will be also tested at the PALS facility in Prague (CZ).

2 INTRODUCTION

At INFN-LNS since many years three exceptional, well-established research areas coexist: ion acceleration and beam transport, plasma ion acceleration and related diagnostic, hadrontherapy and medical physics applications. This favorable presence allowed us to launch in the past months the European ELIMED initiative. ELIMED, acronym of MEDical applications at ELI-Beamlines, is an international venture started by a joined collaboration between INFN-LNS and ELI Experimental Program Department (Prague) researchers. The main aim of the project is the realisation, within the year 2018, of the first facility entirely dedicated to the physics and radiobiological studies of high-energy (60 - 250 MeV) proton beams accelerated by the high-power laser interaction with matter. As reported in many theoretical studies as well as in a vast set of experiments with lower power laser systems, the produced beams will show very peculiar energy spectrum, fluence and temporal distributions. In particular lasers with a very short duration generate extremely intense pulsed beams ($10^9 - 10^{12}$ protons per pulse with 1.0 - 0.1 nsec pulse duration). ELIMED will be a specific laser facility designed and realised with the aim to demonstrate the clinical applicability of these laser-driven proton beams (up to 20 - 30 MeV of kinetic energy in the first phase). Particular care will be devoted to the design, development and test all of the diagnostic devices necessary to monitor the different phases of the particles production (from the laser-target interaction point to the final clinical beam). A specific effort will be dedicated to the dosimetric and radiobiology studies. They will lead to the development of innovative detectors able to perform absolute and relative dose measurements to be used for a quantitative evaluation of the biological effects of the laser-driven beams compared to conventionally accelerated particles. ELIMED will therefore represent the first step towards a feasible reduction in dimensions and costs of future hadrontherapy facilities. From a pure scientific point of view, it will also represent a key opportunity for different and multidisciplinary research activities to converge and for the development of innovative detection techniques and to study and characterise this new kind of beams.

The ELIMED Collaboration is now growing and different research institutes are joining it or expressing the will of an active participation. The list of the actual European ELIMED partners can be found in the Section 1 of this proposal.

The scientific collaboration between INFN-LNS and ELI-Beamlines has been made official through a Memorandum of Understanding (MoU) signed in April 2012. The MoU establishes the scientific program, the time schedule and the specific responsibilities of the two research institutes in connection with the ELIMED Collaboration. A copy of the signed MoU is attached to this proposal. Starting from these considerations, taking in account the extreme novelty

and originality of the ELIMED activity and also the interest shown by the INFN in this field (funds of laser-plasma related projects, development and realisation of the FLAME facility at LNF, disposal into the MoU sign, etc.) we decide to submit to the INFN Fifth Commission this new proposal that we are calling ELIMED.

3 THE ELIMED FACILITY AT ELI-BEAMLINES

The ELIMED European Collaboration is planning the realisation, at ELI-Beamline facility in Prague, of a specific transport beam line to study the potential medical applications of the laser-accelerated ions. ELI-beamlines is one of the four pillars of the pan-European ELI infrastructure (funded in the framework of the European ESFRI process) which is planning the realisation of four different high power (up to 200 PW) laser facilities that will be located in four different European countries. The Prague facility, in particular, named ELI-Beamlines, will be entirely dedicated to the study of the potential applications of the secondary sources (like more energetic ion beams) generated by these lasers class. Of course, one of the potential application of ion sources is the external cancer radiation treatment or hadrontherapy. ELIMED was born by a common initiative proposed by researches of the INFN-LNS in Catania and FZU (Academy of Sciences of Czech Republic) in Prague. The starting idea was the wish to demonstrate the clinical applicability of the laser-driven protons. The proposed initiative has been favorably approved by the scientific committee of ELI-Beamlines and now ELIMED has a dedicated room (Experimental Hall number 6) specifically assigned for the realisation of the medical beam-line. The room will have a surface of about 50 m^2. It will contain the interaction chamber (where the laser impacts on the target), the energy selection system and, finally, the in-air hadrontherapy transport beam line with the connected dosimetric devices. Figure 3.1 shows a graphical layout of the ELI-Beamline structure. Experimental halls are located at the lower floor.

The temporal development of the European ELIMED project will be constituted of four different stages, each related to a well defined phase of the ELI-Beamlines facility development: These phases are:

1. ***The preliminary phase (2013 - 2016)***: during this phase the ELI-Beamline facility will be realised and no laser-driven beam will be available. In this period all the aspects will be analyzed and the first prototype of beam transport and selection systems, detectors and dosimetry will be designed and realized. Preliminary experimental runs with the realized devices will be performed in facilities where laser-driven ions beams are already available even if at lower energies.

Figure 3.1: Graphical overview of the ELI-Beamlines facility. The Exp hall 6 is the one dedicated to the ELIMED project

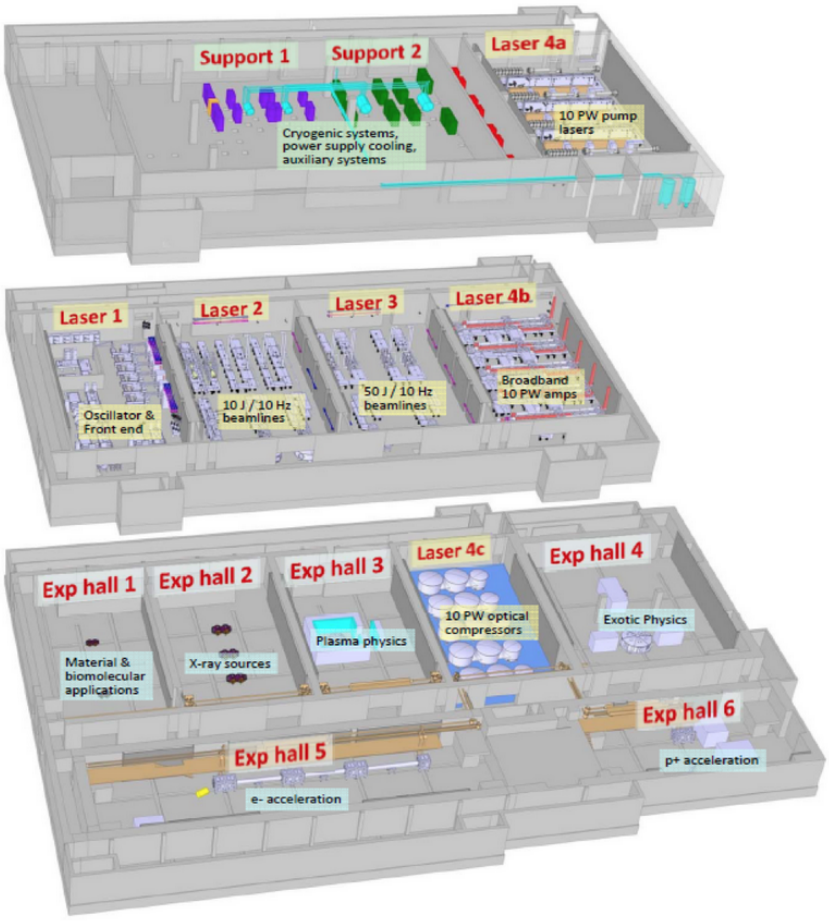

2. ***Phase 1 (2016-2017)***: first laser shots will be available and protons in the 20-30 MeV energy range are expected. The energy selection system would be installed and the first dosimetric studies and cell irradiation could be performed.

3. ***Phase 2 (2017-2019)***: 60 - 200 MeV proton beams are expected after the target. The final configuration of the in-air hadrontherapy transport beam line would be assembled and tested. Final dosimetric characterisation and radiobiological tests would be performed.

4. ***Phase 3 (starting since 2020)***: proton beams with a maximum energy of 1 GeV are expected.

In Table 3.1 the laser system and produced ion beams characteristics we expect at the various ELIMED phases are summarized. In the same Table the estimation of the expected beam characteristics after the energy selection system and dose evaluation at the irradiation point are presented.

Table 3.1: Laser and and laser-driven beams expected at the ELIMED facility in the various phases.

	Phase 1	**Phase 2**	**Phase 3**
Focused intensity $[W/cm^2]$	$10^{19} - 5 \cdot 10^{21}$	$5 \cdot 10^{19} - 10^{23}$	$5 \cdot 10^{19} - 10^{23}$
Energy range [MeV]	20 - 30	60 - 200	100 - 1000
No particle per shot	$10^{9} - 10^{10}$	$10^{10} - 10^{11}$	$10^{11} - 10^{12}$
Bunch duration [nsec]	1	0.1 - 1	< 0.1
Protons per pulse after the beam transport	$5 \cdot 10^{8} - 5 \cdot 10^{10}$	$5 \cdot 10^{9} - 5 \cdot 10^{10}$	$\sim 10^{11}$
Energy spread	$\pm 5\%$	$\pm 5\%$	not still defined
Proton dose per shot to the cells	0.1 - 1 Gy	0.06 - 0.6 Gy	$\sim$ 7 Gy per shot

4 RELEVANCE OF THE PROJECT WITH RESPECT TO THE INFN MISSION AND THE STATE OF THE ART OF THE PROPOSED RESEARCH

The scientific interest of INFN for hadrontherapy and all the related topics is evident. INFN, that is leader in research and development of accelerator machines, has funded in the last twenty years various initiatives related to hadronterapy. INFN supported and realized the first Italian proton therapy center at the LNS Laboratory in Catania that is still active and have

treated more than 300 patients up to now. Starting from 2004 the INFN signed an agreement with the CNAO foundation to actively participate in the realisation of the first Hospital-based Italian hadrontherapy center. The relevance of hadrontherapy and related topics for INFN is also widely declared inside the INFN triennial scientific plan (years 2012 - 2014) [1]. In the same document the study, design and realisation of a therapy beam line for the laser-driven beams is expressly reported as one of the LNS milestones for the period 2012 - 2014. In our opinion is hence evident that the scientific activity we are proposing, perfectly fits with the scientific INFN mission.
Nowadays the international panorama saws the German OncoRay (http://www.oncoray.de/) and Light (http://nnp.physik.uni-frankfurt.de/Light/) projects and the PMRC (Photo Medical Research Center) activity in Japan (even if for the last one, financial support from the Japan government have been momentarily stopped). These three initiatives are strongly working onto the topics related with the future use of the laser-driven protons for therapy purposes and they express, together with the ELIMED project, the status of the art in this field.

5 Project aim and implementation

The activity of the INFN ELIMED project will be entirely focused on the development of innovative instrumentation, technologies and dosimetric methodologies pointed to the development of a beam line for dosimetric and radiobiological studies based on laser-driven beams with energy of interest in hadrontherapy. The project will closely follow the activities of the ELIMED project that will accomplish, within 2017, the first beam line for therapy studies using laser-driven beams accelerated up to 30 MeV at the ELI-Beamlines laser facility in Prague (CZ). One of the main goal of the project will be the realization of a first prototype of energy selector for laser-driven proton beams and the necessary diagnostic systems in order to perform the first dosimetric and radiobiological measurements at three different laser facilities: the TARANIS laser facility in Belfast (UK), the GIST in Korea, the LULI in France and FLAME laser in Frascati (IT). Evidently, one of the intrinsic characteristics of the ELIMED project is its multidisciplinary approach. The realisation of a transport beam line for hadrontherapy studies based on laser-driven beams, in fact, requires many different competences. People with knowledge of targets design and realisation, of plasma characterisation, of the emitted radiation diagnostic from the target, of the selection and transport of the produced charged beam as well as of the dosimetric, radiobiological and beam formation for hadrontherapy, will be involved simultaneously. In the same way, people skilled in the simulation of high power lasers interaction with the matter using realistic Particle In Cell (PIC) codes, are necessary. In the preliminary phases in fact, the theoretical knowledge of the produced radiation from the

targets (in terms of energy, fluence and momentum distributions) will be of topical importance. It will firstly give us the possibility to evaluate the performances of systems and detectors we are planning to experimentally test with laser-driven beams. Secondly, it will give us the possibility to simulate the whole beam line from the target, through the selection system and up to the dosimetry and biologic irradiation point.

We are organizing our proposal in such a way that all these different aspects can be considered and sufficiently and coherently investigated. In order to achieve this objective, researchers with competences in the different involved areas have been joined together to form a complete team having the same scientific goal. The ELIMED scientific proposal have been divided in three Working Packages (WP), each of them dedicated to a specific research aspect of interest for the project. Each WP has its main responsible and it is in turn divided in smaller sub-WPs. The WP-1 is dedicated to all the aspects related to the target, to the development of PIC simulations and to the beam handling (the energy selection and all the transport beam line). The WP-2 is fully related to the diagnostic of the produced radiation and charged particles. Finally the WP-3 will investigate, also by Monte Carlo simulations, all the problematics related to the development and test of new dosimetric systems, to the design of the in-air transport proton beam line, to the absolute and relative dosimetry issues and to the radiobiological tests.
Figure 5.1 shows the ELIMED transport beam line as it is designed at the moment.

Figure 5.1: Schematic layout of the ELIMED final beam line as it will be implemented at the ELI-Beamlines in Prague. The scientific activity we are proposing is divided in three parts corresponding to different section of the beam line and to a well defined Working Package.

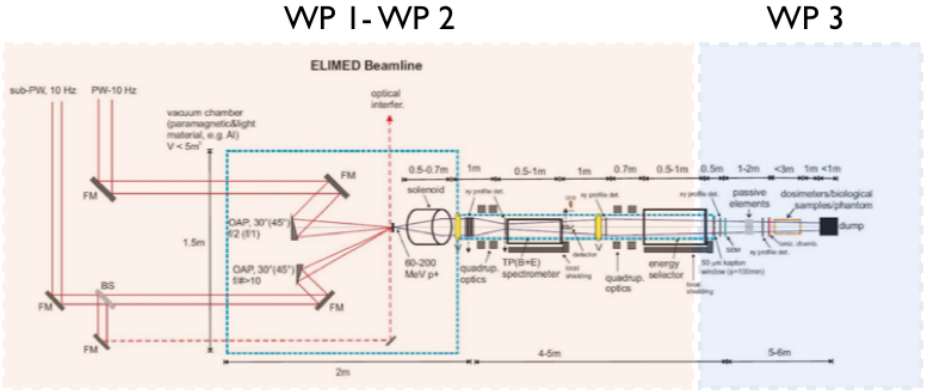

In order to rigorously define our research activity timeline, we assigned to each WP a set of well defined and detailed milestones. These will be discussed with more details in the paragraph Milestones and temporal plan. We estimated that the project activity can be completed in three years, with our actual Full Time Equivalent manpower that is about 38.6.

6 PARTICIPATION OF EXTERNAL AGENCIES CONTRIBUTING TO THE PROJECT FUNDS

The project will be financially supported by the FZU AS CR in Prague that will contribute with 1-2 PhD, 1 three-years post-doc to work on the energy selection system and on the preparation of the Belfast experimental run and, finally, into travel expenses for the part of the people that will perform the planned experimental runs at PALS (Prague), TARANIS (Belfast), GIST (Korea) and FLAME (Italy) laser facilities. At the time in which we are writing, a five-months contract for a technical designer and one half of the travel expenses for a preliminary experimental measure at PALS have been already provided by FZU. The post-doc public announcement has been provided and the deadline fixed for July the 2nd, 2012. We expect to start the contract on September 2012. Support will be also provided for the 2013 experimental run at PALS (already assigned) where travel expenses will be covered for four participants and for the full experiment duration (three weeks).
One will be the Queen's University in Belfast that already gave the full disposal in providing us a set of experimental shifts with the TARANIS laser system there installed. At the same time they will provide us also the full technical support. The disposal of the Queen's University is documented with a letter attached to this proposal. In the same way we will have the access to the PALS femtosecond laser system for the final test of the improved Thomson Spectrometer. Additional contributes will be provided by the Drugs Department of Catania University that will support the radiobiological measurements making at their laboratories available for cells culture and analysis as well as their scientific expertise. Based on more than a decade long collaboration and experience in irradiations with protons and carbon ions of biological samples at LNS, group of researchers (nuclear physicists and molecular biologists) from the Vinca Institute of Nuclear Sciences, University of Belgrade, will give their contribute in the field of radiobiology.

7 PROJECT WORKING PLAN

ELIMED scientific activity is organised in Working Packages (WPs). Each WP corresponds to a well defined research activity in turn connected with those will be performed at ELI-Beamlines.

WP-1: Target, PIC simulations, Beam Handling

WP Responsible: Dr. D. Giove

- WP - 1.1: Targets development and optimisation for proton productions.
- WP - 1.2: Quantitative evaluation of accelerated particles using Particle In Cell (PIC)

simulations.

- WP - 1.3: Innovative energy selection and beam transport systems to transform the laser generated mixed beam in a clinical one.

WP-2: Diagnostics

WP Responsible: Dr. L. Labate

- WP - 2.1: X-ray diagnostics of Laser plasmas: Energy-Dispersive X-ray Spectroscopy, High Resolution X-ray Spectroscopy and 2D space-resolved X-ray Imaging.
- WP - 2.2: Optical and UV imaging and spectroscopy.
- WP - 2.3: Charged beams diagnostic: upgrading of INFN Thomson spectrometer for the diagnostic of charged beams up to 100 AMeV; CR39, SIC, Synthetic Mono-crystal Diamond Detector, Ion Collector (IC) and Ion Collector Ring (ICR); electron detectors.

WP-3: Hadrontherapy transport, dosimetry and radiobiology

WP Responsible: Dr. F. Romano & L. Manti

- WP - 3.1: Monte Carlo simulations of transport beam line and related radioprotection evaluations.
- WP - 3.2: Development of innovative systems for in-air diagnostic of accelerated particles and fluence measurements for absolute and relative dosimetry.
- WP - 3.3: Radiobiology studies and measurements.

Table 7.1 shows the scientific organisation of the proposal with the three research areas, the sub-working packages, the responsible and involved people. It has to be also underlined that the general layout of the ELIMED transport beam line, as it will appear at ELI-Beamlines in Prague, is already defined and divided into three different sections (Figure 5.1).

8 Link with other research Institutions and groups, research impact also respect the Horizon2020 program

The European ELIMED project prefigures multidisciplinary actions and, therefore, it implies the involvement of research groups belonging to different areas and different national and international institutions. The hardware implementation of innovative transport elements and

Table 7.1: Working packages, responsibilities and involved sections of the ELIMED project.

Working package and corresponding scientific activity	**Responsible**	**Involved sections**
WP-1: Target, PIC simulations, Beam Handling	Dr D Giove	INFN-MI (D Giove), INFN-CT, Section of Messina (A Italiano), INFN-LNS (L Torrisi, GAP Cirrone), INFN-LE (V Nassisi), INFN-BO (A Bazzani), INFN-LNL (M Maggiore), INFN-RM1 (P Antici)
WP-2. Diagnostics	Dr L Labate	INFN-LNS (L Torrisi, GAP Cirrone), INFN-MI (D Giove), INFN-CT, Section of Messina (A Italiano), INFN-RM1 (P Antici), INFN-PI
WP-3. Hadrontherapy transport, dosimetry and radiobiology	Dr F. Romano & Dr L. Manti	INFN-LNS (L Torrisi, GAP Cirrone), INFN-NA (L Manti), INFN-RM1 (P Antici), INFN-BO (A Bazzani), INFN-LE (V Nassisi), INFN-TO

dosimetric systems, the development of Monte Carlo applications for transport and treatment planning, and finally the testing of the whole apparatus and cells irradiation with the laser-driven proton beams must be accompanied by a close and fruitful collaboration of each WPs with other research institutions, that have already expressed interest and will contribute to different part of the project. In particular a huge part of the proposed experimental activity is planned to be accomplished in three different top-level laser facility where laser driven proton beams can be already produced (see the section 14). One is the facility hosted at the Queen's University of Belfast (UK), where the TARANIS laser system is available . The second one is the PALS facility, hosted by the FZU Academy of Science in Prague (CZ), where two different lasers are installed. Finally we will have the possibility to use the laser installed at the Korean GIST facility and at the French LULI facility. The listed facility are strongly linked inside the ELIMED collaboration. Of course, we strongly hope in the future availability of proton beams at the Italian FLAME facility. Part of measurement campaigns (Thomson spectrometer calibration, preliminary tests of the energy selector, characterization of the dosimetric systems), at least in the preliminary phase of the project, will be carried out at the CATANA facility (Hadrontherapy Centre and Advanced Nuclear Applications) at LNS-INFN in Catania. CATANA, which is a centre with a direct INFN involvement (one of the research units of the project), was the first proton centre in Italy, born from the collaboration among the Department of Physics, the Institute of Ophthalmology and Radiology of the University of Catania and INFN. The centre, specialized in the treatment of ocular melanomas with 62 MeV proton beams, provides a clinical proton beam, characterized in all its specific spatial, temporal and energy features. Access to this facility will allow characterization of the various hardware components that will constitute the ELIMED apparatus, as well as the check of the diagnostic and dosimetric systems.

As it appears evident reading this proposal, the role of the Geant4 Monte Carlo simulation tool is crucial in different aspects of the project. The scientific activity of the WP-3.1 is, indeed, based on the Geant4 simulations, which have an important role in the ELIMED project both for the beam line design and for the dose/fluence distributions foreseen in the planned experiments. Moreover, in a second phase, also radio protection assessments will be carried out by mean of Monte Carlo simulations. Some components of the ELIMED project are official members of the Geant4 International collaboration and actively contribute to its development. They have the opportunity to directly interact with other members of the international collaboration, through meetings with the heads of the various "working groups" related to the specific areas of development. Geant4 collaboration is composed by more than 100 researchers who constantly update and verify its components. It was born thanks to a Memorandum of Understanding (MoU) between all the institutions involved in

the development and maintenance of the toolkit: CERN, ESA, KEK, SLAC, Triump, LEBEDV, LPNHE, ATLAS, BaBar, CMS, LHCb and INFN. Despite Geant4 has been designed at first for high energy physics, in recent years a huge activity has been undertaken concerning other fields of application, especially in medical physics. Many participants at the proposed ELIMED project are involved in the development of Geant4 applications related to the medical physics field. In particular they are strongly involved in the study of issues related to hadrontherapy, in the simulation of transport beam line for the therapy and in the development of algorithms for the evaluation of dose, LET (Linear Energy Transfer) and RBE (Relative Biological Effectiveness) distributions into biological material.

One of the main goals of the ELIMED project will be to improve as much as possible the international collaborations described above. This would permit to broaden the skills of the scientific community working in this field. In this last aspect we can find a clear link with one of the main goals of Horizon 2020 (Scientific excellence): the expansion and consolidation of excellence, in order to make European research and innovation more competitive. The proposed project would allow, in particular, the consolidation of partnerships between experts on the particles production and acceleration by lasers, on Geant4 applications development, on beam transport and on medical physics.

Finally, it should be stressed that the work toward the realization of the first hadrontherapy facility based on laser-driven beam (that will be the final goal after the preparatory phase of the next three years) could significantly improve the access of the future hadrontherapy treatments. Indeed, one of the main aspect which are boosting such a kind of application is represented by a relevant cost reduction and compactness which should characterize the future commercial lasers respect to the current hadrontherapy centre. If this two points were demonstrated in the next years, hadrontherapy could become a routinely treatment procedure of easy access, as can be considered today the photon radiation therapy. According to that, laser driven acceleration could represent an important step forward in the fight against cancer, which is one of the main causes of disability, early death and poor health conditions. Technological progresses in this direction certainly falls under the first goal of another priority of the Horizon 2020, that is, "Societal Challenges: health and demographic change".

9 Risk assessment of the proposed activity

A multi-disciplinary project, as ELIMED is going to be configured, is based by definition on the mutual interaction of different competencies and skills in order to fulfil specific goals. Therefore, in these cases, milestones are strictly related to each other and the attainment of a comprehensive objective depends on the fulfilment of the cross-related deliverables

scheduled in the time plan. For such a kind of projects a risk assessment is necessary in order to preliminarily evaluate the key phases of the project and foresee the potential effect on the project time schedule. These assessments allow to plan in time the different strategies and the alternative solutions which should be followed to fulfil a specific milestone also in case a probable event risk takes place. Good rule is also to relate each risk assessment with a specific level of probability. The following Table summarizes risk assessments of each sub-WP, the effect on the project and the potential actions to be undertaken to overcome the issue with a minor impact in terms of time delay, cost increasing and lack of commitment:

Table 9.1: Risk assessments for the specific subWP: L = low, M = medium, H = high.

Owner	Risk	Probability	Impact	Effect of Project	If it happens: Actions
WP1.1	Difficult on optimization of thin nanostructered targets.	L	M	Changing in planned targets type to be used and, eventually, in the related diagnostic system.	Investigate other methods of optimizations. Identify alternative possibility of development (Prague group).
WP1.3	Technical issues in the realization of the energy selector according to the specific requirements.	L	H	Lack of commitment. Strong change in strategy. Closure of WP3 activity. Cost increasing.	Inform coordinator of WP3 and national responsible for the quick decisions. Commitment of an alternative system to an external farm.
WP2.1	Not clear assessments about plasma characterization coming from X-spectroscopy.	M	M	Change in strategy.	Change of the diagnostic method with an alternative one (Optical spectroscopy).
WP2.2	Not clear assessments about plasma characterization coming from the use of a VIS and UV ICCD.	M	M	Change in strategy.	Change of the diagnostic method with an alternative one (X-ray spectroscopy).
WP2.3	Issues for the upgrading of the Thomson spectrometer for the required energies.	L	M	Cost-increasing. Time delay.	Replacement of the spectrometer with a new one. Change of the measurements schedule.
WP3.1	Not reasonable results of Monte Carlo simulations	L	M	Change in strategy. Time delay.	Change of the Monte Carlo code used. Alternative analytical simulation for faster preliminary assessments.
WP3.2	Lack of accurate information on particle fluence detected by the innovative monitor system.	M	M	Failure to complete key task (dosimetry, radiobiology).	Investigate alternative system for proton fluence measurement: thin transmission foil or transmission ionization chambers (correction of saturation effects).
WP3.2	Big systematic errors in absolute dosimetry.	M	H	Failure to complete key task (radiobiology). Time delay. Change in strategy.	Investigate alternative detectors for dosimetry: calorimetry, TLD. Plan additional measurement campaign for further tests.
WP3.3	Not reasonable results for cellular response.	M	M	Time delay. Cost increasing.	Review of the considered assays in order to find coherent intercomparisons and/or new kind of response investigations. Increasing statics, if necessary.
WP1 WP2 WP3	Belfast TARANIS laser facility not available.	L	H	Time delay. Cost increasing.	Move to FLAME and/or Korea GIST laser facility or other laser facility.
WP1 WP2 WP3	FLAME laser facility not available.	M	M	Lack of some commitments.	Move to Korea GIST laser facility or other laser facility.

10 PHYSICS BACKGROUND:

PARTICLE PRODUCTION AND ACCELERATION BY HIGH POWER LASERS

The investigation of fast ions emission from laser-plasma interaction is crucial for future applications of laser -accelerated ion beams in different areas, such as warm dense matter generation, probing of high electric and magnetic fields, probing of very dense matter, nuclear applications (compact neutron source, isotope production, fission reactions), medicine, astrophysics laboratory, new accelerator generation, etc..

The ion acceleration is due to the interaction of a high power (intensity $I > 10^8\ W/cm^2$) and sub-nanosecond pulse laser with solid target. The key in reaching such high powers is the chirped pulse amplification (CPA) technique, developed for radar devices more than 40 years ago. In the CPA scheme a pulse produced by a low power laser ables to create a really short packet ($\sim 50\ fs$) is first stretched in time (chirped in frequency) by a factor $\sim 10^4$, then amplified and finally recompressed. In CPA process not only an ultra-short high-intensity main pulse is produced, but also a weaker pedestal, or pre-pulse, due to the amplified part of the pulse that is not compressed again. The pedestal plays an important role in ions acceleration in fact even if its intensity is several order of magnitude smaller than the main pulse, it is enough to create a plasma [148, 149]. The electrons escaping from nuclei will acquire a kinetic energy greater than their rest mass, thus they become highly relativistic. In this context a useful parameter is the so called $laser\ strength\ parameter$, defined as:

$$a_0 = \frac{eA}{m_e c^2} \tag{10.1}$$

namely it is the peak value of the laser potential vector normalized with respect to the electron rest mass. It can be related to the peak intensity, I_0, and the wavelength, λL, of the laser by:

$$a_0 = \frac{e}{m_e c^2}\sqrt{I\lambda\frac{2}{\pi c}} \tag{10.2}$$

Thus, a_0 can be seen as the maximum momentum of an electron quivering in the laser field, normalized with respect to its rest mass, and the previous relation shows that relativistic regime is reached for laser intensity $I > 10^{18}\ W/cm^2$.

When an electromagnetic wave with optical or near infrared frequency ω is focused on a gas, the produced plasma has an electron density n_e less than critical density $n_c = me\omega^2/4\pi e^2$. Hence the plasma is called $underdense$ and the wave can propagate through it. This scenario allows electrons acceleration in the so called $Laser\ Wake-Field\ Acceleration$ regime.

Interaction with a solid target is radically different, in fact the electromagnetic wave promptly

ionizes the target forming an overdense plasma with $n_e > n_c$. The laser pulse can only penetrate in the skin layer $l_{sd} = c/\omega_p = (\lambda/2\pi)\sqrt{n_c/n_e}$ and the interaction is a surface interaction. In the interaction, part of laser light is reflected but a significant fraction of laser energy may be absorbed by the target.

For short laser pulses with relativistic intensity, plasma temperature rises very fast and the collisions in the plasma can be considered ineffective during the interaction. In this situation, different collisionless absorption mechanisms can arise, such as $resonance\ absorption$, $\mathbf{J}\wedge\mathbf{B}\ heating$, $vacuum\ heating$ [150, 151]. In any case the absorbed energy will result in the heating of electrons fraction at temperature much higher than the initial bulk temperature. Laser energy absorption by electrons is a crucial phenomenon in ion acceleration. If normal incidence is considered, the ponderomotive force pushes inward the electrons from the rear surface of the target creating a charge separation which produces an electrostatic field experienced by ions. The first experiments exploiting the interaction of short ($\tau < 1\ ps$) and intense ($I\lambda^2 > 10^{18}\ W/cm^2$) laser pulses with thin solid foils, showed the production of proton beams in the range of several tens of MeV coming from the rear surface of the target.
In most experiments the dominant regime is the so called **Target Normal Sheath Acceleration** ($TNSA$) in which the accelerated protons come from the rear surface of the target and the accelerating field is due to the expansion of heated electrons around the target. In the interaction of an intense electromagnetic wave with a solid, the front surface of the target becomes ionized well ahead the pulse peak. The successive laser-plasma interaction heats the electrons via different absorption mechanism to high temperature ($T \simeq MeV$) and their free path becomes bigger than the plasma skin depth and than the target thickness. These hot electrons have a diffusive motion both in the laser direction and in the opposite one. Thus, they can propagate in the target reaching its rear surface where they expand into vacuum for several Debye lengths forming a cloud of relativistic electrons. The charge imbalance due to the cloud gives rise to an extremely intense ($TVolts/m$) longitudinal electric field, which is responsible for the efficient ion acceleration. The most effective acceleration mechanism takes place at the rear surface of the target where the high intensity electrostatic field can ionize the atoms present on the unperturbed surface and then accelerates the produced ions. The accelerated multi-MeV protons from the rear surface of the irradiated solid foil is achieved no matter its composition, because they come from the hydrogen rich contaminants present on the target surface, such as hydrocarbons or water vapor. The energy spectrum of the protons is typically exponential with a high cut-off in the range of tens MeV. Several theoretical models have been proposed in order to describe the TNSA regime, but the most efficient in predicting the energy cut-off and that gives also a good interpretation of the acceleration mechanism is the one proposed by Passoni at al. [152], despite the strong assumptions. A representation of

the electron expansion and ion acceleration from the rear surface of the target in TNSA regime is proposed in figure 10.1.

When laser intensities exceed $I = 10^{21}\ W/cm^2$, different regimes can be achieved. In these conditions the radiation pressure of the laser dominates on the heating process and the accelerated bunch is composed by ions coming from the irradiated surface of the target. These regimes are called $Radiation\ Pressure\ Acceleration$ (RPA) and the accelerating mechanism depends on the target thickness [153]. The bunches produced exhibit a remarkable collimation and a high energy cut-off; the maximum energy record of 58 MeV has not been beaten yet. On the other hand there have been significant improvement in the control of the beam quality and energy spectra which give the possibility to start feasibility studies on tumor therapy with laser-accelerated ions. Anyway, several studies are still required on the transport of the optically accelerated beams in order to delivery ions with suitable characteristics for clinical applications.

Within the ELIMED collaboration some experimental activities have been already performed

Figure 10.1: Schematic rapresentation of TNSA regime.

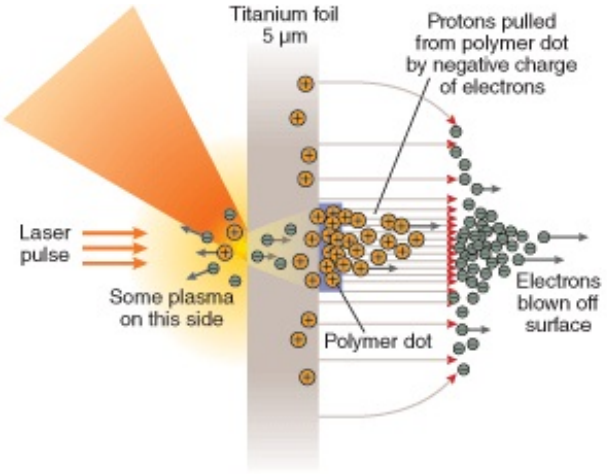

or scheduled at Prague PALS laboratory using the ion beams accelerated by the long pulse (400 ps), medium power (2 TW) infrared ASTERIX IV laser system.

Recently, the production of ions emitted with energy of few $AMeV$ and current densities of few A/cm^2 by the use of the sub-nanosecond, kJ-class lasers in the TNSA regime [6] has been proved [2, 3, 4, 5]. The dependence of ion maximum energy and current on the laser intensity have been investigated and apparently explained. Various parameters involved in laser-plasma ion acceleration mechanisms have been recognized in the last decade, however, the most of them have been investigated only partially and not fully explained. There are some

reasons responsible for this situation which are related to some difficulties in the diagnostic techniques applied in the PALS measurements. It is evident that additional investigation are necessary to obtain more detailed characterisation of ion emission (measurement of angular distributions, individual ions intensity, dependence of ion emission on the type and structure of targets, etc.) and to find threshold conditions at which the mentioned nonlinear effects are starting to develop [7, 8]. The dependence of many plasma parameters (temperature, densities, gradients, electric fields, ion and charge state distributions,...) on the $(laser\ intensity) * (wavelength)^2$ (or $I \cdot \lambda^2$) factor permits to derive that the ion acceleration increases with the laser intensity (Figure 10.2). High energy laser pulses (1-1000 J) and short laser pulses (ps and fs lasers) may produce intense charge separation effects in plasma and develop high electric fields, inducting above $10 AMeV$ ions acceleration [9]. Many international laboratories are accelerating protons in the range of 10-50 MeV, exploiting the TNSA regime for laser intensity of the order of $10^{20} W/cm^2$ (laser facility Vulcan, Luli, Ral PW, Nova PW,...) [10].

Figure 10.2: Experimental data collection showing the scaling law ($I \cdot \lambda^2$ factor) for ion acceleration.

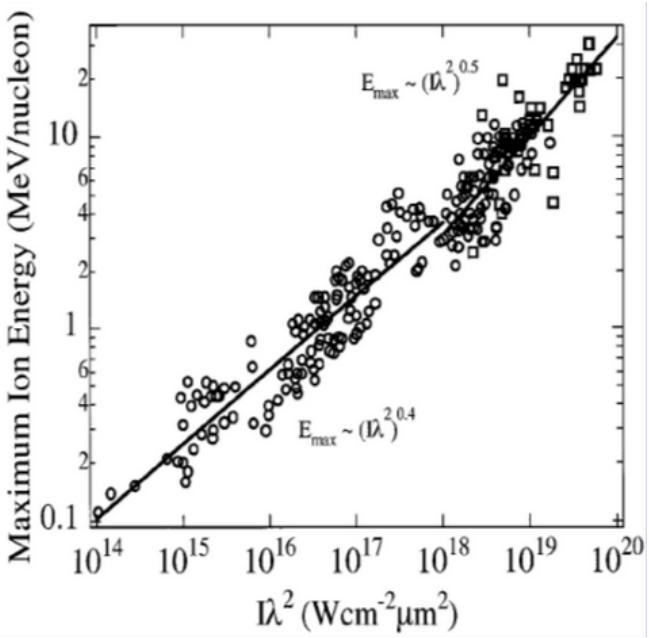

11 DETAILED ACTIVITY OF THE WP-1

11.1 WP-1.1: TARGETS DEVELOPMENT AND OPTIMISATION FOR PROTON PRODUCTION

Although tremendous fundamental research and development on laser-driven proton and ion sources have been performed, still a lot of long-term effort is required for the implementation of laser-driven medical accelerators.

Firstly, the development of a compact, low-cost, energy efficient, stable, ultra-high-intensity and ultra-short pulse laser with a repetition rate of at least 10 Hz. For this purpose, solid-state laser technology is one of the promising candidates.

Secondly, the design and construction of the laser transport line is an issue that includes not only a flexible laser beam pointing but also different techniques to keep the quality of the laser wavefront. Thirdly, the proton acceleration mechanism should be chosen and the target conditions optimized in order to obtain the beam energy, spectrum and divergence which match well the desired application requirements, otherwise the rejected unwanted parts of the spectrum and/or angular distribution can cause significant activation when it is stopped by shields. Ideally, a monochromatic or spectrally tailored low-divergence ion/proton beam produced in the laser-driven plasma itself is desired.

Fourthly, target production and placement may become a limiting factor in future high rep rate experiments. Accurate insertion/injection of targets is a significant challenge and the solutions are intimately related to microtarget design and production. Also insertion mechanisms introduce further experimental complexity (and possibly extra characterization). The source development activities will be focused on the study of the processes involved in the design, construction and alignment of specific targets. We plan to develop specifically designed target holders (to deal with nanometer thickness targets) and optically based alignment tools and to study what is the best targetry for different lasers in term of energies/particle yields and stability of the output beams. Current experiments involved gasjet targets, solid targets etc. First estimations of a proton yield have already been made and should help establishing the efficiency of the laser-driven beamline. In particular, we plan to implement an high-repetition cryogenic targetry systems produced by J-P Perin (CEA/INAC/Service des Basses Temperatures) which has been already installed for the LMJ.

The group of J-P Perin (CEA/INAC/Service des Basses Temperatures) is currently developing a high-precision alignment system for LMJ on a Òsingle shotÓ basis.

They are currently developing a new cryostat system able to produce a continuos 25 μm H_2 solid foil, the thickness will be reduced as soon as they manage to implement this kind of high accuracy. This system will be in operation at the end of 2013.

The ELIMED group has at this moment 3 patents pending - extended to 4:

1. Self-supported thin foil of any gas h2, CO2,É
2. Double layer (1 to 5 microns of metal Au or Al with less than 1 micron to 5 microns of solid gas;
3. Double layer with less of 1 microns metal and solid gas (the thickness is free).

The main difficulties to design the cryostat are:

1. Definition of the rep-rate and how we increase it;
2. The pumping of experimental chamber (we have to maintain the vacuum at a level of 10-6 mbar);
3. Access for diagnostic;
4. The constraints of the experimental hall (cryogenic fluid, vibrations,ÉÉ).

The J-P Perin group propose for the positioning of the target to use a hexapod (Symetrie company) which has been developed for LMJ and it can work under vacuum, we can rent such device.
These activities will take as a reference laser facilities able to delivery laser beams with energies of at least 5J, contrast of the order of 10^9-10^{10}, pulse duration of the order of 100 fs, focal spot of the order of 20 micron (FWHM), intensity of the order of 10^{19} at least.
In particular, the experiments shall be carried out on 200 TW laser ALLS located at the INRS-EMT in Canada. This laser is an exact copy of the FLAME laser located in the Italian National Laboratory of Frascati (Italy) with the only (but important) difference that he contrast has enhanced and therefore higher proton energies are achievable. The laser delivers pulses of 5 J in 25-30 fs with a repetition rate of 10 Hz. The maximum on target intensity reaches 10^{20} W/cm^2. First results of laser-generated particles on this facility have been published recently [11], involving, besides Canadian and French groups, also the Roman Group belonging to the applicant. The ALLS laser represents currently (2013) the state of the art for so called Òtable-topÓ high-repetition rate lasers that are commercially available and therefore can be considered an ideal facility to perform these kind of experiments. Moreover, the facility has a dedicated laser-driven proton line about to be established and has offered beamtime for performing the required experiments. Additional experiments using other laser-facilities are planned, e.g. on the LULI laser that is a longer-pulse laser facility with similar on target intensity (30 J delivered in pulses of 300 fs with repetition rate of 10 Hz) and on the TITAN Laser (delivering 200 J in 1 ps). To both laser facilities one member of the ELIMED collaboration has received several times access.

11.1.1 TARGET PREPARATION

The data available in the specific literature show that, fixed laser parameters, the performance of the emitted protons will vary with respect to the following target parameters:

- target thickness;
- target materials;
- target composition;
- target geometry (lateral size and overall shape).

Thick and thin targets will be prepared in order to control the plasma composition, ion and electron density. In order to increase the concentration of protons, hydrogenate targets will be employed, such as polymers (polyethylene, polystyrene, polymethylmethacrylate, mylar,....), hydrates (titanium hydrate and other metallic hydrates) and metals with absorbent hydrogen (gold, titanium, etc.). In order to increase the electron density for each target heavy metallic elements will be added, such as gold, as embedded nanostructures, nanospheres or as deposited thin films.
Materials as thin diamond-like carbon (DLC) will also be investigated, they combine the advantages of high mechanical strength and high laser-induced damage threshold which make them less contrast-demanding. Target foils with thickness from 500 nm (self supporting) down to a few tens of nm are commercially available from specialized companies. Proton beams with energies up to 15 MeV have been reported from these kind of targets. The different targets will be prepared also taking into account the absorption coefficient of the laser wavelength. For this reason, special nano and microstructures will be embedded into polymers or deposited as thin films in multilayered structured foils. Carbon nanotubes and other nanostructures containing high hydrogen content will be employed to increase the absorption coefficient and the proton amount of the produced plasma. Proposed targets and foams will be employed to enhance the laser absorption and to decrease the reflection of the incident light so that the maximum laser pulse energy can be transferred to the plasma. A special attention will be dedicated to the preparation of thin foils, with a thickness below 10 microns, in order to be employed in experiments well described by TNSA approach that accelerate protons in forward direction. Different techniques, such as thin film deposition, sputtering deposition and spinning solution deposition, will be investigate to generate thin structured foils with thickness of the order of 1 micron. Resonant absorption effects will be also studied to generate non linear phenomena, for which p-polarized radiation can be absorbed at the critical density surface. Targets will be employed in different experiments in order to test their composition

and thickness to obtain the maximum proton acceleration, according the Fuchs experiments (Figure 11.1).

Figure 11.1: Maximum proton energy emitted by an Al target of different thickness

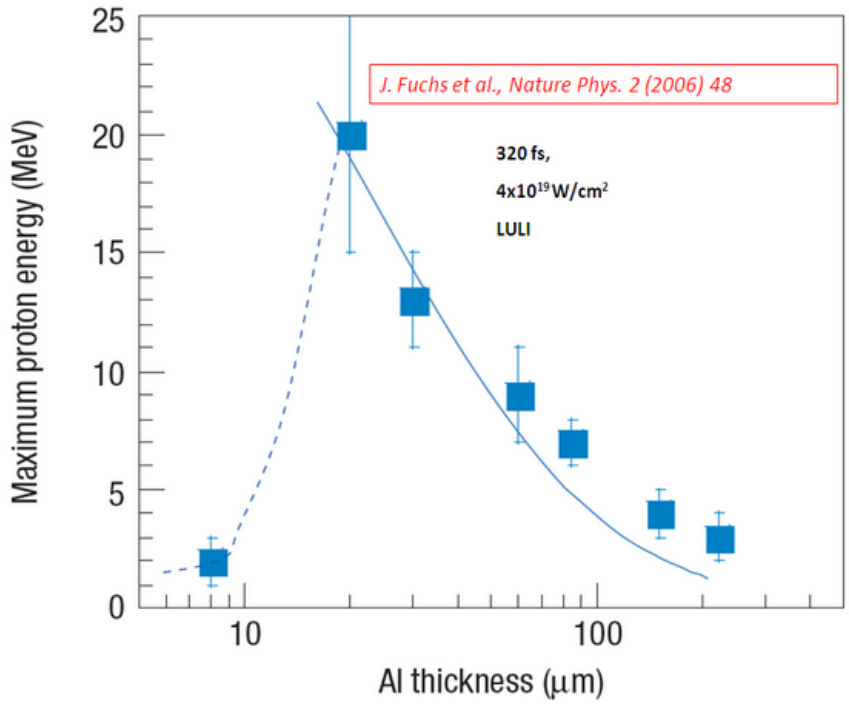

Target geometry is an other parameter that is undergoing deep analysis in different laboratories. The influences of the shape of the target and the effect of its size on proton energies and emission properties (angular extension,...) have been reported in different experiments. We would investigate different aspects of these phenomena. First of all we would try to experimental test the theoretical prediction related to the fact that a reduced surface leads to higher densities of hot electrons at the rear side of the target and, thus, to higher accelerating electric fields. On the other side we would try to design and machine flat-top cone targets, with apertures of the order of 100 microns and depth of the order of 30 microns. Using structures like these, the proton acceleration enhancement is attributed to the guiding and microfocusing of the laser pulse, larger absorption on the cone walls and preformed underdense plasma filling the inner volume, and better conditions of hot electron transport to the flat-top surface. The list of foreseen activities is quite ambitious and we have to face with different and difficult technological issues. For these reasons we propose to start 2014 research experimental

activities focusing on source development in term of target thickness and material and on the design and construction of dedicated laser spot qualification tools.

11.1.2 Laser diagnostic tools and Target Positioning

To qualify the behavior of the targets, so far discussed in literature, we need to have a deep knowledge of the main parameters of the laser beam and to be able to define and reproduce the exact positioning of the target with respect to the laser focus.
In a laser system it is common to observe fluctuations in the functional parameters. A precise control of shot to shot behavior is even more important in experiments where a single measurement cannot be repeated a number of times sufficiently high to authorize a statistical treatment. Nevertheless a strong correlation between the different parameters (energy, direction of the beam, contrast, etc.) is observed; this enables us to limit our observation of the laser status to some key parameters and be able to set a rejection criterion out of them.
The energy of the laser shots may be obtained from the knowledge of the energy before compression and then calculate the efficiency and the losses percentages in the compression processes.
The focusing of the laser may be measured imaging the focal spot. The focused beam is intercepted by a removable mirror and sent through a microscope objective to a linearized camera. The quality of the spot is defined by measuring its transverse size.
The Rayleigh range of a Gaussian laser beam as the ones we are interested range from 20-300 μm. This sets the scale of precision that is needed to align the target. Moreover, a precise absolute reference is important to ensure repeatability and meaningful comparison among different shots. The technique we would like to investigate is the collection of a part of the light that, from an Helium-Neon laser collinear to the main IR beam, is diffused by the rough target surface. A small lens images the helium-neon spot to a camera: the lens is aligned to provide a very big magnification ($\approx \times 20$), that is enough to map a range of 400 μm of movement in target focus to the entire chip of a CCD camera. A small aperture lens may work better, for its small level of detail produces a cleaner spot, which eases the reference. We estimate that the error on target positioning may be smaller than 15μm.

11.2 WP-1.2: Quantitative evaluation of accelerated particles using Particle In Cell (PIC) simulations

The laser acceleration of protons has reached a sufficient maturity in the TNSA regime. It is based on electrons heating and subsequent creation of an electrostatic field due to charge separation. The protons inherit a Maxwellian spectrum and consequently it is exponential in

energy with a cutoff proportional to the square root of intensity.

$$\frac{dN}{dE} = \frac{N_0}{E_0} \cdot e^{-\frac{E}{E_0}} \tag{11.1}$$

where E_0 is the average energy and N_0 is the total number of protons. The cutoff energy E_{max} is given by:

$$E_{max} \sim k \cdot a \tag{11.2}$$

with $a = 8.5 \cdot 10^{-10} \sqrt{I[W/cm^2]} \cdot \lambda[mm]$ and $k \sim 1-2$.

The average energy is typically 1/8 the cutoff energy. Since the energy transferred to protons is a $1-5\%$ of the laser energy, close to the cutoff energy the number of protons is very low. At one half the cutoff energy (4 times the average energy) the number of protons is appreciable. Also the target thickness affects the maximum energy, in fact there is an optimum thickness close to the induced transparency:

$$a = \pi \cdot \sigma \tag{11.3}$$

where

$$\sigma = \frac{nl}{n_c \lambda} \tag{11.4}$$

With a=30, obtained with a 250 TW lasers, the cutoff energy can reach 60 MeV and at 30 MeV the number of protons is more than 10^8. In order to have a similar intensity at 60 MeV the power must be increased to 1 PW. The optimal thickness is quite low (a few hundred nm) and such targets are difficult to deal with. As a consequence, targets with a few microns coating of a foam with $n \sim n_c$ on the illuminated side have been proposed. The simulations confirm that these improvements increase the energy transfer to protons and their cutoff energy up to a factor of two, but more investigation are needed to understand the relation between the target density, the incidence angle of the laser and its intensity for metallic target. Finally an interesting regime occurs for targets having quasi critical density of a $50-100\ \mu m$ thickness (2-3 times the laser pulse length). The laser drills a hole creating at the exit a magnetic vortex and an electrostatic field which efficiently accelerates protons. Simulations show that with a = 30 energies up to 100 MeV can be reached and this regime, known as MVA, is very robust unlikely the shock wave acceleration regime SWA. The full 3D simulations are carried out by Bologna researchers using the PIC code ALaDyn, its version for the GPU and the hybrid architectures Jasmine. The energy and spatial distributions obtained by simulations are suitable for the proton tracking along the transport line (collimators and focusing elements). Typically collimators and a high field solenoid can be used for focusing and energy selection.

The output beam will have small size (a few mm) and small emittance (a few mm-mrad, it will be also suitable for injection into a RF cavity (eventual post-acceleration with a linac). The choice of the targets is crucial and we believe that at present solid targets with thickness slightly below 1 mm (improved TNSA regime) or low density targets (gas or liquid H jets) with thickness near 0.1 mm (MVA regime) offer the best opportunities for proton particle to reach 30 MeV or 60 MeV with adequate intensity for a = 30 and a = 60, obtained with a laser power of 250 TW and 1 PW respectively. Extensive 3D computations are required to guide the experiments. Extending the simulation range from a few hundred μm to a few mm or even a few cm allows to deal with the complex space charge and charge neutralisation effects due to the comoving electrons. The use of thin foils can reduce their number by one order of magnitude but their presence in the transport line needs probably to be taken into account. The space charge effects during beam transport need to be taken into account even though their treatment is not straightforward due the large energy spread. Figures 11.2 and 11.3 show two example of proton spectra obtained with the ALaDyn simulation code under different target condition as detailed in the caption.

Other regimes like Coulomb explosion or RPA promise higher energies and lower energy spread. However they are not well consolidated experimentally and much research work and targets development needs still to be performed. In this framework the benchmarking between the two PIC code, Aladyn and Jasmine, about the an issue in the TNSA regime represents one of the main tasks, in addition to the comparison between the simulation outputs and the experimental results obtained by Ogura et al at KPSI (Nara) [12].

11.3 WP-1.3: Selection and beam transport systems to transform the laser generated mixed beam in a clinical one

11.3.1 Beam selection and transport

Charged particle beams produced with new techniques of acceleration by means of high power lasers have interesting features. For instance, they have a very high peak currents (10^{12} – 10^{13} particles per shot, $I > 500mA$) and rather small transverse and longitudinal emittance. Although the large angular width (up to $30deg$), the transverse emittance has pretty small radial dimension because of the small size of the laser spot interacting on the target ($\times 100\mu m$). The result is a geometric emittance smaller than $0.1\pi \cdot mm \cdot mrad$. The small longitudinal emittance depends on the very short temporal amplitude of the laser pulse ($< 1ps$). The energy spectrum of the produced particles varies from a minimum of energy of few keV to the maximum value derived from the electric fields reached during the process of plasma expansion at the beginning of laser-target interaction. Also the spatial distribution of the

Figure 11.2: Protons spectrum of a 3D simulation of a 0.5 μm solid target with a 2 μm foam layer at critical density for a=30 and a thin layer 0.05μm of contaminants. Average energy 7.4 MeV.

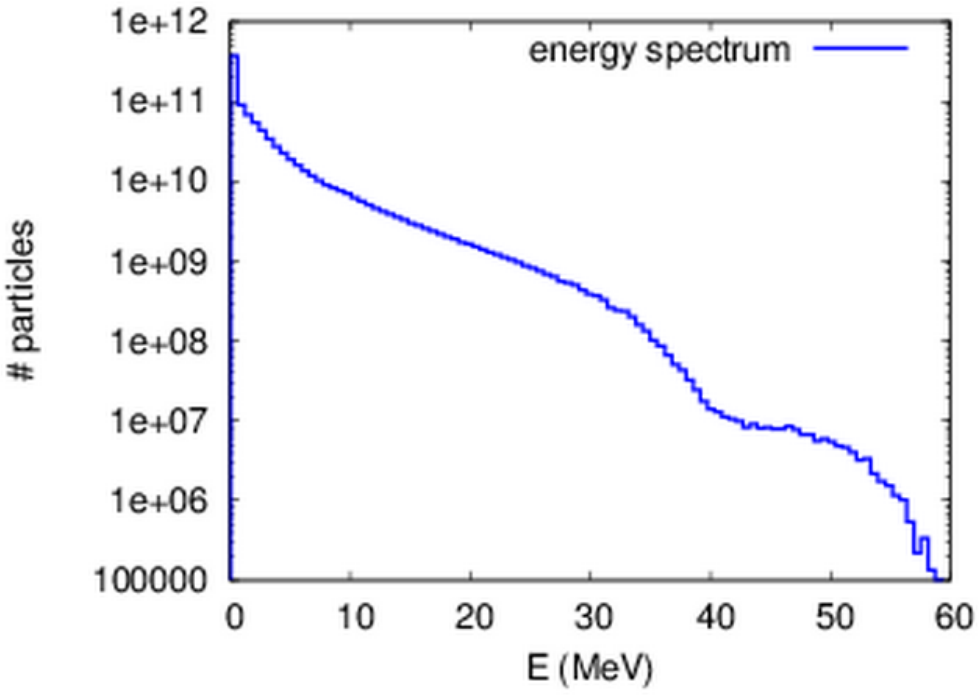

emitted particles depends on the energy as shown in Figure 11.4. In the view of using these beams for interdisciplinary applications [36] they must be characterized in energy and species and properly shaped so that they can be efficiently transferred to the measurement systems through standard beamlines used for particle transport. To do this, it is necessary to study the focusing techniques to maximize the number of particles transported and properly selected in energy and their relative spread [37]. In general, the pattern of focus and selection of the beams produced in the laser-plasma interaction is characterized by the following steps (see Figure 11.5):

1. **Initial Phase of Capturing and Collecting:** it occurs nearby the point of production of charged particles. It aims to collect as many particles as possible and to reduce the angular component of the transverse emittance. The device must be quite compact as it is necessary to place it inside the interaction chamber. This system provides the first coarse selection in beam energy. To do so, typically solenoid magnets are used, and

Figure 11.3: Protons spectrum for a target of critical density of thickness 40 μm with a pulse having a=25 and P=150 TW . Acceleration in the MVA regime.

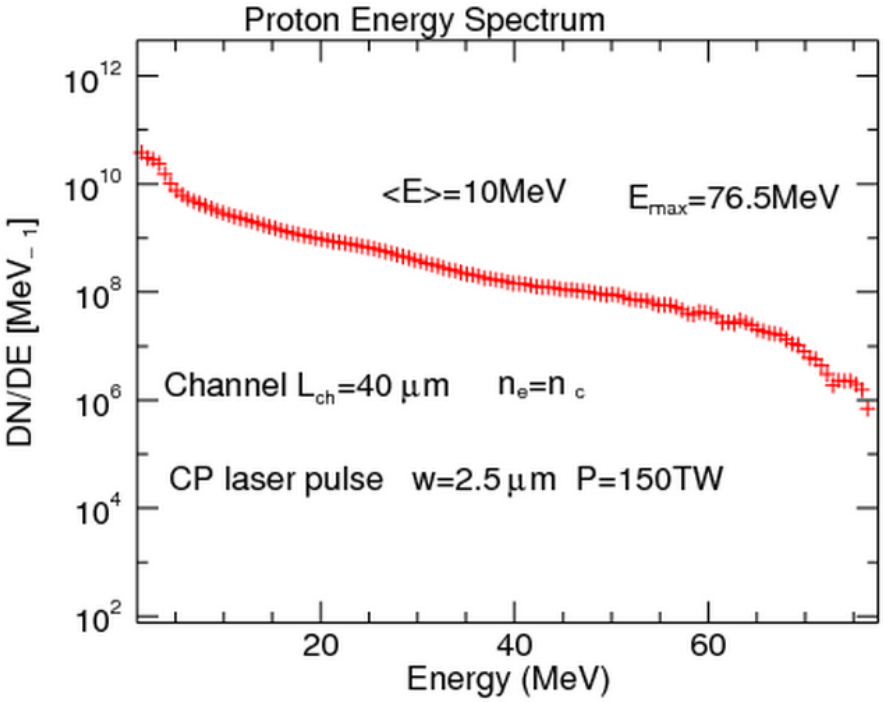

pulsed high magnetic field [38]. In this first step it is necessary to carry out the beam dynamics simulations in presence of space charge effects due to the high current, but also the effects of the de-neutralization, namely the dynamics of electrons component in high intensity magnetic fields.

2. **Secondary Focusing:** It is done by means of the focusing devices which are positioned at the exit from the interaction chamber with the function of focusing on the transverse direction the beam of pre-selected particles by the first phase of collecting. Since the system must be able to focus beams with different energies and with rather large transverse dimensions, it can be constituted by conventional electromagnetic or permanent based quadrupoles [39] with wide acceptance. The triplet configuration would ensure the focusing of particles in the two transverse space to a common point (waist). This would allow a subsequent focusing "point-to-point" of a possible conventional transport system. Also in this case a selection in energy by the above system is performed.

3. **Energy Selection and final beam characterization**: the beam at the end of the second

Figure 11.4: Plot showing the strong angular divergence related with particle energy for a typical laser-driven beam.

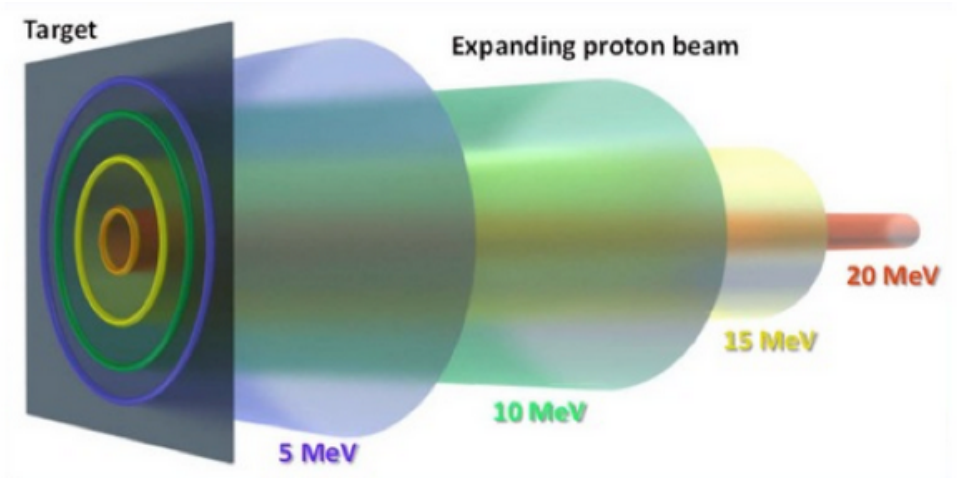

Figure 11.5: Steps into the pattern of focus and selection.

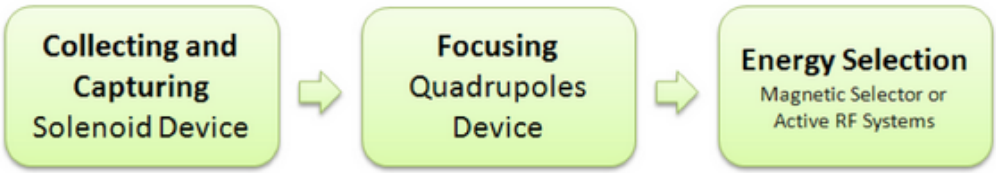

phase should have rather small energy spread and transverse dimension (the first two steps help to reduce the transverse emittance by suppressing part of the beam), then the longitudinal emittance is also reduced. A magnetic system (consisting of a dipole or a series of dipoles with alternating gradient) can be used for final selection [116]. If the energy spread is relatively small and the energy is not excessively high, an active bunching system can also be used [41] to further reduces the spread in energy, keeping the number of particles transported.

The design of a beamline suitable for transporting and attaining a useful proton beam with intensities of the order of 10^{10-12} particles/bunch, energy resolution of the order of 1-5%, and beam emittances of the order 5-6 π mm mrad is the main goal for the Elimed group activities. We will focus on two different configurations:

- proton energies from 5 to 10 MeV
- proton energies of 30 MeV

The first configuration will allow carrying out test and commissioning activities at TARANIS facility coupled with the ESS (Energy Selection System) accomplished by the collaboration during the 2013. The second configuration may be considered a first significant step toward the final application at the ELI-beamlines facility in Prague. Some of us have already published in 2013 a paper on the subject taking as a reference a scheme where we need to provide a laser induced emission proton beam with energy up to 30 MeV, to be injected in a high frequency RT linac. Other researchers of the ELIMED collaboration are developing an energy selection device based on moving permanent magnet elements. The purpose of our activities will be to merge these expertise and converge toward a complete design of a beamline to be coupled with a suitable source (see above activities) able to drive a proton beam of 30 MeV toward beam quality analysis stations.
We would focus on a design based on 'standard' accelerator focusing elements such as PQM (permanent quadrupole magnets) and solenoids. The most significant advantage of a solenoid magnet compared with quadrupole magnets is the high collection efficiency (almost 100%). At the same time a suitable RT solenoid needs a pulsed power supply synchronized with the laser trigger. A possible design that foreseen a superconducting solenoid HTS based will be investigated at least for the first configuration above discussed.
Solenoid based schemes are very challenging for the technological issues involved. Due to these considerations we propose to start an investigation on these possibilities, eventually carrying out a market survey with specialized companies. A first prototype of a pulsed RT solenoid along with a dedicated power supply (limited in power and repetition rate) will be evolved to take experimental data about its working conditions. At the end of the studies and of the survey we will have all the elements to take a decision about the possibility to develop a stable element.

11.3.2 Collecting and Focusing

In 2013, the study and design of the focusing system based on a triplet of permanent magnet quadrupoles was completed in collaboration with the staff of ELI-Beamlines project in Prague. This focusing system is very compact and versatile and it is possible to place it inside a interaction chamber immediately behind the target. Using this system, it is possible to focus beams up to 30 MeV on both transverse planes, allowing a better control on the beam shape. It is possible to vary the focal distance of the whole system triplet modifying the relative positions of three quadrupoles. This allows to focus particles with different energies at different points in order to maximize the transport of particles with a certain energy. The device designed and developed is shown in Fig. 11.6.

The system consists of three quadrupoles made with NdFeB permanent magnets (Fig. 11.7)

Figure 11.6: Different views of the device designed for overall support and move the triplet quadrupoles made with permanent magnets.

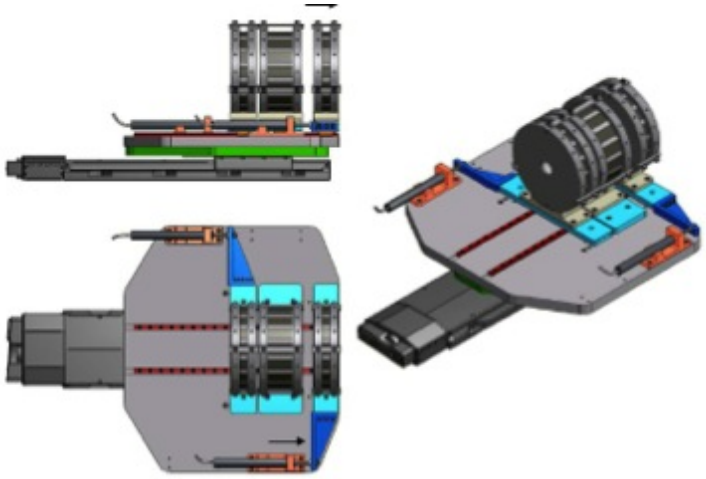

in Halbach configuration (16 sectors) ensuring high magnetic field inside the bore, which is rather large (Φ = 35 mm) for increasing the acceptance of the focusing system. The gradient field is about 70 T / m.

Figure 11.7: Drawing of the triplet quadrupoles in 16 sector Halbach configuration.

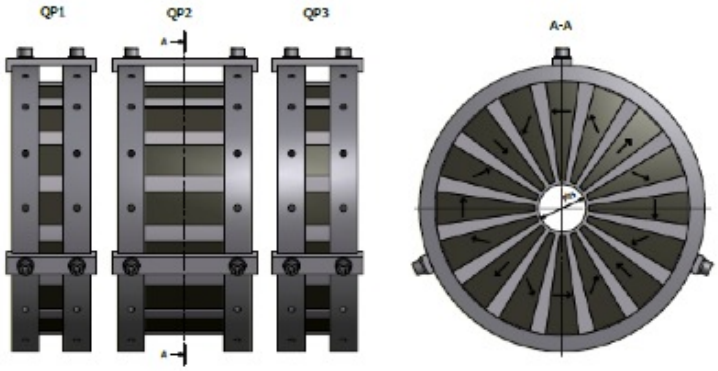

The three quadrupoles are placed on a guide with two linear actuators to change the relative distances among them. The whole system is set on a longitudinal movable plate which permits to change the distance of the entire triplet respect to the source. In this way the selection of the proton beams emitted with narrow divergence (typically particles with higher energy) in the most efficient way is possible. This system can be used also at the facility TARANIS in Belfast for increasing the transmission efficiency of the energy selector already tested at LNS. In fact, the initial testing of the selector provides the positioning of the latter directly inside

the scattering chamber and close to the target, in order to maximize the number of particles transmitted. In fact, due to the initial large divergence, some particles will be disperse during the crossing. To increase the transmission efficiency by a factor of 5, it is necessary that the beam has a minimum divergence as shown in fig. 11.8.

Figure 11.8: Effect on the beam dynamics inside the selector where the input particle have a different divergence.

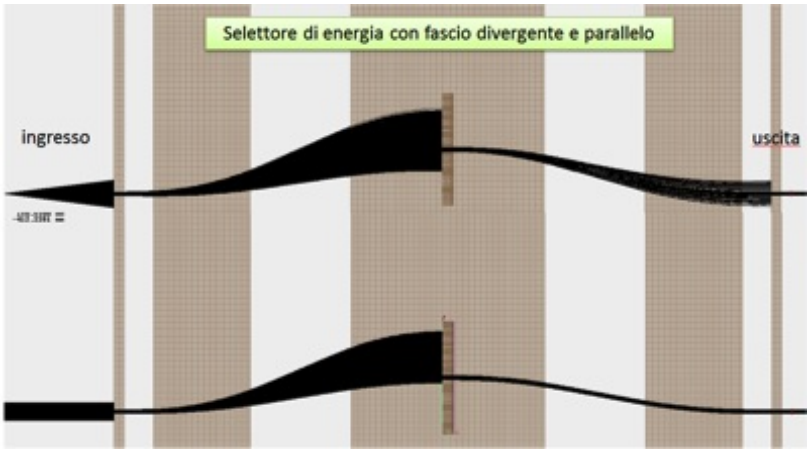

In this regard, the beam dynamics simulations carried out with the code TRACEWIN was developed to verify the system ability to focus different energy components of the beams generated by the laser of Belfast. In the specific case of protons emitted from 5 MeV to 10 MeV with a total divergence of 10 deg the results are shown in fig. 11.9.

The calculations were also validated by simulations with the tracking of FEM codes used to calculate the magnetostatic fields of the triplet as shown in Figure 11.10.

This system is also able to perform a reduction of the beam divergence, for medium-low energy, generated by laser and it constitutes an excellent tool to use in tandem with the energy selector to start the step of characterization of beams produced by laser. The setup for the planned experimental run at TARANIS is represented in fig. 11.11.

11.3.3 Energy Selector

In order to select the energy of the particle beam produced by the target laser interaction, a magnetic system is under study. The device consists in four dipoles based on permanent magnets producing 0.7 Tesla each (see Figure 11.12). The second and the third magnetic fields are parallel with each other but oriented antiparallel to the first and the fourth ones. This configuration allows to increase the separation between the particle trajectories at different energy in correspondence of the central pair of magnets where, by means of a slit device, the

Figure 11.9: Horizontal and vertical beam envelope for energies of 5 MeV and 10 MeV focused by the system of triplet quadrupoles.

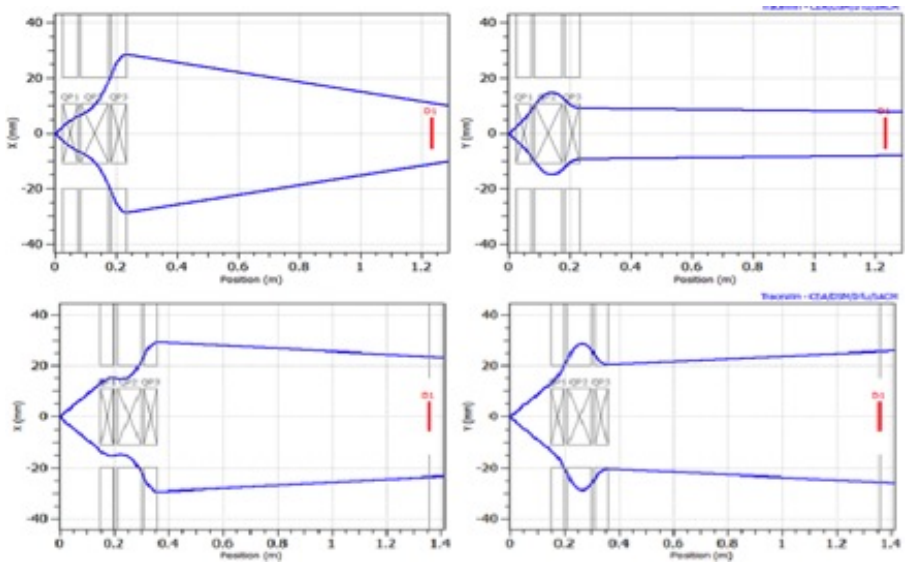

particles with suitable energy are selected.

The energy spread and the amount of particles passing through the slit depends on the size of the aperture. The lower the energy spread, the lower the number of particles will be transported through the energy selector because it needs to use a smaller slit size and vice versa (see Figure 11.13). The energy of the proton beam can be tuned by moving transversely the slit position between 30 mm and 8 mm from the target normal axis. A roller guide system where the central twin magnets are placed, allows to displace radially the two magnets in order to increase the transversal displacement and select the lowest energy particles. In this way the energy could vary within the wide range of 5 MeV and 50 MeV. The energy spread reachable by using 1 mm slit aperture ranges from 3 % for low energy up to 30 % for the highest. The whole magnet system is almost 600 mm long and will be placed into the dedicated vacuum chamber. Two additional collimators are placed both upstream and downstream the selector system in order to control the proton beam size.

The whole system will be simulated with the GEANT4 Monte Carlo toolkit in order to accurately predict the proton trajectories and energy spectrum of the selected beam. These information are crucial for preliminary calculations on proton fluence and dose per pulse. Moreover, the simulation will give also a quantitative estimation of radioactive activation produced by protons inside the energy selector, for further radio-protection assessments.

Figure 11.10: Envelope of a 10 MeV proton beam subjected to the action of the focusing quadrupole triplet.

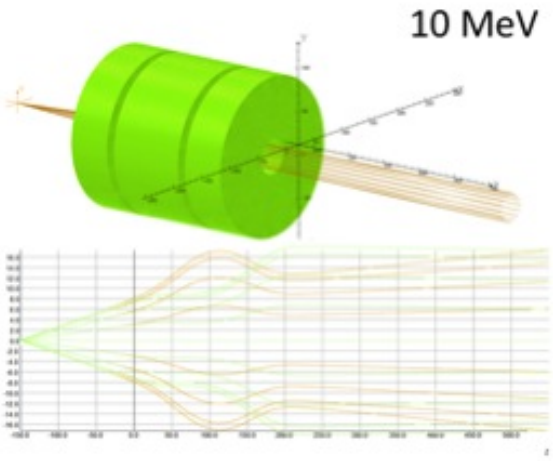

12 Detailed activity of the WP-2

12.1 WP-2.1: X-ray diagnostics of Laser plasmas: Energy-Dispersive X-ray Spectroscopy, High Resolution X-ray Spectroscopy and 2D space-resolved X-ray Imaging

The interest in using X-ray diagnostics for understanding the plasmas produced in laser-target interactions, have grown rapidly in the last decades [30, 31]. In fact the main self-emission from plasma lies in the X-ray domain. Thus, the analysis of the emission spectra (both the continuous bremsstrahlung and the line-spectrum resulting in transitions between bound levels of ionized atoms) can be considered a powerful tool for the non-intrusive investigation of the plasma matter. In particular, X-ray based techniques can be used to gain accurate information on electron temperatures, electronic densities and ionization states [30, 32]. The activity of the present sub-WP will be focused on the development and integration of analytical techniques based on the X-Ray Spectroscopy (both Energy-Dispersive and Wavelength-Dispersive) and X-ray Imaging to be applied in the investigation of the laser interactions with different target-material (i.e high Z and low Z atomic numbers) and target-structure (i.e. multi-layered, nano-structured, etc.). The main scope of the proposed diagnostics will be the investigation of the best experimental conditions for the final protons production (reproducibility, intensity and energy stability).

Figure 11.11: Setup at TARANIS facility for the characterization of laser beams.

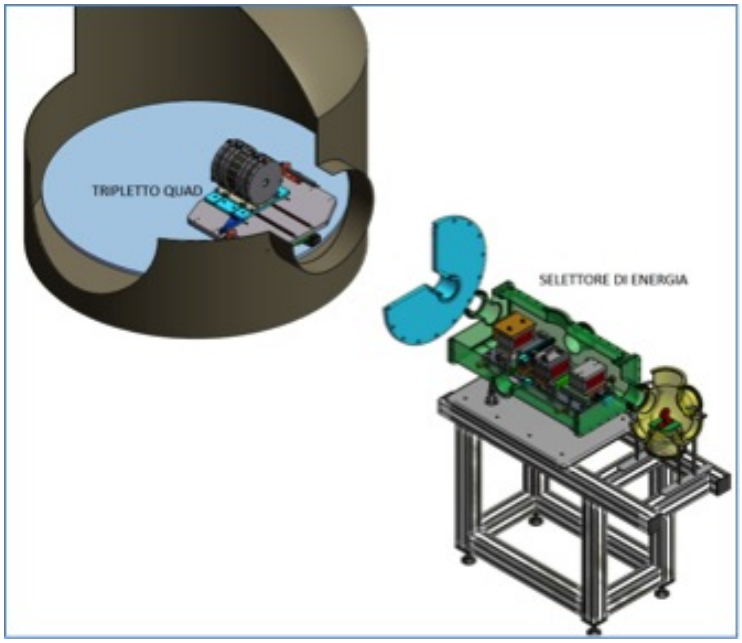

12.1.1 Energy-dispersive X-ray spectroscopy (XRS)

Some of the participants to the ELIMED project have a strong experience in the application of Energy-Dispersive X-Ray Spectroscopy (ED-XRS). In past experiments a number of ED-XRS spectrometers where developed and tested with X-rays of different energies (from 1 keV up to 100-200 keV) emitted by microwave generated plasmas [33, 34]. In particular fast and high efficiency HPGe, and SDD detectors - all equipped with their own electronics and acquisition systems - are already available and will be used for studying the X-ray emissions of laser-plasmas in different energy domains. In particular, since laser interaction with target materials produces high-brilliance emissions (for examples in table-top lasers it is estimated to be about 10^{10}-10^{12} $ph/(sec \cdot mm^2 \cdot mrad^2)$ for metals) [2], measurements will be carried out using large active area (50-80 mm^2) SDD detectors that allow to operate with high counting rates (up to 500 KHz) and optimal energy resolution (133-138 eV at the reference value of 5.9 keV). Information on the electronic temperature can be extracted from the continuous component; also, X-ray lines emitted by atoms with different ionization state can be highlighted through the broadening of the characteristic peaks. Even if ED-XRS presents poor energy resolution in order to gain accurate information about plasma parameters, it represents a fast method in order to perform preliminary studies about the laser-target interactions. During the 1st year the participants will optimize the detection systems using microwave generated plasma

Figure 11.12: The figure shows the layout of the magnet system used as energy selector for the beam produced by the laser-target interaction.

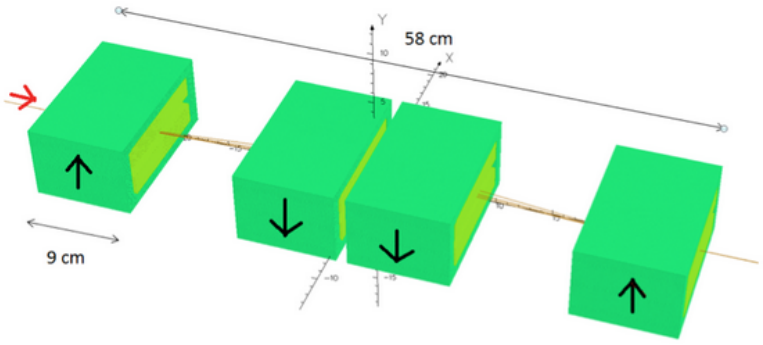

sources already available at the LNS.

12.1.2 High Resolution X-ray Spectroscopy (HR-XRS)

The plasma parameters (i.e. electron temperature, density, charge states) can be accurately measured with the known methods based on the line intensity ratios and on the line broadening [30, 32]. It should be noted that the interaction of the laser with target produces exploding plasmas with atoms in different ionization states. Depending on the Z of the target, few atomic electrons (in H-like, He-like, Be-like, Li-like, etc., configurations) are produced. Such atoms in their own state of charge will undertake electronic transitions between bound levels and emits characteristic radiation. The latter results shifted with respect to the one measured in the neutral state. Also, satellite transitions can be efficiently excited. Thus, in order to approach the accurate measurement of line-shift and line-width, a spectrometer with a challenging spectral resolution ($\Delta l/l=10^{-3}-10^{-4}$) should be developed. Moreover, such a system should be able to operate in a wide energy range in order to investigate different Z target. To satisfy the above requirements a HR-XRS spectrometer suitable for investigating a wide energy range with appropriate energy resolution will be developed . In particular the spectral evaluation will be performed by using 2 complementary line-space gratings (Bragg law based) operating from about 1.241 keV (1nm) down to about 60 eV (20 nm) coupled to a new CCD camera (back-illuminated CCD, 1024 × 1024 pixel, 13.3μm size, 16 bit, 5 MHz redout, QE = 20 % at 10 eV, QE = 95 % at 1 keV). The spectrometer will operate under vacuum. During the 1st year of activity, we will take care about the acquisition of the instruments, we will develop the appropriate goniometric mechanics in order to select the opportune incident angles for the different energies to be investigated. Preliminary tests will be performed at the end of 2013.

Figure 11.13: The plot shows the calculated energy spread as a function of the energy of the selected beam. The curves correspond to the values obtained by using two sizes of the used slit (0.5 and 1 mm).

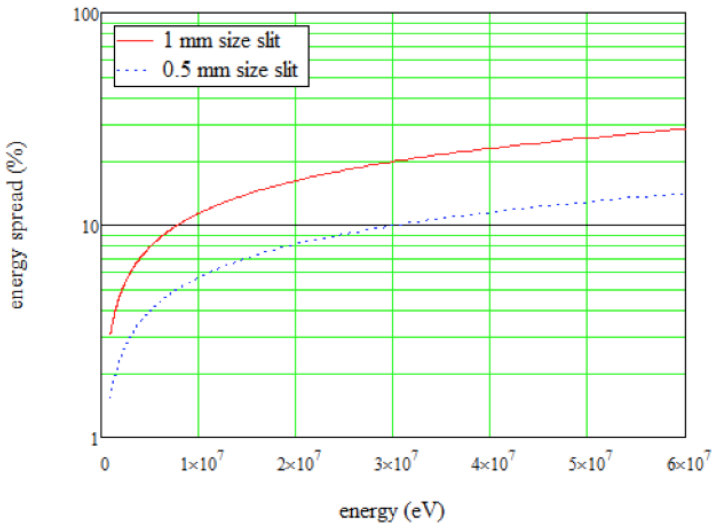

12.1.3 2D X-RAY IMAGING AND SPECTROSCOPY

In the recent research activity of the UTOPIA experiment (5th Group of INFN) a X-ray pinhole camera have been developed and successfully applied in space-resolved imaging and spectroscopy of microwave generated plasma sources [35]. Such a system is particularly suitable to operate in the energy range between 1-30 keV, related to the hotter component of the plasmas (the Quantum Efficiency of the system is 85 % – 90 % in the region 1-10 keV). It consists of a CCD device containing 1024 × 1024 X-ray sensitive silicon pixel. Each pixel presents a 13.3 mm size and it is back-illuminated in order to minimize the absorption of the lower energies. The CCD can be cooled down to a temperature of −100°C (under vacuum) with a strong reduction of the dark-signal (the associated noise is only 5×10^{-3} electrons · pixel^{-1} · sec^{-1}). The CCD operates in Photon Counting mode, with a linear relationship between the number of photoelectrons generated by the X-rays incident in the camera and their energies ($N_{photoelectr.} = E(eV)/3.659$). Finally, the CDD camera is coupled to small aperture pinholes (in particular 5, 50, 75, 100 microns tungsten pinholes). The above experimental configuration allows to perform 2D spatial-resolved imaging and spectroscopy with a spatial-resolution up to 20 microns (mainly depending on the pinhole aperture, geometry and detected energies). During 2013 research activity will be focused to optimize geometry (pinhole apertures, source-pinhole and pinhole-CCD distances) in order to improve the spatial resolution and the magnification of the laser-plasma source with a typical dimension of $50 - 100\mu m$ (de-

pending on the target typology). Moreover, the multi-filtered-pinholes method will be tested with known X-ray sources in order to acquire, in a single acquisition, the different spectral components composing the source. Finally, the use of external TTL coming from an ancillary detector (MCP) will be used as time gating (up to few ns) for the 2 CCDs.

12.2 WP-2.2: Optical and UV imaging and spectroscopy

The understanding of spatial and temporal distribution of plasma parameters in a laser-produced plasma is of great interest to many fields in science. As a matter of fact, between several techniques employed for diagnostics of a laser-created plasma, the photometric and imaging techniques can deeply contribute to plume investigation if they were able to provide a real time, two-dimensional information on the three-dimensional plume propagation [26, 27]. Indeed this capability is essential for hydrodynamic understanding of the plume propagation and reactive scattering. It gives information about the influence of the target nature and geometry on the plume characteristics. Since laser-produced plasma exist on sub-mm spatial and nanosecond temporal scales respectively, plasma diagnostics with these resolutions are needed. The advent of commercial intensified CCDs (ICCD), make it possible to obtain nanosecond time resolution, high spatial resolution and high sensitivity. Thus comprehensive and reliable information can be obtained even on electron density, electron temperature, plume species velocities and ionization balance. Recently [28] a laser plasma imaging technique has been reported. It permits simultaneous spatial, temporal and spectral analysis of the optical emission from laser-produced plasma plumes. The image of an expanding laser-produced plasma is focused on the entrance slit of a stigmatic spectrometer with time-resolved image readout. If the plume expansion axis is aligned with the slit, the obtained images are space resolved along the direction of expansion and spectrally resolved along the orthogonal axis.

Indeed this capability is essential for hydrodynamic understanding of the plume propagation and reactive scattering. Some preliminary experiments have been performed [29] obtaining the time resolved image of two colliding laser-produced expanding plasmas (see Figure 12.1).

Moreover, combining high time and spatial resolved optical spectroscopy with Langmuir probe measurements, the temporally and spatially resolved electron density and temperature at the stagnation layer were extracted (see Figure 12.2).

In this proposal we want to use this novel technique to generate critically evaluated plasma parameters from the time resolved spectral images. It will be made by employing a getable ICCD camera sensitive from 185 up to 850 nm, with a pixel array of the order of 1024 x 1024, an active area of about 20 mm x 20 mm and a minimum optical gate width < 2ns. The laser system

Figure 12.1: Time resolved imaging of broadband at different propagation times: 30 ns, t = 50 ns, t = 100 ns.

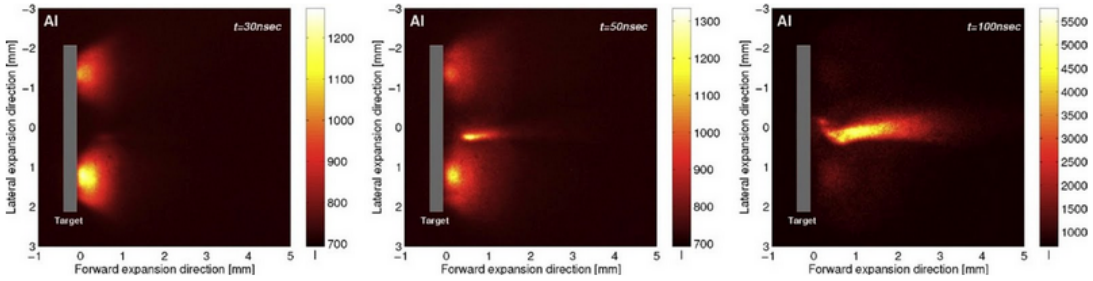

Figure 12.2: Electron density and electron temperature profiles vs. time for the seed and for the stagnation layer.

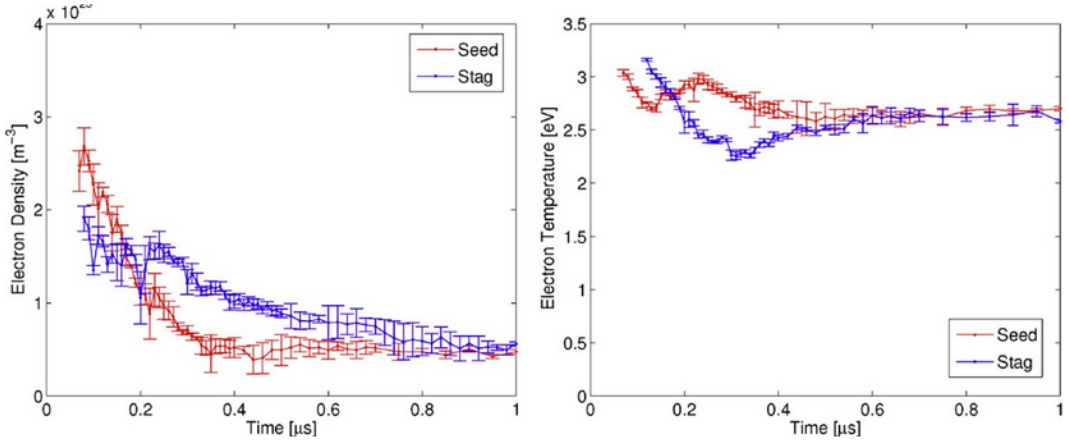

Fig. 2. Electron density and electron temperature profiles vs. time for the seed and for the stagnation layer.

will be synchronized temporally with the main diagnostic systems using a delay generators with a maximum temporal jitter of 1 ns. A suitable optics based on zoom lens, together with an extension tube will allow to the ICCD to acquire highly magnified shots of the plasma. A suitable optical filter will protect the ICCD from any scattered laser radiation. Optical emission spectroscopy will be realized with two suitable imaging spectrograph, one for the UV and the other for the VIS range, with a resolution of 2 nm. The technique will be based on the approach of Siegel et al. described in [28]: the plasma focused on the entrance slit of the spectrograph produces at its output a one-dimensional spatial and spectral plume image. The vertical axis corresponds to its expansion direction (z) and the horizontal axis refers to the wavelength of the emission species. By placing the ICCD at the spectrograph output, will be possible to obtain simultaneously the spectral and spatial information of the plasma propagation; the temporal evolution will be then obtained by gating the ICCD camera.

12.3 WP-2.3: CHARGED BEAMS DIAGNOSTIC

12.3.1 DIAGNOSTIC FOR LASER-DRIVEN IONS

In addition to the more traditional radio-chromic films, CR-39 and MCP based detector, active solid state devices will be studied and tested. The main advantage of the latter is the real-time capability: you can have the measurement result immediately after the shot, using the same detector at high repetition rate. Different materials and structures have been considered and partly characterised: Ion collectors (IC), Ion collector ring (ICR), silicon photodiodes (PD) available in linear array, monolithic silicon telescope (MST) for optimum particle discrimination and large energy range and Silicon Carbide diodes (SiC).

IC and ICR will be employed in time-of-flight (TOF) configuration in order to have immediate information on the average proton energy and yield in different angular directions with respect to the target surface normal direction. IC and ICR will be placed at different angles in forward and in backward directions and at different distances (higher than 1.5 meters) so that TOF measurements will permit to distinguish the photopeak on the collector, the proton contribution and the contribution of the slower ions coming from the other elements of the produced plasma. ICR will be employed in special manner in front of the Thomson parabola spectrometer in order to compare the maximum energy of the proton parabolas and the TOF evaluations. The IC and the ICR will be employed by using different sectors (generally four) equipped with different absorbers (generally thin Al absorbers from 1 microns to 8 microns in thickness) so that it will be possible to select very well proton peak from heavy ion peaks and from the photons producing photopeak.

SiC detectors will be employed because of their energetic gap (3.3 eV) which permits to detect no visible light but only UV and X-ray photons and because of their high response velocity and high sensitivity. SiC will be used in TOF configuration to reduce the background of proton peak and to highlight the proton contribution with respect to that of heavy ions coming from plasma.

At ultra-intense laser experiments also monocristalline diamond detectors will be employed in TOF configuration in order to decrease the background due to the visible and soft UV, to detect very well the proton peak and to measure their mean velocity and energy, that can be compared to the measurements coming from the Thomson Parabola spectrometer.

All those detectors will be placed at different angles in order to have information on the ion angular distributions as a function of the laser and of the target parameters. To achieve this goal, very fast storage oscilloscopes will be employed. Further details on the use of these kind of detectors can be found in our literature [14, 13, 15].

Preliminary tests have already been performed on two silicon structures at INFN-LNS and

INFN-LNL with 30, 1-5 MeV proton beam and 60 MeV/u carbon beam. Results show that charge collection is optimal in the fully depleted structure (MST), being the other affected by long tails and partial collection. The main specifications for these detectors may be so summarized:

- maximum energy of the order of 50/60 MeV;
- energy range of two decades (1-100 MeV for protons) for exploring the high and medium energies;
- identification and selection of the particles with different Z/A ratio;
- single particle detection capability in order to have good energy resolution even at low fluence;
- dynamic range of three decades;
- response to single shot capability in order to sustain real-time operation mode;
- repetition rate equal at least to the laser repetition rate (10 Hz).

These detectors, in 2D array configuration, are thought also for imaging of beam transverse size with proper spatial resolution.
Moreover, we will focus on the development of the following elements:

- non intercepting diagnostics based on AC thoroids and beam profile monitors, to measure longitudinal characteristics and pulse current.
- destructive diagnostics based on pixels, solid state CMOS detectors and scintillating fibers, to measure transverse characteristics

Each one of these devices requires a specific electronic card to handle the signals as close as possible to the device itself. The purpose of the card is to adapt the signals coming from the beam instrumentation to standard high quality electronic data acquisition and analysis systems.
Also electrons play a key role on protons acceleration mechanism [6] and the development of the related diagnostics can in future represent an important task in order to optimize the ELIMED beams that can be done with different detectors.

12.3.2 THOMSON PARABOLA SPECTROMETER

Thomson Parabola Spectrometer (TPS) is a widely and successfully used device for laser-driven beam diagnostic. It has the advantage of a quite simple working principle which allows to get a complete set of information in a single measurement [16, 17, 23, 19]. Within the INFN LILIA project an high resolution, wide acceptance Thomson-like spectrometer have been already developed at LNS [20, 21]. A scheme of the deflection sector with a simulated carbon ions beam passing through the device is shown in Figure 12.3.

Figure 12.3: Simulation of a carbon ions beam passing through the Thomson Parabola developed at LNS

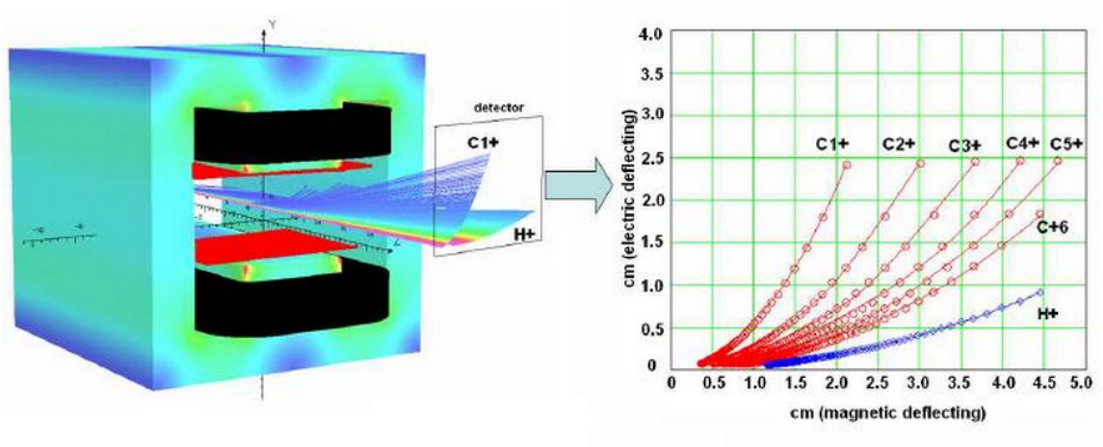

In view of the future ELIMED activity the TPS have been successfully tested at PALS laboratory in Prague, under ions beams accelerated with the ASTERIX IV laser system [22]. The acquired results have been analysed and compared against ICR time-of-flight information showing good agreement. Moreover another TPS developed at PALS and used since several years have been used during the experiment. Further comparison against the data acquired with the reliable PALS spectrometer have been performed successfully. Consistency among data shows the proper operation of the new Thomson Parabola as detector for beam diagnostic, even if some upgrades are still necessary in view to develop an improved spectrometer suitable for the higher energies expected within ELIMED project. Figure 12.4 shows a typical spectrogram obtained with a double-layer Mylar ($2.5\mu m$) and Al (50 nm) target, laser energy was 512 J.

The bright central halo is due to neutral particles streaming form laser-target interaction. It can be cause difficulties in evaluating the maximum energy of ions, as sometimes it overlaps with the starting point of parabolas. A new collimation system is required in order to reduce

Figure 12.4: Image of a tipical shot acquired with the Thomson Spectrometer of LNS. Parabolas of proton and carbonions with different charge states are visible.

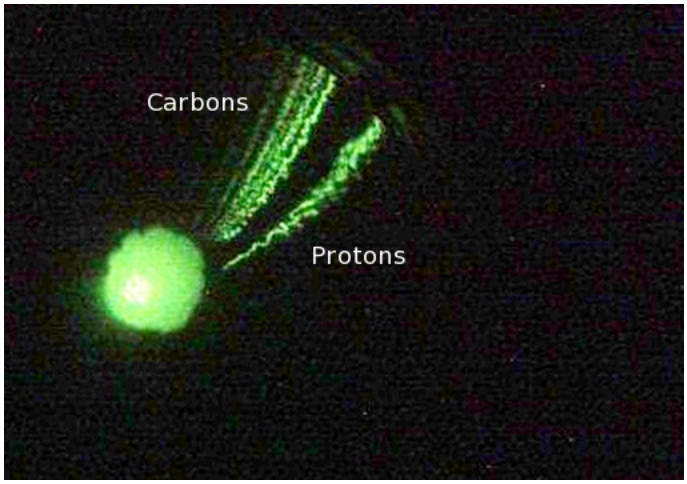

the halo dimensions. Moreover Al and O ions, elements in the target, are not resolved in spectrograms as their parabolas overlap with C ions traces. These issues can be resolved reducing the central halo dimensions and exploiting the whole MCP detector acceptance. In fact the minimum energy region, where parabolas are further from each other, is not visible on the active MCP surface. The main upgrade of the TPS concerns the improvement of the Field of View of the imaging detector. This can be done if all the ions reach the detector not along its axis. This would allow to exploit the whole detector acceptance making easier to resolve parabolas of different ions species.

The experimental phase has also shown some problems with the alignment and collimation systems. It should be possible to control the pinholes relative positions using a micro-metric screws system. This will permit to set the pinholes on the same axis and to control the beam spot position on the MCP detector. The possibility of using smaller pinholes, such as a system with 500μm and 50 μm in diameters, is also under consideration. This would allow to reduce the central halo dimension and to improve the spectrometer spatial resolution and its intrinsic energy resolution as well, as parabolas would be thinner and the energy range inside parabolas width would result smaller [23]. Finally, a pointing laser system ensuring the pinhole alignment and the alignment of the spectrometer with the interaction chamber have to be used. A micro-metric moving system is under testing, it will allow to fix the alignment laser position and set the spectrometer on the proper position with respect to the target in the interaction chamber. The upgraded spectrometer will be tested again at PALS laboratory during another beam shift that has been already approved for 2013. We hope in the possibility to test the system at the FLAME facility in Frascati within the end of 2013 or in 2014. During the same years

the feasibility of a new Thomson spectrometer for proton energies up to 100 MeV will be performed. This study, based on the experience gained with the lower energy spectrometer, aims to realise the final spectrometer system to be used, as part of the diagnostic set-up, along the ELIMED beam line at ELI-Beamlines in Prague.

A specific *R&D* activity is also planned with the purpose to develop a new kind of imaging system for the spectrometer. We are evaluating the possibility to use plastic scintillator coupled with CCD camera as detector, to visualise the parabolic traces. A BC-408 scintillator, for example, can be used to resolve proton spectrum. Taking into account the overall resolution of the imaging system, we could obtain a minimum energy resolution of 100 keV. In order to verify the real possibility of this novel detection approach, we applied the physics evaluations given in [24] on the experimental data acquired during the experimental run at PALS in May 2012. We have calculated the number of protons per shot (9×10^7) entering the spectrometer, analysing ICR signals. Figure 12.5 below shows the estimated number of photons emitted by the scintillator for protons in the energy range 1.8-3 MeV (error bars are evaluated taking into account the solid angle of CCD lens, Quantum Efficency, etc. [24]).

Figure 12.5: Estimated number of photons emitted by the scintillator considering protons in the energy range 1.8-3 MeV.

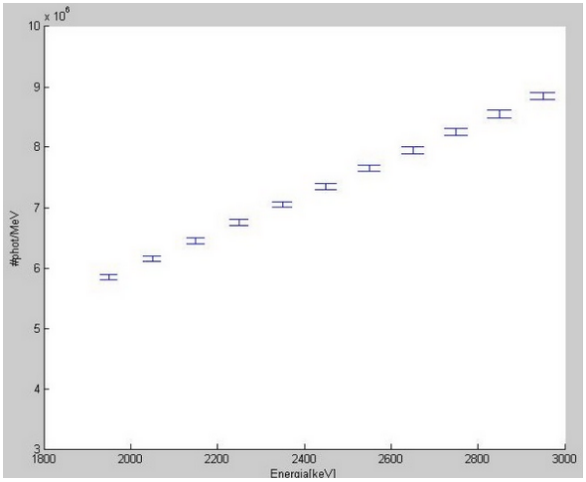

Starting from the experimental data we acquired, we have estimated the number of protons reaching the imaging system per energy slice of 100 keV, which is of the magnitude order of 10^6. Taking into account the CCD (14-bit CHROMA CX3 camera) QE and the scintillator emission spectrum (1 mm thick BC-408), we have estimated that at 2 MeV energy, a minimum of 10 protons are needed to be detected [24]. A scintillator-based ion beam profiler capable of measuring the ions beam transverse profile for a number of discrete energy range has been designed by Belfast researchers. It has been just tested and calibrated with conventional

beams whose features are set similar to laser-generated beams ones. Preliminary results with non-conventional beams was obtained at RAL Laboratory, but many improvement of the detector are still necessary [2].

12.3.3 Rivelatori di Milano

13 Detailed activity of the WP-3

13.1 Introduction

The WP3 is devoted to the study of feasibility of a proton in-air transport beam line for dosimetry and radiobiology studies. Different aspects have to be taken into account for such a kind of study, which involve theoretical calculations with simulations, as regards the part related to the project of the beam line, and experimental one, as regards development and test of detectors for diagnostic and measurements of dosimetry and radiobiology. Before clinical applications of laser acceleration becomes a realistic possibility, several tasks need to be fulfilled. The development of a dedicate therapeutic irradiation equipment, the transition from physical experiments with single shots of poor reproducibility to stable, reliable irradiation of patients with prescribed doses in a few minutes, addressing quality assurance and patient safety are necessary. Moreover, the real time physical and dosimetric characterisation and the investigation of the biological effectiveness are necessary. Thus, four different sub-WPs have been considered, each one related to the mentioned aspects to be investigated

13.2 WP- 3.1: Monte Carlo simulations of transport beam line and related radioprotection evaluations

The WP-3.1 task is crucial for the design of the passive/active elements necessary for the in-air transport of the proton beams, once selected in energy. Depending on the collimation and on the spatial spread a customised system has to be simulated in order to obtain a "clinical beam" with the right requirements in terms of spatial homogeneity and symmetry. Monte Carlo simulations also permits to pre-calculate the environment dose in order to eventually design shielding elements for radioprotection. Moreover, the simulations of the experimental setup used in the laser facilities for the first test (Belfast, Corea, Luli, Flame) will be necessary to foresee dose per pulse and, according to that, reproduce the specific experimental configurations for the planned measurements.
The evaluation of the coming-out beams dose distributions and of the secondary radiation generated inside the selection system; design and Monte Carlo simulation of the in-air transport beam line and radioprotection calculations with Monte Carlo (MC) simulations are today

widely used in different fields. In particular MC codes for physical transport of particles in the matter are largely employed for medical applications because of the high level of accuracy of their predictions, also in very complex configurations. They, indeed, represent a fundamental tool for the study of dosimetric systems, the reproduction of clinical beam lines, the development and test of novel detectors and the verification of the Treatment Planning Systems (TPS). In this proposal we aim to use the MC simulation toolkit GEANT4 (GEometry ANd Tracking) to accurately reproduce the transport of the pulsed proton beam and to foresee all the physical quantities of interest. GEANT4 is one of the most versatile and widespread codes used today for particle tracking and it is widely used for different physical applications. It is a C++ object oriented toolkit permitting the simulation of particle interactions with matter [42, 43, 44]. It provides advanced functionalities for all the typical domains of detector simulation: geometry and material modelling, description of particle properties, physical processes, tracking, event and run management, user interface and visualisation. Initially developed for High Energy Experiments (HEP) simulation, GEANT4 is now widely used also for medical physics application. It allows, indeed, the tracking of any charged and uncharged particle relevant for radio diagnostics and radiation therapy. Some components of the LNS group involved in this proposal are expert users of this MC code and are member of the official GEANT4 collaboration since several years. We are also responsible of an application, currently distributed in the public release of the code, which simulate the CATANA proton therapy facility at LNS-INFN of Catania [45, 46, 47]. In the CATANA facility eye tumours are treated with 62 MeV proton beams [65]. The passive beam line is simulated in details with GEANT4, with the possibility of retrieve depth and lateral dose distributions as well as averaged LET of both primary and secondary particles. Our aim is to gather the LNS expertise in MC simulations, coupled to the Turin researchers, in order to fulfil the followings scopes:

- MC simulations of the experimental setups to be used in the laser facility for the planned experimental activity (Belfast, Korea, Flame, Luli). The preliminary information retrieved by these calculations are important for the optimization of the experimental setup and a prediction of fluence per pulse expected at the measurement point. Accurate dose estimation will be done in order to foresee the response of the different detectors to be used.

- MC simulation of the energy selector. A realistic reproduction of the system and of the particle transport in the magnetic field allows an accurate prediction of the beam characteristics at the exit window and, consequently, to retrieve the expected energy spectrum.

- Feasibility study of the ELIMED beam line. An accurate simulation of the active/passive

elements of the in air transport beam line will be done at the end of the project. The MC simulation will allow to study the best solutions for the spatial shaping of the beam, the homogeneity, the dose delivery system, the collimators and each kind of elements necessary to achieve a "clinical beam".

- Radio-protection studies. The full simulation of the transport beam line, starting from the energy selector to the in-air measurement point, will permits to predict the radiation due to secondary particles and to preliminary identify areas at high level of activation. This study will be helpful for eventual design of shielding elements.
- Radiobiological modeling and simulation: extension of conventional hadrontherapy models for their use in the context of laser-driven beams.
- Study and implementation of simulation strategies for treatment planning with laser-driven beams.

13.3 WP-3.2: Development of innovative systems for in-air diagnostic of accelerated particles and fluence measurements for absolute and relative dosimetry

Absolute and relative dosimetry for high pulsed proton beams is particularly challenging because of the intense dose delivered per pulse. For this reason, we propose a dose-independent system for proton fluence measurements, with a level of accuracy required for absolute dosimetry. An innovative system will be realized in order to overcome the limitations coming from the high current per pulse and to perform in-beam diagnostic with a minimum beam perturbation. This system, named ELIMON, will be also coupled to a Beam Current Transformer (BCT). Moreover, the study and the characterisation of different detectors dedicated to dosimetry will be necessary; the main task will be to select the most appropriate ones and to design a customised and integrated dosimetric system. An innovative Faraday Cup (FC), a new Proton Spectrometer, made of scintillator layers and a new type of Ionization Chamber coupled to gafchromic films (RCF) and CR39 will be developed and tested in order to measure their response as a function of the dose rate and dose per pulse. In particular the CR-39, the RCF and the Proton Spectrometer will be crucial for a precise measurement of the proton spectrum, fundamental for extracting the dose with the FC.

13.3.1 ELIMON

In-beam diagnostic for the intense pulsed proton beam in progress at the ELI facility is a demanding task. Beam specification, as sketched in the ELIMED draft, reports a proton burst

duration Δt=0.1-1 ns with pulsed intensity ranging from 10^{10} to 10^{12} p/burst. In addition it is mandatory to perform an on-line monitoring (negligible beam perturbation) and the detection system must operate in an EM polluted environment. An integrating or fast current transformer (e.g. Toroid) would represent a preliminary choice, since they are world-wide used and commercially available [49], but its reliability could be compromised by EM pollution. In order to match such "tricky" requirements an innovative, still simple, detection setup must be put in place. Simplicity and consequently reliability result as fundamental requirements for such a new diagnostic system. By using the experience developed at INFN-LNS and ISOLDE-CERN [50] and considering the constraints dictated by the beam specifications we propose a proof of concept to be validated. Introducing the ELImon, a compact and scalable in-beam monitor for pulsed beam. The detection system is described in the figure 13.1.

Figure 13.1: Layout of the proposed new detector for the on-line monitoring of the pulsed beam fluence

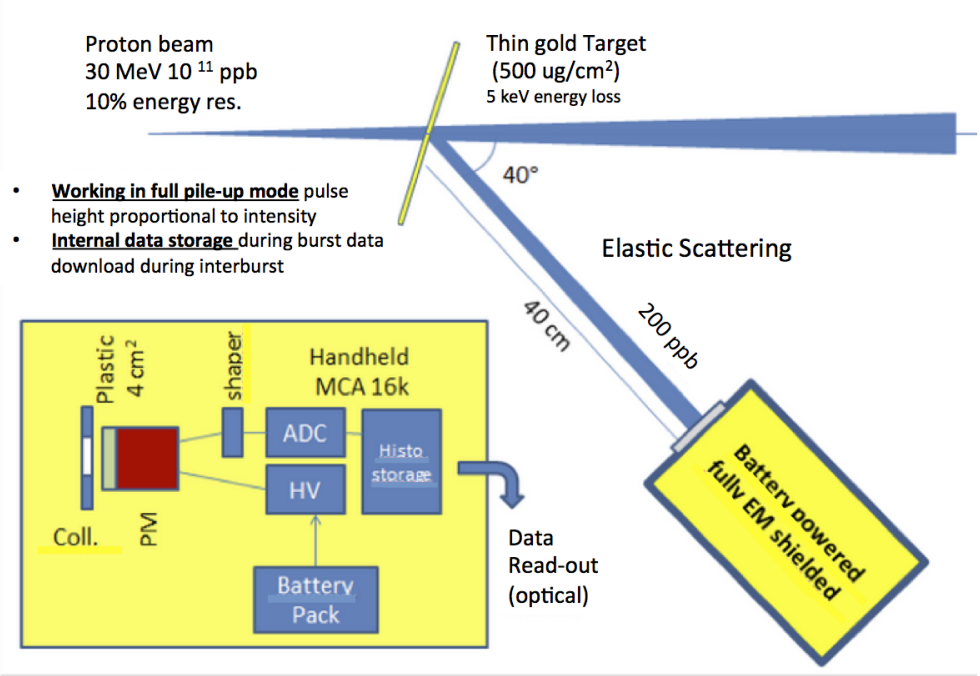

Pulsed beam will be diffused by a thin Au target (on-line monitoring), the elastically scattered protons will be detected at a tunable angle (in order to change the intensity range) by a battery-powered detection system consisting of a plastic scintillator coupled to a PM. Such a detector will work in full pile-up mode (total charge to pulse height conversion), allowing a simple and linear intensity-to-pulse height conversion. In such a way downscaling of beam intensity will be performed by the elastic scattering, intensity measurement by pile-up summing. A

hand-held low-power MCA system will convert each pulse, the histogram will be stored in the internal MCA memory and will show intensity distribution over several beam bursts. The intensity profile will be download via optical link during the inter burst time interval, defeating the strong in-burst EM noise. The set-up geometry is well adapted for beam alignment monitoring too, just by using two or more symmetric modules around the Au target. Due to the simplicity of the set-up we will be ready to test a first prototype at the beginning of 2013.

13.3.2 Beam Current Transformer

The Fast Current Transformer (FCT) is a passive device, it is one of the most suitable device to monitor a short fast pulse, such as the laser-driven beam one, on an oscilloscope when non-contact measurement is a necessity. The output response is a current signal and it can be determined by monitoring the generated magnetic field with a current transformer. The beam passes through a highly permeable torus as the 'primary coil'. An insulated wire around the torus acts as the 'secondary coil' of the transformer.
The FCT main advantage is the possibility to measure beam currents with a minimum distortion up to very high frequency. In particular we would like to use its features for an on-line monitoring of the current in the in-air region of the dosimetric system and also as a cross-check measurement of the ionization chamber.
For the dosimetric purpose, we will use a FCT with a rise time faster than 1 ns, as low as 175 ps, corresponding to 2 GHz up to the frequency cutoff. Exceptional bandwidth and sensitivity with very high permeability and low loss at high frequencies are achieved by using amorphous cobalt-based alloy cores specially annealed in a magnetic field.

13.3.3 Dosimetric system

Due to the broad exponential shaped energy spectrum and the high pulse dose, the dosimetry protocol for such kind of beam quality is challenging. Thus, an independent absolute dosimetry and an online relative dose monitoring system are crucial prerequisites for successful radiobiological and clinical experiments with laser-accelerated protons. Few integrated systems have been already developed for such a kind of application [51]. We propose to develop and test different detectors for dosimetry and to design and realize an integrated system for dosimetrical measurements and cell irradiation. In particular, we aim to use radiochromic films (RCF), CR39, a Proton Spectrometer and an Ionization Chamber for relative dosimetry and to develop a dedicated Faraday cup (FC) for dose rate independent absolute dose measurements. The proton spectrometer, coupled with RCF and CR39 in stack configuration, can be used in order to obtain quantitative information on the accelerated proton energy spectrum

[70, 95, 54, 55, 57]. An accurate measurement of the energy spectrum is fundamental for a precise calibration of the FC. Moreover, the high spatial resolution of the gafchromic films allows a precise measurement of 2-D dose distributions at different depth, which is crucial for the cell irradiation. The integrated dosimetric system will consist of three main sectors: the first one will be dedicated to the relative dosimetry (RCF, CR,39, Proton Spectrometer, Ionization Chamber), the second one to the cell irradiation and the last one to the absolute dosimetry (i.e. the innovative FC). The FC will operate in vacuum, on the other hand all other detectors will operate in air. The characterization of all these detectors with pulsed beams and the realization of an integrated dosimetric system for the absolute dosimetry in combination with a relative on line dose monitoring are a key requirement for in vitro cell irradiation and, therefore, for eventual future in vivo irradiation studies.

Proton Spectrometer

We propose to design and develop a Spectrometer based on the Proton Range measurement. The goal of the system is the real time acquisition of the beam profile and the residual range spectrum for protons produced by the laser acceleration mechanism. The sensitive volume of the proton range detector will be made of a stack of 60 plastic scintillator layers, 3x3 cm^2 area and 100 micron thick, read by means of wavelength shifting fibers. The energy range covered by such a system is [0:30] MeV. The proton spectrometer will be provided with an imaging detector at the entrance window, it will be made of two plane, orthogonally oriented, of 250 micron scintillating optical fibers. The photosensors chosen for the conversion of the scintillation light into an electric signal are matrix of silicon photomultipliers manufactured by ST Microelectronics. The front-end boards, hosting the photosensors and customized for the application, consist of a fast comparator array. The measurement of the scintillation light intensity will be performed with the time over threshold technique. A FPGA based commercial system, manufactured by National Instruments, will be used for the real time read-out, data-acquisition and pre-processing.
This Spectrometer will allow to measure the proton spectrum with good resolution and, consequently, to extract an low uncertain absolute dose measurements using the Faraday Cup (FC) .

Radiochromic films

Radiochromic films, showing small energy dependence, high spatial resolution (up to 50μm) and tissue-equivalence, are a preferable media for ionizing radiation dosimetry measurements in clinical radiation oncology [59]. The radiation sensitivity is based on a solid solution of colourless crystalline diactylene monomer (sensitive component) coated on a flexible film

base; when the active component is exposed to radiation, it reacts to form a blue colored polymer (self-developing films), with the possibility of handling in visible light. Figure 13.2 depicts the absorption spectra of a gafchromic film before and after irradiation. Before irradiation the active component produces little response as highlighted by the low absorbance at 636 nm. The change in optical density following dose deposition in gafchromic films may be measured with transmission densitometers, film scanners or spectrophotometers; a simple readout of the irradiated film can be obtained by using flatbed RGB scanners in the red channel [60].

Figure 13.2: Example of absorption spectra of an EBT3 gafchromic film before and after an exposure of 2 Gy of photon irradiation.

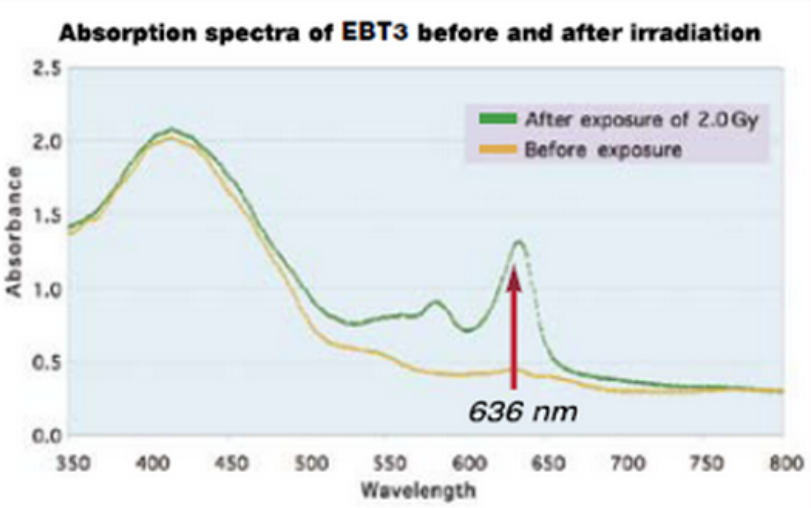

The RCF are presently widely used for absorbed dose measurements of high-energy photon beams produced by medical linear accelerators, including IMRT therapy and IORT [61].

Different models of RCF are available, with different dose sensitivity to be used in different dose ranges and different depths of the sensitive component:

1. **Gafchromic HD-V2**, dimensions 8 ×10 inches, dose range applicability 10 Gy - 1000 Gy; its Equivalent depth in water, Effective point of measurement, is $4\mu m$; the Effective atomic number is 6.5.
   The Gafchromic HD-V2 high-dose dosimetry film has been designed for the use with beams of photons, electrons, protons, ions and neutrons. Its sensitivity is very low for clinical applications, but its effective point of measurement is at a depth of 4 microns and represents the shallowest point we were able to establish with radiochromic films.

2. **Gafchromic MD-V3**, dimensions 5× 5 inches, dose range applicability 1 Gy - 100 Gy; its

Equivalent depth in water, Effective point of measurement, is at 125μm; the Effective atomic number is 6.7.

As INFN-LNS Catana team we have investigated the above mentioned films with proton beams of the eye proton therapy facility in the energy range from 20 to 62 MeV. MD films have been characterized at LNS-INFN with a low energy proton beam of 21.5 MeV directly in a water phantom [62]. The films have been used also for the commissioning of Catana eye protontherapy facility [63, 64]. Moreover, they are currently used for routinely dosimetry measurements for the characterization of the clinical proton beam [65, 66].

3. **Gafchromic EBT3**, dimensions 8×10 inches, dose range applicability 1 cGy - 40 Gy; its Equivalent depth in water, Effective point of measurement, is 140 μm; the Effective atomic number is 6.98, very close to water (7.30).

   The GAFCHROMIC EBT3 dosimetry film has been developed specifically for applications in conventional radiotherapy. The response of EBT3 films to medical ion beams has been extensively investigated by many authors for the use in protontherapy and carbon ion facilities, as passive and active facilities, resulting in effectiveness of radiochromic films for absolute and relative dosimetry. The EBT film response was found comparable for protons and photons. From the acquired experience, EBT films are at the moment extensively used at passive proton-therapy facilities for lateral beam profile measurements in clinical beams of different proton energies and for measurement of unmodulated and modulated (clinical) depth dose curves. EBT films are used also for the commissioning of the pencil beams in hadrontherapy facilities with active scanning beam delivery (p,^{12}C) [67, 68, 69, 70].

   In ocular proton therapy EBT3 films are routinely used for beam profile measurements in unmodulated and modulated beams, including accurate determination of lateral penumbra, for the determination of output factor in the narrow beams of eye protontherapy and for 2D dosimetry. EBT calibration is carried out with 62 MeV mono-energetic proton beams, using a 25 mm diameter circular collimator. Several $3 \times 3 cm^2$ strips are irradiated in a solid water phantom at 1mm depth in the entrance plateau of the Bragg curve, corresponding to a dose rate of 25 Gy/min. Calibration curve is well in agreement with the corresponding curve for 6 MeV photons (Figure 13.3), demonstrating the water equivalence of EBT film.

   EBT has minimal dependence of response (< 2%) upon the residual range beyond the

Figure 13.3: Curve calibrations of the EBT3 Gafchromic detectors irradiated with proton and photon beams.

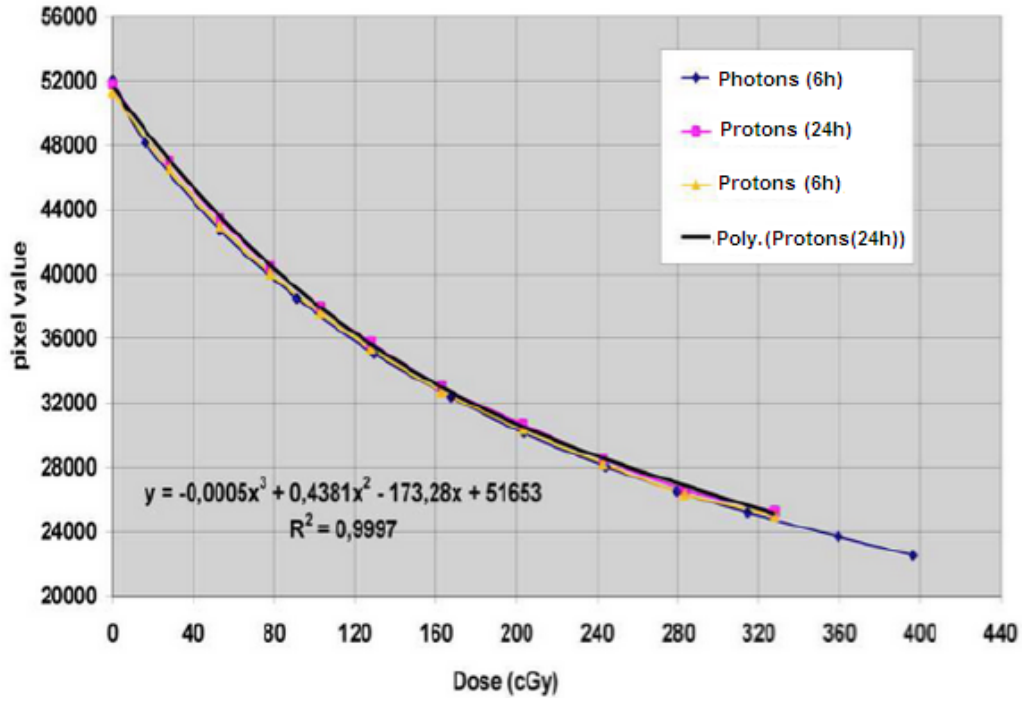

irradiation depths in the interval of residual ranges from 6 mm (25 MeV) to 30 mm (60 MeV); as a consequence, only one calibration file is required to obtain off-axis beam profiles at different depths in SOBPs. In this project we aim to gather the LNS expertise in dosimetry with RCF in order to use them for the followings scopes:

- as a relative dosimeter to be calibrated against an absolute one
- for dose measurements to measure 2D spatial dose distributions in stack configuration to perform laser driven proton beams spectroscopy.

Moreover, recent experimental studies show their dose-rate independence (< 5%) also for high peak dose rate of the order of 10^{10} Gy/s, typical of laser-based acceleration [71].

CR39 detectors

The SSNTD (Solid State Nuclear Track Detector) CR-39 is a polycarbonate plastic largely used as detector of protons and heavy ions [72]. A particle impinging on it produces a molecular damage in the cylindrical region of the crossed material. This region extends for few tens of nano-meters along the particle trajectory. It is the so-called LT (Latent

Track). REL (Restricted Energy loss) is instead the energy lost by particle to form the LT. A chemical etching transforms these damaged trails into permanent structures called ion track.

The detection sensitivity s of a CR-39 detector is defined as:

$$s = \frac{v_t}{v_b} \tag{13.1}$$

where v_t = track etch rate and v_b = bulk etch rate
This detector response is proportional to $\left(\frac{dE}{dx}\right)_{REL}$, namely to the loss of energy to form the LT.
Note that v_t is greater of v_b and therefore s is greater of one. The etch rate v (either v_t as v_b) is a function of etchant temperature and concentration [73].

Several authors have performed tests of sensitivity at low energies with different ions.

With regard to the protons we have:

50 KeV L = 0.19 ± 0.05 μm
100 KeV L = 0.40 ± 0.06 μm
200 KeV L = 0.41 ± 0.04 μm

where L is the length of the particles trace measured after etching [72].
On the other hand, for higher energies (order of Mev) protons the range L is of the order of a few hundred microns (150 μm at 3.5 MeV) [74].

CR39s do not detect electrons and electromagnetic radiation, hence they can be used, together with ion collectors (IC) and RCFs, for detecting energetic protons produced by ultra-intense laser [75]. In these experiments we have bunch of protons greater than $10^8\ cm^{-2}$. Therefore, Al foils ($> 0.65\mu m$) have to cover the CR39 detectors in order to avoid overlapping of proton craters. This way, the low energy component of proton flux is absorbed in the foil and only the higher energy part of the bunch reaches the detector, allowing better crater separation. In such a way it is possible to estimate the flux of protons as a function of its energy [74].

At LNS we have worked with this detector type in several experiments to detect alfa particles from nuclear reaction ^{11}B+ p present in a plasma formed after interaction of a laser pulse with solid target containing natural B [76]. We have done the calibrations

Figure 13.4: Photos of craters induced in the CR39 by protons which were generated by one laser shot and penetrated through Al-foils of different thickness [74].

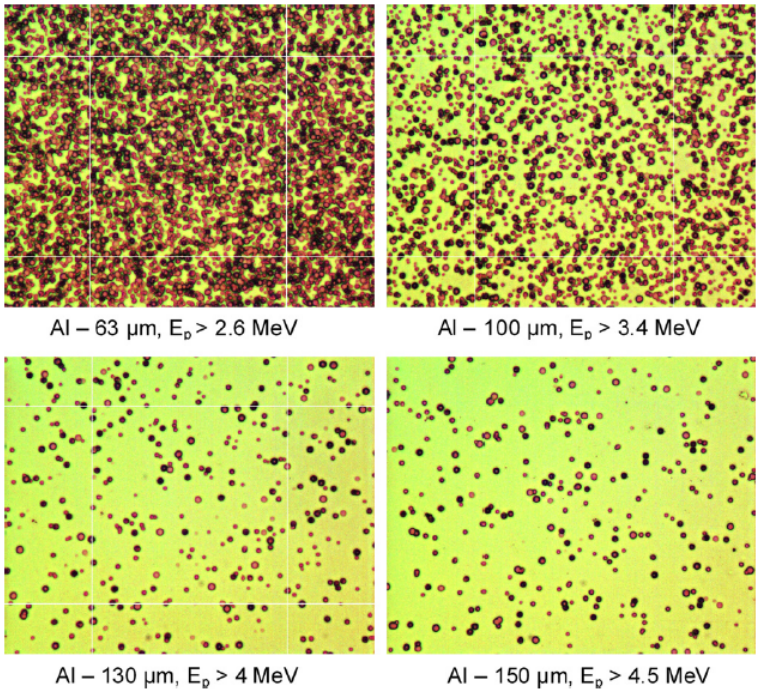

with both alpha sources that with proton beams at several energies. We have a chemical batch and a motorized microscope controlled by a LabVIEW based software developed by our group, for the readout of the tracks. The analysis of the tracks was done by means of *ImageJ*, a public domain Java image processing software [77].

Ionization Chamber

Beam monitors for high intensity beams The widespread use of parallel plate ionization chambers is motivated by the several advantages in terms of uniformity, linearity, transparency and robustness, making it the preferred choice for dosimetry and beam monitoring in current hadrontherapy applications. However their use with highly pulsed beams, where the ionization density would be larger by several orders of magnitude than with uniform beams, would lead to reduced collection efficiency due to the large recombination effects, an important concern for dosimetric applications. In particular, the correction for recombination effects would depend on the dose rate, which is the quantity to be measured. The INFN group of Torino is currently facing this problem by proposing the development of ionization detectors with multiple successive gas gaps

of different thicknesses and operated at different voltages. Since the recombination depends both on the thickness of the gas gap and on the electric field in the gap, the ratio of the charges collected in different gaps is directly related to the recombination effect occurring in the gas. If a thorough calibration of the multi-gap chamber is performed using a Faraday cup, the measurement of this ratio would allow determining the inefficiency and hence correcting for it. The proposal of the development of a simple 2 gap chamber is currently financed by the INFN within the RDH experiment (Research and Development in Hadrontherapy) with a special focus on future syncro-cyclotrons or cyclinacs. The design of a new readout chip for pulsed beams is also part of this proposal. As the dosimetric system for a laser-accelerated beam facility such as ELIMED would be facing the same problems, although at a different scale, the group of Torino is willing to cooperate in the design of the dosimetric system for ELIMED by exploring the possibility of applying the same concept as developed within the RDH experiment. In particular, calculations and simulations of the recombination using the ELIMED beam parameters will be performed. In addition, the prototype developed in RDH will be possibly made available for any beam tests foreseen in the ELIMED proposal.

Faraday cup

A procedure to develop a calibration method for absolute dose measurements must be implemented since no protocol for absolute dosimetry with laser-driven beams has been defined up to now. In TRS-398, it is suggested that the charge collection efficiency in an ionization chamber should be verified by a dose rate independent system such as a calorimeter. A Faraday Cup (FC) can perform absolute dose measurements, since it has a linear response for a given number of particles and a signal independent from dose rate [78]. When the energy spectrum of the beam and the particle fluence distribution are known, a FC can be used to determine the absorbed dose [79]. The absolute dose can be extract with a Faraday Cup using the following expression:

$$D_w(z) = \Phi \cdot \frac{S_w(z)}{\rho_w} \cdot \prod k_i \tag{13.2}$$

where $S_w(z)$ is the stopping power of the proton spectrum at depth z and $\prod k_i$ is the product of the correction factors for beam divergence, scatter, field nonuniformity, beam contamination and secondary particle build-up. This method relies also on an accurate value of the proton stopping power in water for which the uncertainty is estimated to be 1-2 % according to the ICRU Report49 [80].

The previous relation, in the concrete implementation, can be written as:

$$D_w = \frac{1}{A(\frac{S(E)}{\rho})_w} \cdot \frac{Q}{e} \cdot 1.602\ 10^{-10}\ \ Gy \tag{13.3}$$

where A is the effective beam area in cm^2, $(\frac{S(E)}{\rho})_w$ is the mean stopping power in water in $MeV\,cm^2\,g^{-1}$ at the given proton energy E, Q is the total charge transported by the beam in Coulomb, e is the elementary charge in coulomb. For the experimental proton beam the stopping power in water is $\frac{S(E)}{\rho} = 10.516 MeV \cdot cm^2 g^{-1}$. Elastic nuclear interactions are also included: their ratio to the electronic stopping power is about 0.3 %.
Faraday Cup (FC) dosimetry will be implemented in connection with other dosimetric system (like Gafchromic, CR39 plates, Proton Spectrometer) to perform a preliminary on-line dose measurement. In order to obtain the effective beam area entering the FC, the proton beam spot size will be measured by using a scintillator window and a CCD camera [81] or with Gafchromic films. Among the ELIMED activities we propose to develop an innovative FC for absolute dosimetric measurements downstream the beam transport line with an accuracy as close as possible to the one required for clinical applications, i.e. less than 5%. Starting from the several studies published in literature of the existing FC designs for conventional proton beams [83, 84, 85, 86, 82, 63, 51], a prototype will be built, tested and optimized to be suitable for the specific features of the laser-driven proton beams. Moreover, Monte Carlo simulations with the GEANT4 toolkit will be performed in order to specifically investigate the best construction parameters, such as materials and shapes, the influence of the entrance window on the secondary particle production and on the beam angular and energy straggling. The FC prototype design will be based on a typical FC developed for conventional proton dosimetry, such as in [82, 63]. The FC prototype will be made of two electrodes: a suppressor or guard ring placed upstream of a cylindrical cup, both encased in a common cylindrical grounded housing and electrically insulated from it. In order to achieve a minimal leakage current value, particular care will be devoted to the cup shielding, the signal connection and to the insulation between the cup and the suppressor ring. The FC prototype will operate in vacuum, so the device will be provided with a thin vacuum window. A preliminary study of the cup materials, dimensions and geometry, insulation and vacuum parameters is already ongoing and a schematic design result of the FC prototype performed with GEANT4 simulation is shown in figure 13.5.

As it appears clear from the proton fluence-to-dose relation 13.3, the uncertainties affecting the particle fluence and dose determination using a FC strongly depend on

Figure 13.5: A schematic layout of the FC prototype obtained with GEANT4 simulation.

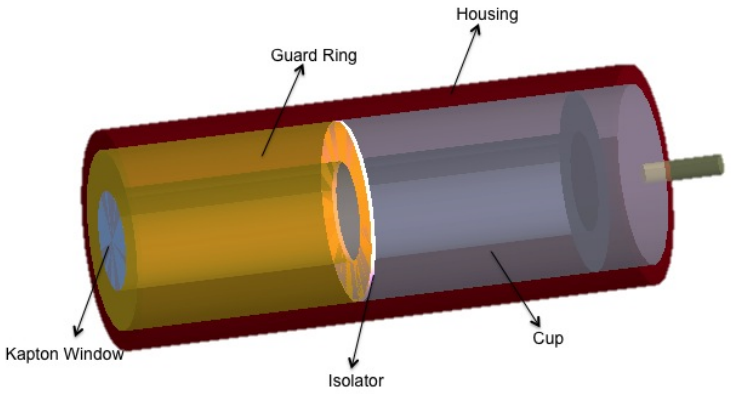

accurate measurements of the effective beam area and of the proton energy spectrum. As discussed before the measurement of the laser-accelerated proton energy spectra will be performed by means of a spectroscopic method using Gafchromic films, CR-39 and a Proton Spectrometer.

Concerning the beam area measurement, it has been pointed out in several works [83, 85, 86, 82, 63] that the effective beam area determination is affected by large uncertainties mainly due to the influence of the scattering from the last collimator edge on the beam profile. We are currently studying innovative technologies to perform an on-line direct measurement of the effective beam area. Up to now the main studied solutions for the FC entrance window consist of: a scintillator coupled to a CCD or two (x,y) scintillating fiber ribbons in a vitreous matrix for the vacuum maintenance. Both these options could be useful for an on-line control of the beam profile and thus for the measurements of its effective area.

The new device will be developed in 2014 and in the same year we plan to perform the first dosimetric tests with conventional proton beams available at the INFN-LNS, in a large dose-rate range (1 - 500 Gy/min). At the end of 2014 we plan to perform its first characterisation with the laser-driven beams at the TARANIS facility in Belfast, at Luli in Paris and Gist on Korea.

13.4 WP- 3.4: Radiobiology studies and measurements

13.4.1 Premise

The ELIMED project will investigate the radiobiological properties of very high-dose rate and (ultra) short-pulsed proton beams, according to the rationale outlined in the

Dosimetry and Radiobiology WP. The aim is to validate the use of such beams for clinical cancer treatment. Beams generated from laser-matter interaction possess almost unique physical features: Whether and how the peculiar temporal structure of proton beams bursting from high-power laser-matter interaction affects cellular radioresponse is basically unknown.
Although a limited amount of data has been already published, a number of radiobiological endpoints that are crucial to clinical outcomes are still unexplored, such as long-term degenerative effects in healthy tissues and secondary cancer risk. In order to fill existing gaps in the knowledge of the biological consequences from exposure to protons accelerated by such innovative technique, we shall need to establish irradiation protocols for hitherto overlooked assays and accumulate statistically robust data to highlight possible differences in biological effectiveness using conventionally accelerated beams whose physical characteristics are as close as technically achievable to those from laser-target interaction. This will help optimizing irradiation schedules and obtaining original information with laser-driven proton beams.
The expertise of, and activity proposed by the ELIMED Radiobiological Units, therefore, timely fits with the scope and work in progress of the project since in 2014 the preparatory phase concerning beam analysis, selection and dosimetry will allow measurements of radiobiological relevance to be made at facilities where laser-driven sources are already operating.

13.4.2 State of the art

Demonstration, more than a decade ago, by large high-power glass lasers operating at a few pulses per day and generating intense proton pulses with peak energies in the range of 60 MeV [87], triggered proposals concerning the suitability of such acceleration techniques for therapeutic applications [88]. Since then, studies on laserÐplasma ion acceleration of proton beams have made tremendous progress [89]. Continued interest in laser-driven acceleration stems from its potential cost-saving compared to conventional ion beam radiotherapy [104, 91, 92, 93, 94, 95]. The rationale for using accelerated charged particles (protons and carbon ions) as cancer radiotherapy strategy is based on their superior ballistic properties compared to photons and generally higher RBE, by which same level of cancer cell inactivation is attained by delivering a lower radiation dose, translating in advantages in terms of dose distribution to the tumour and increased sparing of normal tissue [96, 97]. As a result, particle radiotherapy is preferred than conventional one [98]. In particular, although protons show a lower RBE

respect to carbon ions, a growing number of accelerators dedicated to proton therapy are being planned at hospital-based centers. This is mainly because protons present less complex and costly technology for beam transport as well as radiation shielding [99, 100]. However, today economic climate has made even more stringent the issue of building and running costs for an ion radiotherapy facility, due to the requirement of a synchrotron or cyclotron often associated with large gantry systems. The cost-benefit debate highlights, for example, that the costs per fraction are estimated to be up to 5 times higher than those for photon therapy [101], thereby hampering the large-scale spread of these facilities. From these reasons, it is evident the demand for more compact and flexible acceleration and beam transport techniques, thus strengthening the case for laser-driven acceleration of particles, combined with the hope for a reduction of costs and required space.

In a typical laser-ion acceleration experiment, a high power laser pulse (of intensity above 10^{19} W cm^{-2}) is focused onto a thin foil. The highest proton energies observed by this method so far are about 20 MeV [102]. This has been achieved with a laser power intensity of 6 10^{19} W/cm^2 and a pulse length of 320 fs. Extrapolation of model calculations to deliver a 200 MeV beam (the energy range for non-superficial proton therapy), indicates that the needed laser power would be 10^{22} W/cm^2, at which no experimental results have yet been obtained [103]. Although the energies achieved at present are far from those required for radiation therapy and many questions remain unresolved (e.g. regarding energy selection, beam preparation and transport, repetition rate, stability and dosimetry) it is important to point out that the pulse properties of laserÐplasma-accelerated proton beams differ significantly from those commonly provided by medical accelerators in pulse duration, peak current and correspondingly energy spectrum and pulse dose rate [104].

The ion beams resulting from laser-matter interactions will be emitted as bursts of ultra-short pulses at variable pulse frequency. In a clinical scenario, thus the operational dose rates will be orders of magnitude greater than those presently used in proton or carbon-ion cancer treatment, for instance 10 Gy/min used at LNS CATANA facility. Hence, before clinical application of laser-driven ions can be considered, basic radiation biology research, starting from systematic in vitro cell irradiation experiments with very high dose-rate and pulsed proton beams resembling actual laser-driven beams, then moving through animal experiments to clinical trials with patients, will constitute an important preliminary step to demonstrate the maturity of this technology [105].

In fact, the biological effectiveness of these new kind of beams, characterized by high intensity (10^{10-12}p/bunch) bunches with short duration, compared to quasi-continuous

beams coming from conventional accelerators (cyclotrons or synchrotrons) is basically unknown. Although recent modeling studies [106, 107] have shown a possible reduction of reactive oxygen species (the main mediators of in direct radiation action on biologically relevant macromolecules) for ion tracks overlapping in time (i.e., during initial level of DNA damage), in principle, the impact of a pulsed beam on cells or tissues remains unclear. In a more general context, time-resolved radiobiological studies with sub-nanosecond particle bunches might help to elucidate the ultrafast processes underlying the biological response of cells. Characterized by ultra-short relativistic particle beams and high dose delivery rates, these new irradiation sources would represent interesting tools for the specific treatment of deep tumours or radio-resistant cancers. In this context, spatiotemporal radiation biology is expected to provide new insights into yet unknown domains such as cell and tissue responses to pulsed high dose rate irradiation regimes.

The biological effects at these ultra-high dose rates are virtually unknown. As a matter of fact, most of the radiobiological datasets on which current models of the cellular and molecular response to ionising radiation are based and used for radioprotection guidelines and radiotherapy strategies, derive from in vitro as well as in vivo experiments or epidemiological studies, with dose rates rarely exceeded 1-2 Gy/min. Cellular exposure to radiation is indeed determined by the rate at which dose is delivered, in addition to the total absorbed dose and the phase of the cell cycle in which the cell is located at the time of irradiation. Dose-rate effects are well documented when irradiation regimes are lowered towards chronic exposure conditions (i.e. down to cGy/s). On the other hand, there is very little knowledge of the effects very high dose rates may have, most studies have being performed only recently. Moreover, such limited experimental evidence has been accumulated either exposing cells to ultra-short laser-driven pulsed electron beams [108], intra-operative radiation therapy (IORT) electron beams [109] or using conventionally accelerated, but pulsed, low-energy (up to 20 MeV) proton beams [110, 111, 112, 113, 114]. The results did not show any significant difference in relative biological effectiveness (RBE) at causing several endpoints (cell killing, micronuclei, chromosome aberrations DNA damage-associated γ-H2AX foci), except in the case of IORT electrons, which appeared to be less effective than high-energy photons at inducing clonogenic death [109]. Also the yield of chromosome aberrations seemed to be slightly less after pulsed compared to continuous proton beams [112]. To date, however, only a few studies have been performed using actual laser-driven protons: Kraft et al. described a preliminary experimental set-up for radiobiological studies at the 150 TW DRACO facility in Dresden, Germany, highlighting the need for further

dosimetric and radiobiological studies [115]. Two more recent studies examined the clonogenic survival of the human salivary cancer line HSG to quasi monoenergetic proton beams of 2.5 MeV in 20 ns bunches [116], and the clonogenic survival of the rodent V79 cell line to laser-accelerated beams up to 10^9 Gy/s in the energy range 0-5 MeV [32]. These studies provided somewhat conflicting results pointing to a higher RBE of laser-driven protons [116] with a lack of a significant difference by such beams compared to photons [117]. Overall, work carried out so far employing laser-driven particles has shown some deviations from the known cell response to the longer ion bursts used in radiotherapy. However, these investigations have been limited to examining mainly cell survival, hence overlooking sub-lethal cytogenetic stress and heritable DNA damage, which are clinically important for long-term consequences in healthy tissue, and in most cases Gy-level doses have been obtained by accumulating multiple irradiations with an effective dose rate of Gy/s, as in ÒconventionalÓ irradiations.

Early studies also investigated the effects of very high dose rates (in the order of 10^{11} Gy/min) on mammalian cell survival: an apparently lower effectiveness was reported for X-rays administered in the form of very short impulses (7 ns) and it was found that the cell survival curve resembled that observed under anoxic conditions [118]. Early animal studies also showed an effect, albeit in the opposite direction, i.e. towards an increase in radiosensitivity of intestinal epithelium when the dose rate increased from 1 to 60 Gy/min [119]. However, using electron beams at much higher rates (10^3 to 10^9 Gy/min), Field and Bewley [120] using 7 MeV electrons and Inada et al. [121] using 8 MeV electrons on mouse and rat skin found a decreased effectiveness compared to conventional regimes. In these studies, the decrease in radiation effectiveness was attributed to oxygen depletion under regimes of ultra-high dose rates since experiments done on skin under hypoxic conditions did not show a similar behavior. In other words, normal cells that are at low oxygen tension may potentially become anoxic at high doses delivered at high rates. This is in agreement with the observation that, at high dose rates, dissolved gaseous oxygen in bacteria may be depleted, which would render the cells more radioresistent [122]. Indeed, some of the much more recent results obtained with IORT electron beams [109] point to this direction, showing a diminished cell killing of high-dose rate and dose per impulse electrons compared to photons. Although radiotherapy doses are considerably lower than what been reported/simulated for the oxygen depletion to occur, this critically depends on the initial level of oxygen inside the cell (and there is a wide range of oxygenation especially in close proximity of the tumour) and the re-oxygenation parameter, which may be cell type dependent.

Thus far, high-dose rate investigations have not addressed the issue of complex damage

caused by overlapping (in time and space) ionizations from secondary electrons. The biological outcome of radiation exposure is dominated by the amount and complexity of DNA damage. While the absorbed dose by cells is a good indicator of the amount of damage induced, the complexity of the damage is linked to the clustering of DNA lesions, which results from direct ionizations from ions and electrons as well as reactions with radical species. If the spatial distribution of DNA lesions is a critical parameter for all charged particle exposures (due to the increasing Linear Energy Transfer or LET by the slowing particle), pulsed laser-driven ion sources push the temporal aspect to limits, which have not been achieved/investigated so far. Several effects related to the ultra-short nature of the energy deposition have been suggested as possible mechanisms that may influence the biological response of laser-driven beams and diversify it from that seen after ÒconventionalÓ particle exposure:

- possible alteration of the radical production (the above mentioned oxygen depletion effect);
- spatio-temporal overlap of independent tracks resulting in collective effects;
- lack of interaction between direct (caused promptly by direct DNA-ion and secondary electron interaction) and indirect (caused by radicals, with diffusion time up to 1 μs) DNA lesions.

Enhancement of the biological effectiveness of overlapping particle tracks has also been demonstrated using microbeam facilities [123]. Although relatively few ion traversals per cell will be required for radiotherapy, questions remain regarding the probability of the ionization overlap from secondary electrons and how this scales with the energy of the main particle beam. Finally, very little is known about the impact of generating a large, almost simultaneous amount of radicals, that is all the radicals produced in a time scale shorter than their average diffusion, contrary to what happens with conventional irradiations where radicals produced at the beginning of the irradiation exposure will have already chemically reacted when further radicals are produced during second- or minute-long irradiation. Thus, the influence of very high dose rates and high doses per impulse warrants further experimental data.

13.4.3 Expertise and international collaborations

The Radiation Biophysics groups of ELIMED collaboration have a long-standing research record in the biological effects of ionizing radiation and have focused particularly on the radiobiological properties of charged particle beams, for space radiation protection

and hadrontherapy applications. They have carried out several INFN-funded projects in close association with the LNS, at whose facility irradiations with protons, and other heavy ions, had been performed recently to study the dependence of radiobiological effectiveness on particle track structure. The laboratories of Naples Unit have state-of-the art equipment for measurement of radiation-induced cytogenetic damage; a 3-MV TTT-3 Tandem accelerator and a 250 V_p X-ray machine are routinely used for irradiations at Naples. Therefore, with respect to the overall economy of the ELIMED project, their expertise guarantees the achievement of the objectives planned within the Dosimetry and Radiobiology WP. Furthermore, it will be working in close collaboration with other national and international groups for the investigation of radiobiological properties exhibited by laser-driven ion beams as part of the European ELI (Extreme Light Infrastructure) initiative. The groups involved are from the Vinca Institute of Nuclear Sciences, University of Belgrade, Serbia; the Department of Physics; the Department of DrugÕs Science, University of Catania, Italy; the Polo Oncologico di CefalÌ, Italy. Collaborating institutions include the QueenÕs University Belfast, UK, the National Physical Laboratory, Teddington, UK and the INRS-EMT, Montreal in Canada.

13.4.4 Relevance of the proposal in relation to INFN mission

INFN actively supports interdisciplinary research. Our participation in ELIMED, in which several fields of experimental and theoretical physics are already present (from plasma physics to dosimetry and computational modeling), adheres to this mission by strengthening the collaboration in the field of radiation physics applied to biology and medicine. In the 2012-14 INFN Strategic Plan it is explicitly stated (pag. 29) that Ò Application of fundamental physics to human health and environment is becoming a primary need that is well-acknowledged by modern research In the field of hadrotherapyÉthe modellization and radiobiology studies are bound to assume a even greater role, producing also important by products on human space explorationÓ. The scientific interest shown by INFN in the application of charged particles to radiotherapy is evident by its funding of the first protontherapy centre in Italy at LNS and in participation to the construction of the National Centre for Oncological Hadrontherapy (CNAO, Pavia). ELIMED activities will contribute to the strengthening of the scientific initiatives devoted to the improvement of the hadrotherapy approach and will benefit INFN visibility in the field of medical application of accelerator and high-energy laser physics.

13.5 FEASIBILITY, SUSTAINABILITY AND RISK ASSESSMENT

The power of lasers foreseen by the ELI initiative for medical application, whose intermediate realization falls within the objectives of the ELIMED project, is yet to be achieved. Hence, validation of the biological effectiveness of proton beams that will be generated by the laser bursts must be performed using current state of the art radiobiological research and available ÒconventionallyÓ accelerated sources of proton beams that mimic as close as possible those physical conditions in order to obtain useful information. Therefore, before performing radiobiology experiments at the facilities employing existing, less powerful laser sources, we had planned preliminary studies at the LNS cyclotron. We have also planned to carry out feasibility studies and proof-of-principle radiobiology experiments at the Naples Tandem, using pulsed, low energy proton beams (pulse length will need to be brought down to tens of ns and requests to the Technical Services at Naples INFN Section have been put forward). This will allow us to fine-tune the choice of eligible assays and experimental conditions and the set-ups for the comparison of the radiobiological effectiveness of higher dose rate and pulsed proton beams at LNS, while performing preliminary measurements at abroad laser-driven proton beam irradiation facilities (TARANIS, LULI, KOREA, FLAME). Our aim is to cross-compare the results in order to assess eventually differences in the cell response.

13.5.1 RESEARCH IMPACT AND HORIZON 2020

The research carried out within the ELIMED project can be expected to implement the theoretical predictions of the fundamental physics of laser-matter interaction in the field of medical applications by validating the approach of using proton beams accelerated by this novel modality. Also, the radiobiological investigation of such exquisitely peculiar beams, with unique spatiotemporal features in their interaction with living cells, is still unexplored, and results will contribute to the understanding of processes underlying DNA damage formation and radiation track interactions, of potential interest for unraveling novel biomolecular pathways of genetic damage formation and recognition. Horizon 2020 Priority: ÒSocietal ChallengesÓ, under the Specific objectives: ÒHealthÓ, is well in line with such expected impact. Moreover, for the main objective of the ELIMED project to be achieved, that is the application of a novel technology for clinical applications, the radiobiological validation of the laser-driven proton beams is the ineludible final step: if successful, the expected reduction in costs and complexity

of this important treatment strategy will definitely represent a goal of valuable social impact in the Horizon 2020 framework.

13.6 Objectives and proposed radiobiological endpoints

The objectives we aim at accomplishing derive from the open questions concerning the radiobiological properties of laser-driven proton beams, which are:

- Whether and how extremely high dose rates of charged particles influence the cellular radioresponse and these are clinically exploitable;
- Whether and to what extent such biological effects by beams exhibiting the physical features attainable from the interaction of very high-power lasers with matter translate in therapeutical advantages in the inactivation of tumour cells without, at the same time, increasing the risk of complications in healthy tissues;

In particular, we aim at studying the dependence of biologically relevant effects from the beam dose rates and beam pulse frequency by measuring the Relative Biological Effectiveness (RBE) of the tested irradiation regimes by means of the clonogenic cell survival assay, the induction of DNA damage and its repair kinetics by comet assay and immunofluorescence, and the onset of premature cellular senescence, which is useful to investigate as a non-cancer late effect of radiation possibly affecting tissue physiological homeostasis. Moreover we will determine the levels of Reactive Oxygen Species (ROS) responsible for the indirect effects of radiation, being also considered to be important signal molecules for the cell and possibly responsible for the perpetuation of late-occurring effects such as genomic instability. Finally, we will analyze different pathways involved in cellular response to radiation, particularly some cellular processes such as apoptosis, DNA repair and oxidative stress response by analysis of gene expression (measured with Affymetrix GENE chip Human Genome U133 plus platform), with a method based on ”gene enrichment” with "a priopri biological knowledge" (hypergeometric distribution method) [143, 144]. In addition, we propose to implement the experimental set-up ARETUSA developed at LNS-INFN for the single photon counting measurement of the low-level photoinduced Delayed Luminescence (DL). By this approach we were able to discriminate between normal cell and tumoral ones [145] and recently we have correlated the DL signal intensity to apoptosis level induced in leukemia cells [124, 125]. Thus, we shall compare the results of this technique with those obtained from both Comet assay and gene expression analysis, which will in turn help to develop an on-line diagnostic technique that could provide real-time information on

the effects of treatments on the cells.
Naples, Pisa and Roma Units will have the role of coordinating, in close association with LNS, the radiobiological studies and measurements as envisaged by the Dosimetry and Radiobiology WP. Their main objective will be the radiobiological characterization of pulsed and high dose rate proton beams accelerated at TTT-3 Tandem, Naples and the superconducting cyclotron at LNS, Catania. These studies will yield data that will be compared with those obtained by the same beams under conventional dose rate and produced in continuous fashion. Such activity will lead to the optimization of the measurements that will be carried out at facility where laser-driven proton beams are already in use.
Limitations affect most of the published results from radiobiology studies that carried out with the existing laser-driven beamlines. In these papers cell survival and almost exclusively of cancer cells have examined; it is sensible if the main concern is the effectiveness at tumour sterilization by these beams, hence overlooking sub-lethal cytogenetic stress and heritable DNA damage, which are clinically important for long-term consequences in healthy tissue. However, in hadrotherapy, one of the main concerns for patients undergoing radiotherapy remains the onset of secondary cancers [126]. The tumorigenic potential of ionizing radiation has been long known as well as its dependence on dose, dose rate and radiation quality, e.g. LET [127]. However, non-cancer late effects such as organ impairment and tissue degeneration may also undermine overall treatment success. For instance, only recently evidence has emerged a significantly higher risk of developing cardiovascular disease in patients cured for breast cancer, possibly as a result of heart and/or blood vessel exposure; this is in line with the results from the epidemiological studies on the Japanese atomic bombs survivors, showing a higher than expected incidence of cardiovascular complications and heart failure [128]. Both cancer and non-cancer late effects of radiation treatment represent sub-lethal effects since they are brought about by proliferating cells surviving the initial radiation insult, and originate by the inevitable exposure of healthy tissue to radiation. Very little experimental data exist on the induction of such effects and hadrotherapy patient-based reliable follow-up data are not fully available. The dependence of sub-lethal effects on unprecedented factors, such as the exceedingly high dose rates and/or the pulsed nature of beams originated by laser interaction with target materials, is unknown and needs investigation prior to a therapeutic use of such beams.
We therefore propose a much wider range of radiobiological endpoints, which will allow us to study also long-term effects that are the major concern as sequelae of radiation cancer treatment. Prostate cancer cells will be used since this type of cancer is amenable for

hadrotherapy. Human foetal fibroblasts will be used for testing effects on healthy tissue. Endothelial cells will also be used, as they are present in both the cancer vessel network and the healthy tissue. Specifically, we shall measure the induction of clonogenic cell death in cancer cells to measure the RBE for cell inactivation: Correct evaluation of the RBE in the treatment planning is critical for the use of ions in radiotherapy. Its value is used to calculate the physical required dose in order to achieve the desired biological effective dose to the tumour. Moreover, the efficiency with which sublethal damage in normal cells will measured by studying the onset of cellular premature senescence and the frequency of radiation-induced chromosome aberrations. Physiological senescence has been recognized as a natural barrier to tumorigenesis in vivo [129]. Cells exposed to sub-lethal insults of various nature undergo a process defined as Stress-Induced Premature Senescence (SIPS) [130, 131]. In particular, ionizing radiation is capable of inducing SIPS and, more interestingly, charged particles have proven particularly effective at eliciting a senescence response at very low dose and dose rates [132]. Radiation-induced premature senescence can be thus very promptly observed in endothelial and fibroblast cells and can persist for a very long time post-exposure [133]. In vivo accumulation of senescing cells could result in organ and/or tissue dysfunction, genomic instability and cancer [134]. In hadrotherapy patients, healthy tissue receives sub-lethal doses of radiation, which may trigger a SIPS response, whose role is still undetermined [135]. In addition to the risk of complications it may represent for normal tissue and organ function, the existence of the so-called SenescenceÐAssociated Secretory Phenotype (SAPS) poses even more serious questions as to the implications this effect may have on the primary cancer: secretion of factors released by cells undergoing SIPS have been associated with either the inhibition or even the promotion of cellular proliferation in surrounding tumour cells [136, 137].

Chromosome aberrations (CAs) are the most extensively studied type of DNA damage and are universally acknowledged as a biomarker of increased cancer risk in healthy individuals [138]. At low doses, mainly simple, hence transmissible CAs are induced that do not prevent the host cell from dividing. Thus, viable cells carrying CAs will propagate such genetic alterations through proliferating descendants increasing the risk of pre-malignant cellular transformation. The type of genetic damage detectable, as CAs is a function of radiation quality since high-LET radiation is known to elicit a higher proportion of complex-type exchanges [139]. The more complex the aberration the least chances a cell has to proceed undisturbed through mitosis, hence to divide. Although such an increase in complexity is therefore the main reason of the greater efficiency at clonogenic cell killing associated with charged particle-based radiotherapy, there exists

evidence that a fraction of such complex damage can be transmitted through cell division to the progeny of the initially exposed cell population [140, 141, 142]. Persistence of CAs in healthy proliferating cells may lead to genomic instability and represent the driving force of cellular transformation, hence of secondary cancers. Moreover, because at DNA level the formation of CAs neatly reflect the spatio-temporal ionization pattern along and around the radiation track, the unique dynamics characterizing the physical properties of dose deposition from particle beams generated by high-energy lasers is expected to impact the spectrum of CAs: to what direction, that is whether resulting in more complex vs. simple exchanges, is currently unknown.
Irradiation at LNS will be performed at the CATANA beamline hence using 62 MeV protons, with radiation being delivered in acute shots contrary to most experimental studies by others where Gy-level doses were obtained by accumulating multiple irradiations with an effective dose rate of Gy/s, as in ÒconventionalÓ irradiations. High-energy protons will allow to explore a therapeutically relevant energy range, in contrast to most studies carried out with conventionally accelerated, pulsed proton beams (typically of 20 MeV). This will also enable us to study the possible effects due to the spatio-temporal overlapping of the more energetic secondary electrons thus generated.

13.7 Activity plan for 2014

Radiobiological measurements will be carried out on dermal human fibroblasts (a typical normal cell line) and DU145 prostate cancer cells will be used since this type of cancer is amenable for hadrotherapy, human foetal fibroblasts and endothelial cells for testing effects on healthy tissue. Cells will be grown in standard tissue culture flasks.
The experimental activity for 2014 is as follows:

- Feasibility study for optimization of protocols and proof-of-principle irradiation of human and normal cell lines at the TTT-3 Naples tandem with pulsed proton beams up to 6 MeV (pulse duration in the order of tens of ns, dose rates of tens of Gy min-1);
- Irradiation with highly pulsed 62 MeV protons at LNS-Catana set-up (pulses in the order of ns, dose rates of hundreds of Gy min-1);
- Irradiations with laser-driven proton beams of up to tens of MeV (peak energy) at TARANIS (UK) and/or LULI facilities (Fr);
- Coordination between and data mining from the collaborating groups examining other radiobiologically relevant endpoints (e.g. cell survival, DNA damage and

repair, cellular senescence, gene expression and Reactive Oxygen Species levels, apoptosis by photoinduced delayed luminescence); The Table below summarizes the endpoints that will investigated and the information that they will convey.

Table 13.1: Biological endpoints that will be investigated during the experiment.

Endpoint	**Assay**	**Information**
Cell death	Colony formation assay	Radiation-Induced loss of proliferative potential
Functional assay	MTT assay	Metabolic components necessary for cell growth
DNA double-strand breaks	Immunochemical detection of γ-H2AX foci	Induction of DSBs and kinetics of repair
Different DNA damage and repair capability	Comet Assay	Evaluation of DNA fragmentation and/or repair capacity of irradiated cells
Cellular senescence	Beta-galactosidase Assay	Determination of cellular premature senescence induced by radiation
Gene expression measurements	Affymetrix GENE chip Human Genome U133 plus	Determination of genes and pathways involved in response to radiation
Reactive Oxygen Species (ROS) measurements	Fluorescence Microscope Analysis with H_2DFFDA and DHE	Quantification of the level (concentration) of ROS following exposure to radiations

14 PLANNED EXPERIMENTAL SECTIONS

14.1 TARANIS FACILITY AT QUEEN'S UNIVERSITY (UK)

The **TARANIS** laser is a hybrid $Ti:Sapphire-Nd-glass$ system operating in the chirped pulse amplification mode. This unique laser model can simultaneously deliver two 1053 nm beams in each of the two existing target areas, in different combinations of 700 fs/1 ns pulse and with intensities up to 10^{19} W/cm^2 in the short pulse mode and up to 30 J on target in the ns pulse mode. The laser rep rate is 1 shot every 10 minutes [146]. The laser front-end consists of a Ti:Sapphire oscillator, followed by a folded all-reflective stretcher, and by a Ti:Sapphire regenerative amplifier (RA). The oscillator provides a train of transform-limited, 120 fs long pulses at a wavelengh of 1053 nm, with a repetition frequency of 76 MHz. The wavelengh is chosen to match the peak of the Nd:glass amplifiers gain curve in the glass amplification chain, and, although the gain of the Ti:Sapphire crystal is not peaked at 1053 nm, the oscillator delivers an average power of 400 mW. Pulse stretching is achieved within the double-pass stretcher, equipped with diffraction grating and a spherical mirror, arranged in an inverting telescope configuration. The stretcher bandpass is chosen to be about 4 times the oscillator output bandwith and the streching factor is about 10^4, providing at the output 1.2 ns long optically chirped pulses. Pre-amplification of the laser pulse is obtained in the Ti:Sapphire RA, pumped by a Q-switched Nd:YLF laser operating at the wavelengh of 527 nm. Optimization of the Ti:Sapphire RA for amplification at 1053 nm and a double set of Pockels cells located after the RA cavity contribute to limiting and controlling amplified spontaneous emission and pre-pulse activity. Amplification to multi-TW levels is achieved within a three stage Nd:glass amplification chain , optically pumped with flash lamps. As a result of the tailoring (by 3.4 mm diameter serrated aperture, located at the input of the glass amplification chain) and relay-imaging (by spatial filters between the different amplifications stages), the beam conserves a near-uniform top-hand spatial profile through the amplification chain, allowing optimal energy extraction from the glass rods. The two pulses from the glass amplification chain can be separately re-compressed in two double pass grating compressors.

A maximum proton energy of ~ 12 MeV was obtained with 10 μm thick aluminum targets [147]. The typical proton spectrum has been used to perform some preliminary dose evaluation of the beam selected with the first prototype of energy

selector. The selecting device is placed 1.5 m far from the target. The collimator has 1mm diameter and the slit size is 1 mm. Two energies values (4 and 8 MeV) are taken in account. Following table reports data on the simulated energy spread and transmission efficiency.

$Energy$ $[MeV]$	$Energy\ Spread$ $(FWHM/E_0)$	$Simulated\ transmission\ efficiency$	$Expected\ transmission\ efficiency$
4	3.5%	7.5%	15%
8	5%	2.6%	4%

According the information on the beam, the total number of particles produced per shot is 1.7763×10^9. After energy selection the expected number of particles are reported in the following table.

	$Particle\ per\ shot\ (out)$
4 MeV	228945
8 MeV	70000

Using the above data, preliminary MC simulation with $Geant4$ have been performed in order to evaluate the amount of dose delivered to a water phantom per each shot. Results are reported in the following table.

Number of Particle per Pulse	Incident Energy (MeV)	SD of Incident Energy (keV)	Phantom Length (mm)	Lateral Dimension of Phantom (mm)	Peak Position (μm)	Absorbed Dose (mGy)
70000	8	169.8643	1	4×4	765	5.47873
228945	4	59.45	0.4	4×4	205	21.1206

In order to calculate the dose as a function of the depth, phantom is divided to slices with 0.01 mm length. Depth dose profile related to 8 MeV protons is reported in Figure 14.1.

14.2 GIST Facility (Republic of Korea)

In the **GIST** Laboratory, in Gwangju (Korea), there is a 0.1 Hz, 1.0 $PW\ CPA\ Ti:Sapphire$ laser system, the typical pulse duration is 30 fs (FWHM). This

Figure 14.1: Depth dose profile specified by colour for 8MeV proton beam

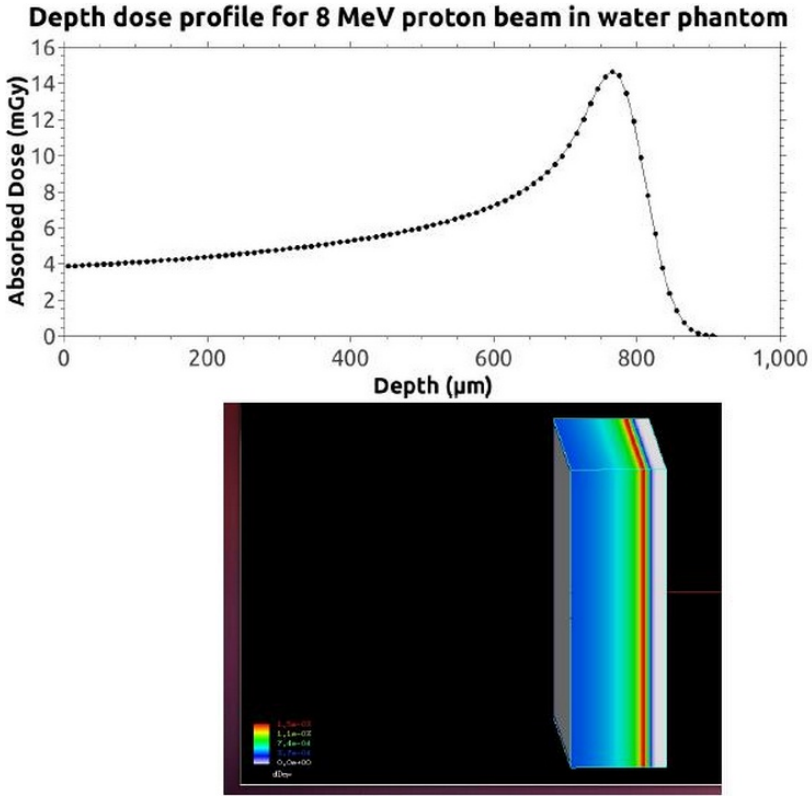

laser system is shown to have very low energy fluctuation and an almost homogeneous flattop spatial profile; it consists of a 1 kHz multi-pass amplifier system, a grating stretcher, a preamplifier, two power amplifiers, a final three-pass booster amplifier, and a grating compressor. A commercial 1 kHz multi-pass amplifier system is used as a front end to provide seed pulses for the amplifiers. Laser pulses from the 1 kHz amplifier system are stretched to about 0.9 ns with a grating. After stretching, the laser pulse is amplified in the preamplifier and the two power amplifiers thus its energy reaches 4.5 J. Before being injected into the final booster amplifier, the amplified laser pulses are upcollimated to a 60 mm diameter optical aperture through an achromatic beam expander. After passing through the expander, the laser pulses are amplified in the final three-pass booster amplifier. An $Nd:glass$ laser system (527 nm laser pulses in 12 beams at a 0.1 Hz repetition rate, each of the 12 beams delivers 8.0 J of energy) is used to pump the final booster amplifier. The measured spatial beam profile is close to a homogeneous flattop and agrees well with the calculated profile. From the laser beam image of

the central area occupying 80% of the whole energy, the standard deviation of the intensity level in the central area was calculated. The standard deviation was found to be 13% in the central area. Note that this homogeneous flattop spatial beam profile could be achieved with no image relay method or spatial filter. There is also a good reproducibility shot-to-shot, for example the shot-to-shot fluctuation for 25 successive laser pulses was as low as 0.53% in rms value.

14.3 PALS Facility in Prague (CZ)

The terawatt iodine laser system **ASTERIX IV** is implemented in Prague, at **PALS** Laboratory. It is a single beam iodine photodissociation laser system, based on a Master Oscillator-Power Amplifier (MOPA) configuration. It supplies up to 1 kJ of energy at the fundamental wavelength 1.315 nm, in pulses of 400 ps duration.
The lasing medium is composed of a mixture of perfluoralkyliodide C_3F_7I and Ar acting as a buffer gas that reduces the small-signal amplification. The lasing action occurs on the magnetic dipole type transition between the two fine structure levels of ground state doublet of the iodine atom

$$I(5\,^2P_{1/2}) \longmapsto I(5\,^2P_{3/2}) + h\nu(1.315mm)$$

produced by a photodissociation of C_3F_7I by UV light in the region 240-300 nm, generated by Xe flash-lamps:

$$C_3F_7I + h\nu(240-320nm) \longmapsto C_3F_7I + I(5\,^2P_{1/2})$$

The primary pulse is generated in an opto-acoustical mode-locked oscillator equipped with a high-extinction ratio pulse selection system (contrast ratio 10^9). This pulse is seeded into a chain of one preamplifier and five power amplifiers separated by spatial filters which remove the high spatial components from the angular beam spectrum and simultaneously act as image relay pairs ensuring optimum coupling between adjacent amplifiers through increasingly large diameter sections. The beam at the output of the last amplifier is 29 cm in diameter. According to the need of a given experiment it may be frequency doubled to 658 nm or tripled to 438 nm, using the $DKDP$ (deuterated potassium dihydrogen phosphate) crystals, prior to the final focusing down into the target chamber. At the present arrangement, the conversion efficiency of up to 60% and 30% is expected at 3ω at 2ω, respectively. The characteristic feature of both the fundamental and frequency

up-converted output beam is a high spatial uniformity, typically within 66% of the mean value. The laser is capable to fire a full-energy shot each 20 minutes, delivering on the target in the vacuum interaction chamber the focused power density up to $3 \times 10^{16}\ W/cm^2$, the focal spot on target is 50-70 μm and the spatial uniformity is very high (±6% of the average value).

14.4 FLAME FACILITY AT LNF-INFN (I)

The **FLAME** laser system is a CPA laser, with $Ti:Sapphire$ as active medium. It supplies up to 250 TW of power at the fundamental wavelength 800 nm, in pulses of 25 fs duration, with a repetition rate of 10 Hz. FLAME project, as other new generation laser system, looks for an improvement of the beam temporal profile (ASE contrast of 10^{-9}), shot-to-shot energy stability (0.77% rms of the energy) and the high beam spatial quality. It consists of an oscillator, a booster (the main innovative part for the improvement of the temporal contrast), a grating stretcher, a regenerative amplifier, two multi-pass amplifier and a final power amplifier.

LILIA project have been established in order to study and characterize the beam produced in FLAME facilty. In phase **1** laser intensities up to $10^{20} W/cm^2$ are expected and proton with energy up to 6 MeV will be produced. A bunch of 10^{10} protons compatible with those characteristics have been simulated with a PIC code. The bunch have been used to perform a simulation on the energy selector and results are reported in the following table.

	$Particle\ per\ shot\ (out)$
4 MeV	228945

In phase two the highest laser intensity will be reached using adaptive optics. The maximum proton energy will be about 30MeV using thin metal targets. A bunch of 10^{10} protons compatible with those characteristics have been simulated with a PIC code. The bunch have been used to perform a simulation on the energy selector and results are reported in the following table.

	$Particle\ per\ shot\ (out)$
4 MeV	142500
8 MeV	104000

The high laser rep rate could allow a great increasing in the number of protons selected.
Using the above data, preliminary MC simulation with Geant4 have been performed in order to evaluate the amount of dose delivered to a water phantom per each shot. Results reported in the following table are related to the first phase of the project.

Number of Particle per Pulse	Incident Energy (MeV)	SD of Incident Energy (keV)	Phantom Length (mm)	Lateral Dimension of Phantom (mm)	Peak Position (μm)	Absorbed Dose (mGy)	Total Energy Deposition (MeV)
217500	4	59.45	0.4	4×4	205	20.0646	801494.772

Results for high energy particles available in the next phase are reported in the table below.

Number of Particle per Pulse	Incident Energy (MeV)	SD of Incident Energy (keV)	Phantom Length (mm)	Lateral Dimension of Phantom (mm)	Peak Position (μm)	Absorbed Dose (mGy)	Total Energy Deposition (MeV)
104000	8	169.8643	1	4×4	765	8.14129	813022.702
142500	4	59.45	0.4	4×4	205	13.14591	525120.57

15 MILESTONES AND TEMPORAL PLAN

WP	Milestones 2013
All WPs	Periodic report in slides and/or text format of each WPs
WP-1: Target, PIC simulations, plasma and laser-driven beams diagnostic (WP-1.1, WP-1.2, WP-1.3, WP-1.4)	**M-1.1.a:** Realisation and test of nanostructured and porouses targets up to 1 micron thickness **M-1.2.a:** Test and data analysis of IC, ICR, SiC and Diamonds using TOF approach at PALS laboratory (I=10^{16} W/cm^2) - Dec. 2013 **M-1.2.b:** Upgrading of the Thomson spectrometer - Dec. 2013 **M-1.3.a:** Test of time resolved imaging with ICCD and optics at LNS and/or PALS- April 2013 **M-1.4.a:** ED-XRS measurements and 2D X-ray imaging in different energy domains of brilliant plasma source - April 2013 **M-1.4.b:** Design and development of the new High Resolution X-Ray Spectrometer - Sept. 2013 **M-1.4.c:** Feasibility studies of Time-resolved X-ray imaging and spectroscopy by using ancillary MCP detectors coupled to X-ray diagnostic tools - May 2013
WP-2. Energy selection system and beam transport (WP-2.1, WP-2.2, WP-2.3)	**M-2.1.a:** Study of the beam optics: Solenoid and quadrupole focusing system **M-2.2.a:** Monte Carlo Simulation of the ESS **M-2.3.a:** Design, Construction and Assembly of the Energy Selector System (ESS) **M-2.3.b:** Preliminary calibration of the ESS (TANDEM at LNS or CN at LNL)
WP-3. Hadrontherapy transport, dosimetry and radiobiology (WP-3.1, WP-3.2, WP-3.3, W-P3.4)	**M-3.1.a:** Monte Carlo simulations for the evaluation of dose distribution in different experimental configurations **M-3.2.a:** Full assembling of the first ELImon prototype, on-line monitor detector **M-3.2.b:** In-beam test of the ELImon prototype (PALS and Belfast facilities) **M-3.3.a:** Study and design of a dosimetric system for the irradiation of dosimetry and biological samples (Dec. 2013) **M-3.3.b:** Design and development of a dedicated Faraday Cup for absolute dose measurements **M-3.3.c:** GafChromic measurements **M-3.4.a:** Radiobiological measurements at very high dose rates for conventionally accelerated protons

WP	Milestones 2014
All WPs	Periodic report in slides and/or text format of each WPs
WP-1: (WP-1.1, WP-1.2, WP-1.3, WP-1.4)	**M-1.1.:** TARGET **M-1.1.a:** Periodic report in slides and/or text format of each WPs. Coordinator of each WP is responsible for each report. Submission of a beam request proposal at RAL Lab. (UK), LOA (Paris) and Kansai Photon Science Institute (Kioto-Japan)(s.j.) **M-1.1.b:** Experimental tests of relations between proton beam characteristics and target parameters (December 2014) **M-1.1.c:** Design and feasibility study for micro machined targets (June 2014). Construction of conical shaped targets and related holders (S.J. December 2014) **M-1.1.d:** Realization of thin target based on transition metals (Ta, Ti, Nb e Pd) hydrogen riched, using UV laser **M-1.1.e:** Study and Development of a specialized optical station for the alignment of the laser on the target and focus determination (S.J. June 2014) **M-1.1.f:** Feasibility studies about the best targetry for currently available high-repetition laser (June 2014) **M-1.1.g:** Development and potential implementation during experimental compaigns of a high-repetition cryogenic targetry systems **M-1.2.:** PIC SIMULATION **M-1.2.a:** Benchmarking between Aladyn e Jasmine PIC code (TNSA regime model) (June 2014) **M-1.2.b:** Matching between experimental and PIC code results (December 2014) **M-1.2.c:** PIC simulation of output beam product by laser interaction with metallic target (December 2014) **M-1.2.d:** Simulation of different transport schemes for generating a 30 MeV beam suitable for post acceleration using a Linac (June 2014) **M-1.2.e:** Theoretical studies about charge spatial effects after the interaction laser-target (December 2014) **M-1.3.:** BEAM HANDLING **M-1.3.a:** Design, development and pre-manufacturing analysis of a High Field Pulsed Solenoid for pre-selection and focusing nearby the target (June2014) **M-1.3.b:** design and manufacturing of 3 QP based on PM and related movement system (June 2014) **M-1.3.c:** Feasibility study of an Energy and Species selection system based on Wien Filter device (Dec. 2014) **M-1.3.d:** Test and Calibration of the ESS and the QP device at the TARANIS facility (Dec. 2014) **M-1.3.e:** Validation of the MC simulation about the ESS with experimental data (Dec. 2014)
WP-2. (WP-2.1, WP-2.2, WP-2.3)	**M-2.1.:** X-ray diagnostics **M-2.2.:** Optical and UV diagnostics **M-2.2.a:** Pre-plasma diagnostics with an optical spectrometer and plasma diagnostics using a VIS and UV ICCD (june 2014) **M-2.3.:** Beam diagnostics **M-2.3.a:** Development of pixel, solid state CMOS detector for destructive diagnostics (june 2014) **M-2.3.b:** Study and design of AC thoroids and Beam Profile Monitors for non-intercepting diagnostics (june 2014) **M-2.3.c:** Construction of AC thoroids and Beam Profile Monitors for non-intercepting diagnostics (S.J. december 2014) **M-2.3.d:** Proton detection using of IC, ICR, SiC and Diamonds with high sensitivity and energy resolution during the experimental campaigns (june 2014) **M-2.3.e:**Quantitative analysis of IC, ICR, SiC and Diamonds spectra in order to have information about the angular and energy distribution and to compare with the TP measurements (December 2014)
WP-3. (WP-3.1, WP-3.2, WP-3.3, W-P3.4)	**M-3.1.:** Monte Carlo Activity **M-3.1.a:** Dose evaluation at the end of the transport beam line (June 2014) **M-3.1.b:** Preliminary studies of different dosimetry detectors (June 2014) **M-3.1.c:** MC simulations of the experimental setups for the planned experimental campaigns (June 2014) **M-3.1.d:** MC simulation for the optimization of new FC (materials, shape, secondary electrons) (June 2014) **M-3.1.e:** Feasibility studies of the ELIMED beam line to deliver a clinical beam (Dec. 2014) **M-3.1.f:** Radioprotection and shielding studies (Dec. 2014) **M-3.2.:** Dosimetry **M-3.2.a:** Development and test of a Scintillating Proton Spectrometer (SPS) (June 2014) **M-3.2.b:** Test of the ELImon detector (June 2014) **M-3.2.c:** Development of an integrated system for the dosimetry positioning and irradiation (Dec. 2014) **M-3.2.d:** Development of innovative and high precision Faraday Cups for absolute dosimetric measurements (June 2014) **M-3.2.e:** Tests of the dosimetric system and detectors (FC, GAF, CR-39, SPS) at the TARANIS facility (Belfast, UK) (Dec. 2014) **M-3.3.:** Radiobiology **M-3.3.a:** Feasibility studies and proof-of-principle irradiations at Naples tandem. (June 2014) **M-3.3.b:** First measurements with laser-driven proton beams (June 2014) **M-3.3.c:** First measurements at LNS with very high-dose rates beams (Dec. 2014) **M-3.3.d:** Preliminary conclusions on cellular responses by conventionally accelerated and laser-driven beams (Dec. 2014)

WP	Milestones 2015
All WPs	Periodic report in slides and/or text format of each WPs
WP-1: Target, PIC simulations, plasma and laser-driven beams diagnostic (WP-1.1, WP-1.2, WP-1.3, WP-1.4)	**M-1.1.a:** Use of target realized at ultra intense laser lab for TNSA irradiation. The target geometry and structure will be devoted to promote resonant absorption effects, maximum proton energy and narrow energy spread **M-1.2.a:** Measurements with IC, ICR, SiC an Diamonds at Ultraintense laser labs (>10^{19} W/cm^2). Such detector will be improved to be used in TOF approach measuring the proton and other ion contributions **M-1.3.a:** Use of a VIS and UV ICCD for plasma diagnostic at ultra intense laser lab **M-1.4.a:** Use of X-ray based techniques for plasma diagnostic at ultra intense laser lab (early 2015, to be established by the collaboration)
WP-2. Energy selection system and beam transport (WP-2.1, WP-2.2, WP-2.3)	**M-2.1.a:** Final Design of the beam Trasport line for ELIMED **M-2.2.a:** Monte Carlo simulations for radio-protection studies related to the ESS
WP-3. Hadrontherapy transport, dosimetry and radiobiology (WP-3.1, WP-3.2, WP-3.3, W-P3.4)	**M-3.1.a:** Monte Carlo simulation of the in air transport beam line for the ELIMED facility and radioprotection assessments **M-3.2.a:** assembling and commissioning the final ELImon set-up at the test facilities **M-3.3.a:** Irradiation tests at FLAME facility (if available) and/or at the GIST facility (Gwangju, Republic of Korea) - Dec. 2015 **M-3.3.b:** FC and Ionization Chamber measurements with the FLAME (Frascati, IT) beams (if available) and/or and GIST beams (Gwangju, Republic of Korea) - Dec 2015 **M-3.4.a:** Determination of conclusive RBE values of high-energy laser-driven protons for all major endpoints

REFERENCES

[1] INFN (2012), *Piano Triennale dell'INFN 2012-14*

[2] L. Laska et al., Experimental studies of generation of 100 MeV Au-ions from the laser-produced plasma
Laser and Particle Beams 27 (2009) 137Ð147.

[3] J. Krasa et al., Generation of high currents of carbon ions with the use of sub-nanosecond near-infrared laser pulses
Rev. Sci. Instr. 81 (2010) 02a504.

[4] D. Margarone et al., New methods for high current fast ion beam production by laser-driven acceleration
Rev. Sci. Instr. 81 (2010) 02a506.

[5] D. Margarone, et al., High current, high energy proton beams accelerated by a sub-nanosecond laser
Nucl. Instr. and Meth. A, 653 (2011) 159

[6] S.C. Wilks et al. Energetic proton generation in ultra-intense laser-solid interactions
Phys. Plasmas 8 542, 2001.

[7] E. L. Clark et al., Energetic Heavy-Ion and Proton Generation from Ultraintense Laser-Plasma Interactions with Solids
Phys. Rev. Lett. 85 (2000) 1654.

[8] L. Torrisi et al., Tantalum ions production by 1064 nm pulsed laser irradiation
J. Appl. Phys. 91(5), 4685-4692, 2002

[9] P. McKenna et al., High-intensity laser-driven proton acceleration: influence of pulse contrast
Phil. Trans. R. Soc. A (2006) 364, 711.

[10] E. L. Clark et al. Energetic heavy-ion and proton generation from ultraintense laser-plasma interactions with solids
Phys. Rev. Lett. 21(85-n.8), 1654, 2000.

[11] S. Fourmaux et al. *PHYSICS OF PLASMAS* 20, 013110 (2013)

[12] K. Ogura M. Nishiuchi, A. S. Pirozhkov, T. Tanimoto, A. Sagisaka, T. Z. Esirkepov, M. Kando, T. Shizuma, T. Hayakawa, H. Kiriyama, T. Shimomura, S. Kondo, S. Kanazawa, Y. Nakai, H. Sasao, F. Sasao, Y. Fukuda, H. Sakaki, M. Kanasaki,

A. Yogo, S. V. Bulanov, P. R. Bolton and K. Kondo, Proton acceleration to 40 MeV using a high intensity, high contrast optical parametric chirped-pulse amplification Ti:sapphire hybrid laser system
Opt. Lett. 37, 2868 (2012)

[13] L. Torrisi, G. Foti, L. Giuffrida, D. Puglisi, J. Wolowski, J. Badziak, P. Parys, M. Rosinski, D. Margarone, J. Krasa, A. Velyhan and J. Ullschmied, Single crystal silicon carbide detector of emitted ions and soft x-rays from power laser- generated plasmas
J. Appl. Phys. 105, 123304 (2009).

[14] L. Torrisi, D. Margarone, L. Laska, M. Marinelli, E. Milani, G. Verona-Rinati, S. Cavallaro, L. Ryc, J. Krasa, K. Rohlena and J. Ullschmied, Monocrystalline diamond detector for ionizing radiation emitted by high temperature laser-generated plasma
J. of Appl. Physics 103, 083106, 1-6, 2008.

[15] D. Margarone, J. Krasa, L. Laska, A. Velyhan, T. Mocek, J. Prokupek, E. Krousky, M. Pfeifer, S. Gammino, L. Torrisi, J. Ullschmied and B. Rus, Measurements of the highest acceleration gradient for ions produced with a long laser Pulse
Review of Scientific Instruments 81, 02A506, 2010.

[16] M. J. Rhee, Compact Thomson spectrometer
Rev. Sci. Instrum. 55 (8), August 1984.

[17] R. F. Schneider, C. M. Luo, M. J. Rhee, Resolution of the Thomson spectrometer
J. Appl. Phys. 57 (1), 1 January 1985.

[18] D. Jung, R. Horlein, D. Keifer, S. Letzring, D. C. Gautier, U. Schramm, C. Hubsch, R. Ohm, B. J. Albright, J. C. Fernandez, D. Habs, B. M. Hegelich, Development of a high resolution and high dispersion Thomson parabola
Review of Scientific Instruments 82(1):013306, 2011.

[19] K. Harres, M. Schollmeier, E. Brambrik, P. Audebert, A. Blaevi, K. Flippo, D. C. Gautier, M. Geibel, B. M. Hegelich, F. Nurnberg, J. Schreiber, H. Wahl, M. Roth Development and calibration of a Thomson parabola with microchannel plate for the detection of a laser-accelerated MeV ions
Rev. Sci. Instrum. 79, 093306 (2008).

[20] G. A. P. Cirrone, G. Cuttone, M. Maggiore, L. Torrisi, F. Tudisco, Diagnostic for the radiotherapy use of laser accelerated proton beams
Radiation Effects and Defects in Solids Vol 00, No. 00, January 2008,1-7.

[21] M. Maggiore, S. Cavallaro, G. A. P. Cirrone, G. Cuttone, L. Giuffrida, F. Romano, L. Torrisi, Design and realisation of a Thosom Spectrometer for Laser Plasma Facilities
Nejaka Hlavicka 123(2020), 123-456.

[22] K. Jungwirth et al, The Prague ASTERIX Laser System
Physics of Plasmas Volume 8, number 5, May 2001.

[23] D. Jung, R. Horlein, D. Keifer, S. Letzring, D. C. Gautier, U. Schramm, C. Hubsch, R. Ohm, B. J. Albright, J. C. Fernandez, D. Habs, B. M. Hegelich, Development of a high resolution and high dispersion Thomson parabola
Review of Scientific Instruments 82(1):013306, 2011.

[24] A. Pappalardo, L. Cosentino, and P. Finocchiaro, An imaging technique for detection and absolute calibration of scintillation light
Rev. Sci. Instrum. 81, 033308 (2010); doi: 10.1063/1.3360931

[25] J. S. Green, M. Borghesi, C. M. Brenner, D. C. Carroll, N. P. Dover, P. S. Foster, P. Gallegos, S. Green, D. Kirby, K.J. Kirkby, P. McKenna, M. J. Merchant, Z. Najmudin, C. A. J. Palmer, D. Parker, R. Prasad, K.E. Quinn, P. P. Rajeev, M. P. Read, L. Romagnani, J. Schreiber, M. J. V. Streeter, O. Tresca, M. Zepf and D. Neely, Scintillator-based ion beams profiler for diagnostic laser-accelerater ion beams
Laser Acceleration of Electrons, Protons, and Ions; and Medical Applications of Laser-Generated Secondary Sources of Radiation and Particles. Edited by Ledingham, Kenneth W. D.; Leemans, Wim P.; Esarey, Eric; Hooker, Simon M.; Spohr, Klaus; McKenna, Paul. Proceedings of the SPIE, Volume 8079, pp. 807919-807919-8 (2011)

[26] D. B. Geohegan, Diagnostics and Characteristics of Laser Produced Plasma in Pulsed Laser Deposition of Thin films
edited by D. B. Chrisey and G. K. Hubler (John Wiley Sons, New York, 1994).

[27] A. Misra, A. Mitra, and R. K. Thareja,
Applied Physics Letters 74, 929 (1999).

[28] Siegel J, Epurescu G, Perea A, Gordillo-V'azquez F J, Gonzalo J and Afonso
C N 2004 Opt. Lett. 29 2228

[29] N. Gambino, P. Hayden,D. Mascali, J. Costello, C. Fallon, P. Hough, P. Yeates, A. Anzalone, F. Musumeci, S. Tudisco, Dynamics of colliding aluminium plasmas

produced by laser ablation
Applied Surface Science (2012).

[30] D. Giulietti et al., X-ray emission from laser produced plasmas
La Rivista del Nuovo Cimento, 21, (1998), pp. 1-101.

[31] I. Mantouvalou et al., Study of extreme ultraviolet and soft x-ray emission of metal targets produced by laser-plasma-interaction
Rev. Sci. Instrum. 82, (2011), art. N. 066103

[32] H.J. Kunze, Introduction to Plasma Spectroscopy, in Spinger Series on Atomic *Optical and Plasma Physics*, Spinger, London, 2009, ISBN978-3-642-02232-6.

[33] Castro et al., Comparison between off-resonance and electron Bernstein waves heating regime in a microwave discharge ion source
Review of Scientific Instruments , 82, 2012, art.n. 02B501.

[34] Celona et al. Technical issues related to the design of third generation ECR ion sources
Radiation effects and defects in solids 160, 2005, 457-465.

[35] Mascali et al., Preliminary studies on the X-ray emission from an innovative plasma-trap based on the Bernstein waves heating mechanism, oral presentations at the ÒEuropean Conference on X-ray Spectrometry
EXRS 2012 18-22 June 2012, Vienna

[36] H. Daido, *REP. PROG. PHYS.* 75 (2012) 056401

[37] I. Hofmann et al. *PHYS.REV. ST AB* 14, 031304(2011)

[38] K. Harres et al. *PHYS. of PLA.* 17, 023107 (2010).

[39] M. Schollmeier et al.*PHYS. REV. LET.* 101, 055004 (2008)

[40] A. Yogo et al *NUCL. INST. METH.* A 653 (2011).

[41] M.Nishiuchi et al. *PHYS. REV. SP-AB* 13,071304 (2012).

[42] S. Agostinelli et al., Geant4 - a simulation toolkit
Nucl. Instr. and Meth. in Phys. Res. A, 506, 250, 2003.

[43] J. Allison et al., Geant4 developments and applications
IEEE Trans. Nucl. Sci. 53(1), Part 2, 270, 2006

[44] J. Allison, Facilities and methods: Geant4- a simulation toolkit
Nuclear Physics News Vol. 17, 2 , 20-24, 2007

[45] Cirrone G.A.P. et al.
IEEE Trans. Nucl. Sci. 52 (2005) 262.

[46] G.A.P. Cirrone et al., Hadrontherapy: a Geant4-Based Tool for Proton/Ion-Therapy Studies
Progress in NUCLEAR SCIENCE and TECHNOLOGY Vol. 2, pp.207-212 (2011)

[47] Romano F. et al., Applications of Monte Carlo methods to special radiotherapeutic techniques
IL NUOVO CIMENTO C vol. 034 (01), pp. 167-173 (2011). ISSN: 2037-4909

[48] Cuttone G et al., CATANA protontherapy facility: The state of art of clinical and dosimetric experience
THE EUROPEAN PHYSICAL JOURNAL PLUS vol. 126, 65 (2011), ISSN: 2190-5444, doi: 10.1140/epjp/i2011-11065-1

[49] *Bergoz Instrumentation* www.bergoz.com

[50] A. Di Pietro et al.
PRL 105(2010)022701

[51] Richter et al., A dosimetric system for quantitative cell irradiation experiments with laser-accelerated protons
2011 *Phys. Med. Biol.* 56 1529

[52] Daniel Kirby et al., LET dependence of GafChromic films and an ion chamber in low-energy proton dosimetry
2010 *Phys. Med. Biol.* 55 417,

[53] F Fiorini et al. Dosimetry and spectral analysis of a radiobiological experiment using laser-driven proton beams

[54] 2011 *Phys. Med. Biol.* 56 6969.

[55] D. Kirby et al., Radiochromic film spectroscopy of laser-accelerated proton beams using the FLUKA code and dosimetry traceable to primary standards
Laser and Particle Beams June 2011 29 : pp 231-239.

[56] S.D. Kraft et al., Dose-dependent biological damage of tumor cells by laser-accelerated proton beams
New Journal of Physics 12 (2010) 085003

[57] D.S. Hey et al. Use of GafChromic film to diagnose laser generated proton beams
Rev. Sci. Instrum. 79, 053501 (2008)

[58] F. Numberg et al., Radiochromic film imaging spectroscopy of laser-accelerated proton beams
Rev. Sci. Instrum. 80, 033301 (2009)

[59] G.F.Dempsay, Validation of a precision radiochromic film dosimetry system for quantitative two-dimensional imaging of acute exposure dose distributions
Med Phys. 2000 Oct;27(10):2462-75

[60] S.T. Chiu-Tsao, Dose response characteristics of new models of GAFCHROMIC films: Dependence on densitometer light source and radiation energy
Med Phys. 2004 Sep;31(9):2501-8.

[61] O.A. Zeidan, Characterization and use of EBT radiochromic Þlm for IMRT dose veriÞcation
Med Phys. 2006 Nov;33(11):4064-72.

[62] A. Piermattei, Radiochromic film dosimetry of a low energy proton beam
Med Phys. 2000 Jul;27(7):1655-60.

[63] G. Cuttone et al., First Dosimetry Intercomparison Results for the CATANA Project
Physica Medica Vol. XV, No. 3, July-September 1999, 121-130.

[64] G.A.P. Cirrone et al. A 62-MeV Proton Beam for the Treatment of Ocular Melanoma at Laboratori Nazionali del Sud-INFN
IEEE TRANSACTIONS ON NUCLEAR SCIENCE VOL. 51, NO. 3, JUNE 2004.

[65] G. Cuttone et al., CATANA protontherapy facility: The state of art of clinical and dosimetric experience
THE EUROPEAN PHYSICAL JOURNAL PLUS, vol. 126, 65 (2011).

[66] L. Raffaele et al., Dosimetry of clinical proton beams
Rivista Medica, Vol.14, N.1, 2008

[67] M. Martisõkova et al., Dosimetric properties of Gafchromic EBT films in monoenergetic medical ion beams
Phys. Med. Biol. 55 (2010) 3741Ð3751.

[68] L. Zhao et al., Gafchromic EBT film dosimetry in proton beams
Phys. Med. Biol. 55 (2010) N291ÐN301.

[69] S.V. Peterson et al., Experimental validation of a Monte Carlo proton therapy nozzle model incorporating magnetically steered protons
Phys. Med. Biol. 54 (2009) 3217Ð3229.

[70] D. Kirby et al., LET dependence of GafChromic films and an ion chamber in low-energy proton dosimeter
Phys. Med. Biol. 55 (2010) 417Ð433.

[71] L. Karsch, Dose rate dependence for different dosimeters and detectors: TLD, OSL, EBT films, and diamond detectors
Med. Phys. 39, 2447 (2012).

[72] S. Cecchini et al., *Il Nuovo Cimento* 109 A (1996) 1119.

[73] Mukhtar A. Rana , I.E. Qureshi, Studies of CR-39 etch rates
NIM B 198 (2002) 129Ð134.

[74] D.Hermsdorf, Measurement and comparative evaluation of the sensitive V for protons and hydrogen isotopes registration in PADC detectors of type CR-39
Radiation Measurement 44 (2009) 806-812.

[75] A. Szydlowski et al., Application of solid state nuclear track detectors of the CR-39/PM-355 type for measurements of energetic protons emitted from plasma produced by an ultra-intense laser
Radiastion measurements 44(2009) 881-884.

[76] S. Kimura, A. Anzalone, and A. Bonasera, Comment on "Observation of neutronless fusion reactions in picosecond laser plasmas"
Phys. Rev. E 79, 038401 (2009).

[77] http://rsb.info.nih.gov/ij/, Wayne Rasband (wayne@codon.nih.gov), *National Institute of Mental Health*, Bethesda, Maryland, USA

[78] S Lorin, E Grusell, N Tilly, J Medin, P Kimstrand and B Glimelius Reference dosimetry in a scanned pulsed proton beam using ionisation chambers and a Faraday cup
Phys. Med. Biol. 53 (2008) 3519Ð3529.

[79] E Grusell, Isacsson U, Montelius A and Medin J 1995, Faraday cup dosimetry in a proton therapy beam without collimation
Phys. Med. Biol. 40 1831Ð40.

[80] Stopping Powers & Ranges for Protons & Alpha Particles (I C R U Report No 49).
Intl. Commission on Radiation (June 1993).

[81] Boon S N, van Luijk P, Bohringer T, Coray A, Lomax A, Pedroni E, Schaffner B and Schippers J M 2000 Performance of a SSuorescent screen and CCD camera

as a two-dimensional dosimetry system for dynamic treatment techniques
Med. Phys. 27 2198Ð208.

[82] Cambria R et al., Proton beam dosimetry: a comparison between the Faraday cup and an ionization chamber
Phys Med Biol. 1997 Jun;42(6):1185-96.

[83] Verhey L J, Koehler A M, McDonald A C, Goitein M, Chang Ma, Schneider R J and Wagner M The Determination of Absorbed Dose in a Proton Beam for Purposes of Charged-Particle Radiation Therapy
Radiat. Res. 79 34Ð54 (1979).

[84] Vynckier S, Meulders J P, Robert P and Wambersie A The proton therapy program at the cyclotron "Cyclone" of Louvain-la Neuve (first dosimetric results)
J. Eur. Radiother. 5 245Ð247 (1984).

[85] Kacperek A and Bonnet D E Development of a Faraday cup for proton beam dosimetry at the MRC cyclotron unit at Clatterbridge Hospital
Proc. Int. Heavy Particle Therapy Workshop (Villigen) pp 53Ð6 (PSI, 18Ð20 Sept. 1989).

[86] Grussell E, Isacsson U, Montelius A and Medin J Faraday cup dosimetry in a proton therapy beam without collimation
Phys. Med. Biol. 40 1831Ð1840 (1995).

[87] Snavely R.A., Key M.H., Hatchett S.P., Cowan T.E., M. Roth M., Phillips T.W., Stoyer M.A., Henry E.A., Sangster T.C., Singh M.S., Wilks S.C., MacKinnon A.J., Offenberger A., Pennington D.M., Yasuike K., Langdon A.B., Lasinski B.F., Johnson J., Perry M.D., Campbell E.M. Intense High-Energy Proton Beams from Petawatt-Laser Irradiation of Solids
Phys. Rev. Lett. 85, 2945Ð2948 2000

[88] Bulanov S.V., Esirkepov T. Zh., Khoroshkov V.S., Kuznetsov A.V., Pegoraro F. Oncological hadrontherapy with laser ion accelerators
Phys. Lett. A 299, 240 -247, 2002

[89] Borghesi M., Fuchs J., Bulanov S.V., Mackinnon A.J., Patel P.K., Roth M. Fast ion generation by high-intensity laser irradiation of solid targets and applications
Fusion Sci. Technol. 49, 412-439, 2006

[90] Malka V., Friztler S., Lefevbre E., dÕHumieres E., Ferrand R., Grillon G., Albaret C., Meyroneinc S., Chambaret J.P., Antonetti A., Hulin D. Practicability of proton

therapy using compact laser systems
Med. Phys. 31, 1587Ð1592, 2004

[91] Ledingham K W, Galster W, Sauerbrey R., Laser-driven proton oncology-a unique new cancer therapy
Br J Radiol. 2007 Nov;80(959):855-8

[92] Tajima T., Habs D., Yan X. Laser Acceleration of Ions for Radiation Therapy
Reviews of Accelerator Science and Technology 2, 201-228, 2009

[93] Martin M. Laser accelerated radiotherapy: is it on its way to the clinic?
J. Natl. Cancer Inst. 101, 450-451, 2009

[94] Schell S., Wilkens J.J., Advanced treatment planning methods for efficient radiation therapy with laser accelerated proton and ion beams
Med. Phys. 37 (10), 5330-5340, (2010).

[95] Fiorini F., Kirby D., Borghesi M., Doria D., Jeynes J.C.G., Kakolee K.F., Kar S., Kaur S., Kirby K.J., et al., Dosimetry and spectral analysis of radiobiological experiment using laser-driven proton beams
Phys. med. Biol. 56, 6969-6982 (2011).

[96] Fokas E., Kraft G., An H., Engenhart-Cabillic R. Ion beam radiobiology and cancer: Time to update ourselves
Biochim. Biophys. Acta 1796, 216Ð229, 2009

[97] Durante M., Loeffler J.S. Charged particles in radiation oncology
Nat. Rev. Clin. Oncol. 7, 37-43, 2010

[98] http://ptcog.web.psi.ch/ptcentres.html

[99] Weber U., Kraft G Comparison of Carbon Ions Versus Protons
Cancer J. 15, 325-332, 2009

[100] Suit H., DeLaney T., Goldberg S., Paganetti H., Clasie B., Gerweck L., Niemierko A., Hall E., Flanz J., Hallman J., Trofimov A. Proton vs carbon ion beams in the definitive radiation treatment of cancer patients
Radiother. Oncol. 95, 3-22, 2010

[101] Peeters A., Grutters J.P., Pijls-Johannesma M., Reimoser S., De Ruysscher D., Severens J.L., Joore M.A., Lambin P. How costly is particle therapy? Cost analysis of external beam radiotherapy with carbon-ions, protons and photons
Radiother. Oncol. 95, 45-53, 2010

[102] Fuchs J., Antici P., dÕHumiŕres E., Lefebvre E., Borghesi M, Brambrink E., Cecchetti C. A., Kaluza M., Malka V., Manclossi M., Meyroneinc S.,Mora P, Schreiber J., Toncian T., PŐpin H., Audebert P. Laser-driven proton scaling laws and new paths towards energy increase
Nature Phys. 2, 48 Đ 54, 2006

[103] Schippers J. M., Lomax A.J. Emerging technologies in proton therapy
Acta Oncol. 50, 838Đ850, 2011

[104] Malka V., Faure J., Gauduel Y.A. Ultra-short electron beams based spatio-temporal radiation biology and radiotherapy
Mutat. Res. 704, 142Đ151, 2010

[105] Daido H, Nishiuchi M., Pirozhkov A.S. Review of laser-driven ion sources and their applications
Rep. Prog. Phys. 75, 056401 (71 pages) 2012

[106] Kreipl M.S., Friedland W., Paretzke H.G. Time- and space-resolved Monte Carlo study of water radiolysis for photon, electron and ion irradiation
Radiat. Environ. Biophys. 48, 11Đ20 (2009)

[107] Kreipl M.S., Friedland W., Paretzke H.G. Interaction of ion tracks in spatial and temporal proximity
Radiat. Environ. Biophys. 48, 349Đ359 (2009).

[108] Laschinsky L., Baumann M., Beyreuther E., Enghardt W., Kaluza M., Karsch L., Lessmann E., Naumburger D., Nicolai M., Richter C., Sauerbrey R., Schlenvoigt H.P., Pawelke J. Radiobiological effectiveness of laser accelerated electrons in comparison to electron beams from a conventional linear accelerator
J. Radiat. Res. 53, 395-403, 2012

[109] Scampoli P. , Bisogni M.G, Carpentieri C., di Martino F., Durante M., Gialanella G., Giannelli M., Grossi G., Magaddino V., Manti L., Moriello C., Pugliese M., Righi S., BIORT: an experiment for the assessment of the biological effects of of very high dose rate and dose per pulse electron irradiations
Il Nuovo Cimento C, 31, 3-9 (2008)

[110] Auer S., Hable V., Greubel C., Drexler G.A., Schmid T.E,. Belka C., Dollinger G., Friedl A.A. Survival of tumor cells after proton irradiation with ultra-high dose rates
Radiat. Oncol. 6, 139-146, 2011

[111] Schmid T.E., Dollinger G., Hauptner A.,Hable V., Greubel C., Auer S., Friedl

A.A.,Molls M.,Roper B., No evidence for a different RBE between pulsed and continuous 20 MeV protons
Radiat. Res. ,172,567-574 (2009)

[112] Schmid T.E., Dollinger G., Hable V., Greubel C., Zlobinskaya O., Michalski D., Auer S., Friedl, A.A., Schmid E., Molls M., Roper B. The effectiveness of 20 MeV protons at nanosecond pulse lengths in producing chromosome aberrations in human-hamster hybrid cells
Radiat. Res. ,175,719-727(2011)

[113] Zlobinskaya O., Dollinger G., Michalski D., Hable V., Greubel C., Du G., Multhoff G,. Roper B., Molls M., Schmid T.E. Induction and repair of DNA double-strand breaks assessed by gamma-H2AX foci after irradiation with pulsed or continuous proton beams
Radiat. Environ. Biophys. ,51, 23-32 (2012).

[114] Schmid T.E., Dollinger G., Hable V., Greubel C., Zlobinskaya O., Michalski D., Molls M., Roper B. Relative biological effectiveness of pulsed and continuous 20 MeV protons for micronucleus induction in 3D human reconstructed skin tissue
Radiother Oncol. 95, 66-72 (2010).

[115] Kraft D.K., Richter C., ,Zeil K., ,MBaumann M., Beyreuther E.,Bock S., Bussmann M.,Cowan T. E., , Dammene Y.,Enghardt W.,Helbig U.,Karsch L., Kluge T.,Laschinsky L.,Lessmann E.,Metzkes J., Naumburger D., Sauerbrey R.,.Sch§rer M. ,Sobiella M.,Woithe J.,Schramm U., Pawelke J. Dose-dependent biological damage of tumour cells by laser-accelerated proton beams.
New J. Phys. , 12, 1-12 (2010).

[116] Yogo A.,Maeda T., Hori T., Sakaki H., Ogura K.,Nishiuchi M.,Sagisaka A., Kiriyama H., Okada H.,Kanazawa S.,Shimomura T.,Nakai Y., Tanoue M.,Sasao F., Bolton P. R.,Murakami M.,Nomura T., Kawanishi S.,Kondo K., Measurement of relative biological effectiveness of protons in human cancer cells using a laser-driven quasimonoenerge32. Doria tic proton beamline
Appl. Phys. Lett., 98, 053701-3 (2011)

[117] Doria D.,Kakolee K. F., Kar S.,Litt S. K., Fiorini F.,Ahmed H.,Green S., Jeynes J. C. G.,Kavanagh J.,Kirby D.,Kirkby K. J., Lewis C. L.,Merchant M. J.,Nersisyan G.,Prasad R.,Prise K. M.,Schettino G.,Zepf M., Borghesi M. Biological effectiveness on live cells of laser driven protons at dose rates exceeding 10^9 Gy/s
AIP Advances, 2, 011209-6 (2012)

[118] Berry R. J., Forster D. W., Storr T. H., Goodman M. J. Survival of mammalian cells exposed to x rays at ultra-high dose-rates
Br. J. Radiol. 42, 102-107 (1969).

[119] Hornsey S. and Alper T. Unexpected dose-rate effect in the killing of mice by radiation
Nature, 210, 212-3 (1966).

[120] Field S.B. and Bewley D. K. Effects of dose-rate on the radiation response of rat skin
Int. J. Radiat. Biol. Relat. Stud. Phys.Chem. Med. ,26, 259-67(1974).

[121] Inada T. Nishio H. Amino S., Abe K., Saito K. High dose-rate dependence of early skin reaction in mouse
Int. J. Radiat. Biol. 38, 139-45 (1980).

[122] Dewey J. L. and Boag J. W. Modification of the oxygen effect when bacteria are given large pulses of radiation
Nature, 183, 1450-1 (1959)

[123] Schettino G., Ghita M., Richard D.J., Prise K.M. Spatiotemporal investigations of DNA damage repair using microbeams
Radiat. Prot. Dosimetry 143,340-343, 2011

[124] BARAN I.,GANEA C., SCORDINO A., MUSUMECI F., BARRESI V., TUDISCO S., PRIVITERA S., GRASSO R., CONDORELLI D. F., BARAN V., KATONA E., MOCANU M-M., GULINO M., UNGUREANU R., SURCEL M.,URSACIUC C. Effects of menadione, hydrogen peroxide and quercetin on apoptosis and delayed luminescence of human leukemia Jurkat T-cells
Cell Biochem. Biophys. 58, 169-179 (2010)

[125] BARAN I.,GANEA C., PRIVITERA S., SCORDINO A., BARRESI V., MUSUMECI F.,MOCANU M.-M. CONDORELLI D. F., URSU I., GRASSO R., GULINO M., GARAIMAN A., MUSSO N., CIRRONE G.A.P.,CUTTONE G. Detailed analysis of apoptosis and delayed luminescence of human leukemia Jurkat Tcells after proton-irradiation and treatments with oxidant agents and flavonoids
Oxidative Med. Cell. Longevity (2012)

[126] Hall E.J. Intensity-modulated radiation therapy, protons and the risk of second cancers
Int. J. Radiat. Oncol. Biol. Phys. 65, 1Ð7 2006

[127] Yang T.C.-H., Craise L. M., Mei M.-T., Tobias C.A. Dose protraction studies

with low- and high-LET radiations on neoplastic cell transformation in vitro
Adv. Space Res. 6, 137-147, 1986

[128] S. Schultz-Hector and K. R. Trott Radiation-induced cardiovascular diseases: is the epidemiologic evidence compatible with the radiobiologic data?
Int. J. Radiat. Oncol. Biol. Phys. 67, 10-18, 2007

[129] Campisi J. Cellular senescence as a tumour-suppressor mechanism
Trends Cell. Biol. 11, 27-31, 2001

[130] Serrano M., Lin A.W, McCurrach M.E., Beach D., Lowe S.W. Oncogenic ras provokes premature cell senescence associated with accumulation of p53 and p16INK4a
Cell 88, 593Ð602, 1997

[131] Toussaint O., Medrano E.E., von Zglinickic T. Cellular and molecular mechanisms of stress-induced premature senescence (SIPS) of human diploid fibroblasts and melanocytes
Exp. Gerontol. 35, 927Ð945, 2000

[132] Suzuki M., Tsuruoka C., Uchihori Y., Ebisawa S., Yasuda H., Fujitaka K. Reduction in life span of normal human fibroblasts exposed to very low-dose-rate charged particles
*Radiat. Res.*164, 505-508, 2005

[133] Fournier C., Winter M., Zahnreich S., Nasonova E., Melnikova L. , Ritter S. Interrelation amongst differentiation, senescence and genetic instability in long-term cultures of fibroblasts exposed to different radiation qualities
Radiother. Oncol. 83:277-282. (2007),

[134] Pazolli E., Stewart S.A. Senescence: the good the bad and the dysfunctional
Curr. Opin. Genet. Dev. 18, 42-47, 2008

[135] Suzuki M., Boothman D.A. Stress-induced premature senescence (SIPS) - influence of SIPS on radiotherapy
J. Radiat. Res. 48, 105-112, 2008

[136] Tsai K.K., Stuart J., Chuang Y.Y., Little J.B., Yuan Z. M. Low-dose radiation induced senescent stromal fibroblasts render nearby breast cancer cells radioresistant
Radiat. Res. 172, 306-313, 2009

[137] Davalos A. R., Coppe J.-P., Campisi J. and Desprez P.-Y. Senescent cells as a

source of inflammatory factors for tumor progression
Cancer Metastasis Rev. 29, 273Ð283, 2010

[138] Bonassi S., Znaor A., Norppa H., Hagmar L. Chromosomal aberrations and risk of cancer in humans: an epidemiologic perspective
Cytogenet. Genome Res. 104, 376-382, 2004

[139] Durante M., George K., Wu, Cucinotta F. A. Karyotypes of human lymphocytes exposed to high-energy iron ions H.
Radiat. Res. 158, 581-59, 2002

[140] Savage J. R. K. The transmission of FISH-painted patterns derived from complex chromosome exchanges
Mutat. Res. 347, 87-95, 1995

[141] Anderson R. M., Marsden S. J., Paice S. J., Bristow A. E., Kadhim M. A., Griffin C. S., Goodhead D. T. Transmissible and nontrasmissible complex chromosome aberrations characterized by three-color and mFISH define a biomarker of exposure to high-LET ?-particles
Radiat. Res. 159, 40-48, 2003

[142] Manti L., Durante M., Grossi G., Ortenzia O., Pugliese M., Scampoli P., Gialanella G. Measurements of metaphase and interphase chromosome aberrations transmitted through early cell replication rounds in human lymphocytes exposed to low-LET protons and high-LET ^{12}C ions
Mutat. Res. 596, 151-165, 2006

[143] Francesconi M., Remondini D., Neretti N., Sedivy J. M., Cooper L. N., Verondini E., Milanesi L.,Castellani: G. Reconstructing networks of pathways via significance analysis of their intersections
BMC Bioinformatics , 25, 9(2008).

[144] Remondini D., O'Connell B., Intrator N., Sedivy J. M., Neretti N. , Castellani G., Cooper L. N. Targeting c-Myc activated genes via a correlation method: Detection of global changes in large gene expression network dynamics
Proc. Natl. Acad. Sci. U S A ,102, 6902-6 (2005).

[145] MUSUMECI F., PRIVITERA G., SCORDINO A., TUDISCO S., LO PRESTI C., APPLEGATE L. A., NIGGLI H. J. Discrimination between normal and cancer cells by using spectral analysis of delayed luminescence
Appl. Phys. Lett. 86 , 153902-04 (2005)

[146] Dzalainis et al., *Proc. of SPIE Vol. 7451 45119-2*

[147] Dzalainis et al., *Laser and Particles Beams, 2010 doi: 10.1017/S026303*

[148] G. E. Cook, *Pulse Compression-Key to More Efficient Radar Transmission*, IEEE Proc. IRE 48, 310 (1960)

[149] D. Strickland and G. Mourou, Compression of amplified chirped optical pulses
Opt. Commun. 56, 219 (1985)

[150] S. Eliezer, The Interaction of High-Power Laser with Plasmas
IOP Publishing Ltd, 2002.

[151] P. Gibbon, Short Pulse Laser Interaction with Matter
Imperial College Press, 2005.

[152] M. Passoni, L. Bertagna, A. Zani, Target normal sheath acceleration: theory, comparison with experiments and future perspective
New J. Phys. 12 045012 (2010).

[153] A. Macchi and C. Benedetti, Ion acceleration by radiation pressure in thin and thick targets
Nucl. Inst. Meth. Phys. Res. A (2010) DOI: M10.1016/j.nima.2010.01.057

[154] I. Petrovic, A. Ristic-Fira, D. Todorovic, L. Valastro, P. Cirrone, G. Cuttone, Radiobiological analysis of human melanoma cells on the 62 MeV CATANA proton beam
International Journal of Radiation Biology, 82(4): 251-265, (2006).

[155] I. Petrovic, A. Ristic-Fira, D. Todorovic, L. Koricanac, L. Valastro, G.A.P. Cirrone, G. Cuttone. Response of a radio-resistant human melanoma cell line along the proton spread-out Bragg peak
International Journal of Radiation Biology, 86(9): 742-751, (2010).

[156] A. Ristic-Fira, D. Todorovic, J. Zakula, O. Keta, P. Cirrone, G. Cuttone, I. Petrovic. Cellular Response to Conventional Radiation and Hadrons
Physiological research, 60: 129-135, (2011).

[157] A. Ristic-Fira, L. Koricanac, J. Zakula, O. Keta, G. Iannolo, G. Cuttone, I. Petrovic. Proton inactivation of melanoma cells enhanced by fotemustine
Radiation Protection Dosimetry, 143: 503-507, (2011).

[158] L. Koricanac, J. Zakula, G. A. P. Cirrone, G. Privitera, G. Cuttone, I. Petrovic, A. Ristic-Fira. Variation of apoptotic pathway regulators by fotemustine and protons in a human melanoma cell line
Advanced Science Letters, 5: 552-559, (2012).